



LUND UNIVERSITY

Moisture redistribution in screeded concrete slabs

Åhs, Magnus

2007

[Link to publication](#)

Citation for published version (APA):

Åhs, M. (2007). *Moisture redistribution in screeded concrete slabs*. Division of Building Materials, LTH, Lund University.

Total number of authors:

1

General rights

Unless other specific re-use rights are stated the following general rights apply:

Copyright and moral rights for the publications made accessible in the public portal are retained by the authors and/or other copyright owners and it is a condition of accessing publications that users recognise and abide by the legal requirements associated with these rights.

- Users may download and print one copy of any publication from the public portal for the purpose of private study or research.
- You may not further distribute the material or use it for any profit-making activity or commercial gain
- You may freely distribute the URL identifying the publication in the public portal

Read more about Creative commons licenses: <https://creativecommons.org/licenses/>

Take down policy

If you believe that this document breaches copyright please contact us providing details, and we will remove access to the work immediately and investigate your claim.

LUND UNIVERSITY

PO Box 117
221 00 Lund
+46 46-222 00 00

LUND INSTITUTE OF TECHNOLOGY
LUND UNIVERSITY

Division of Building Materials

Moisture Redistribution in Screeded Concrete Slabs

Magnus Åhs

ISRN LUTVDG/TVBM--07/3136--SE(1-54)
ISSN 0348-7911 TVBM

Lund Institute of Technology
Division of Building Materials
Box 118
SE-221 00 Lund, Sweden

Telephone: 46-46-2227415
Telefax: 46-46-2224427
www.byggnadsmaterial.lth.se

Preface

This licentiate thesis is the result of three years of research conducted at the division of Building Materials, Lund Institute of Technology, Lund University. It was funded from SBUF, the Development Fund of the Swedish Construction Industry, FORMAS, the Swedish Research Council for Environment, Agricultural Sciences and Spatial Planning, maxit Group AB, and Strängbetong.

I would like to thank my supervisors, Professor Lars-Olof Nilsson and Ph.D. Anders Sjöberg at division of Building Materials, for their never-ending encouragement and support throughout this project. Their support and guidance put me on back on track, when the intertwined and multifaceted maze of research led me astray both in theory and practice.

The practical works in this research has been performed in cooperation with the technical crew at division of Building Materials, Stefan Backe, Bo Johansson, Ingemar Larsson and last but definitely not least Bengt Nilsson. Their technical skills and experience have made life easier in the laboratory. Marita Persson and Britt Andersson, the administrative spinal cord at division of Building Materials, have contributed to the completion of my thesis with their organizational skills. Special thanks goes to Lars Wadsö, the Matlab-guru, who provided appreciated support with computer aided measurement evaluations.

Representatives from the construction industry are hereby acknowledged for their contributions to this work. Skanska Sverige AB is hereby recognized for giving me the opportunity to attempt to push the frontier forward within the area of Building Materials.

All my fellow Ph.D. students and other colleagues are hereby recognized for their abilities of making my time here well spent.

Finally, I would like to thank my wife Jessica, for her endless patience of enduring having an absent minded husband for the last three years.

Magnus Åhs
February 2007, Lund

Abstract

The principal objective for this licentiate thesis is to develop a methodology and evaluation model in order to make the future relative humidity in a screeded concrete slab predictable.

Residual moisture in screeded concrete slabs may redistribute to the top screed surface under semi-permeable flooring, thus elevating the relative humidity, RH, and possibly exceed the critical humidity level. Passing the critical humidity level may result in material damages on the flooring and adhesive. In order to avoid such damages there is a need of a methodology to estimate the maximum humidity obtained underneath flooring.

Several screeded concrete slabs with PVC flooring, were prepared to reproduce and monitor moisture distribution and the occurring redistribution. The moisture distribution before flooring and after a certain time of redistribution is presented. In addition, sorption isotherms including scanning curves were determined in a sorption balance for materials used in the floor constructions, viz, w/c 0.65 concrete, w/c 0.4 concrete, w/c 0.55 cement mortar, and Floor 4310 Fibre Flow, a self leveling flooring compound. Repeated absorption and desorption scanning curves starting from the desorption isotherm were also investigated.

Performed measurements enabled the development of both a qualitative and quantitative model designed to resemble the actual moisture redistribution and quantify the humidity achieved under flooring respectively. The hysteresis phenomenon of the sorption isotherm is considered in the model.

The model is well suited for estimations of the future RH underneath flooring in a screeded concrete slab and may also be used on homogenous slabs.

Key words:

Moisture redistribution
Relative humidity
Screeded slab
Sorption isotherms
Hysteresis
Scanning

This licentiate thesis is based on the following papers.

Paper I Åhs, M., (2005). “Remote monitoring and logging of relative humidity in concrete”. Proceedings of the 7th Symposium on Building Physics in the Nordic Countries, The Icelandic Building Research Institute, Reykjavik, Iceland, pp 181-187

Paper II Åhs, M., Sjöberg, A., Anderberg, A., (2005) “A method for study sorption phenomena”, Proceedings of the 10th International Conference on Indoor Air Quality and Climate, Beijing, China, pp 1969-1973

Paper III Åhs, M., “Scanning sorption isotherms for hardened cementitious materials”,
(Submitted)

Paper IV Åhs, M., Sjöberg, A., “Moisture distribution in screeded concrete slabs”,
(Submitted)

Contents

- 1 Introduction 1
- 2 Theoretical background..... 3
 - 2.1 Structure of cement based materials..... 3
 - 2.2 Moisture fixation in cement based materials..... 5
 - 2.3 Moisture transport in cement based materials..... 12
- 3 Models..... 17
 - 3.1 Previous model..... 17
 - 3.2 Qualitative model 18
 - 3.3 Quantitative model 19
- 4 Experimental 23
 - 4.1 General description of experimental works 23
 - 4.2 Sorption measurements 25
 - 4.3 Scanning curves..... 30
 - 4.4 Moisture transport properties 39
- 5 Model validation 43
- 6 Discussion and conclusions..... 47
- 7 Future research 51
- 8 References 53

Appendix

Paper I

Paper II

Paper III

Paper IV

1 Introduction

Moisture frequently challenges the building industry worldwide, not only as heavy downpours where flooding demolishes building foundations but also as environmental actions on buildings and as residual moisture in building materials causing less striking damages. Large quantities of residual moisture may be found in concrete, especially in high w/c ratio concrete. This moisture may cause damages to adjacent materials if the humidity level exceeds a certain critical level.

In order to prevent damages caused by residual moisture the expected maximum humidity level should remain below the critical level. A typical example is concrete floors where this maximum humidity level is achieved just beneath flooring when residual moisture inside the slab has been given time to redistribute. A lot would be gained if this expected humidity could be estimated, for instance, based on measurements performed prior to flooring. The critical humidity often is expressed in relative humidity, RH, which is convenient as RH in a material is a good measure of the expected moisture condition in adjacent material. In addition RH measurements on cement based materials are reliable and less affected by uncertainties compared to moisture content measurements [1].

In Sweden, there is a standardized method to examine the humidity in homogenous slabs prior to flooring in order to avoid exceeding the critical humidity level. An RH measurement is performed at a certain depth to estimate the RH obtained beneath flooring of homogenous slabs. Drying of a concrete slab on grade mainly occurs through the flooring. The RH in such a slab is determined at a depth of $0.4h$, where h is the thickness of the slab. This depth is said to correspond to the maximum achieved RH beneath flooring.

The Swedish RH measurement method includes detailed instructions of how to report determined RH levels together with an estimation of the achieved uncertainty. Among others one factor adding to the uncertainty is possible temperature fluctuations. Former standards included such fluctuations with an estimated uncertainty. Logged in-situ measurements performed with certified equipment have shown unexpectedly large disturbances as a consequence of temperature fluctuations. This logging equipment developed to monitor the drying progress in concrete floors described in detail in paper I appendix, has changed the standards to also include temperature logging.

Swedish building industry still lacks an established method to employ on screeded slabs applied with flooring. Drying of screeded floors is besides surrounding climate affected by, i.a.,

- Individual thickness of structural slab and screed
- Internal moisture distribution of the screeded slab
- Moisture related properties, such as sorption isotherms and diffusion properties
- Diffusion properties of the flooring to be installed

This thesis presents a method to estimate moisture redistribution in a screeded concrete slab after the flooring is applied. The outcome is dependent on not only the comprising materials and initial conditions, but also the desorption and scanning isotherms. The method is also applicable on homogenous slabs with consideration taken to scanning. Moisture distribution

and its redistribution are described both qualitatively and quantitatively in chapter 3. The required inputs are described in chapter 4, where moisture properties like sorption isotherms and examples of repeated scanning curves, are shown. In chapter 5 a number of moisture profiles of screeded concrete slabs before and after flooring are shown. The suggested quantitative model has been applied on all these slabs in order to verify the model presented in chapter 3.

2 Theoretical background

2.1 Structure of cement based materials

Concrete may from a structural point of view, be treated as a structure of finite elements assembled together to form a unity. The model resolution is dependent on what experimental data that needs to be explained. Concrete may be treated as a homogenous material when results from moisture transport measurements through concrete are evaluated. Even though moisture has to move through very small pores there is no reason to begin from a pore flow model to reproduce the complete moisture transport through a concrete slab. Moisture transport through one single pore on the other hand definitely requires a finer resolution. Here moisture transport becomes affected by water molecules interacting with pore walls, cohesion forces, surface tension, and adsorbate, even polarity of the water molecules becomes increasingly important.

Fresh concrete made of water, cement and aggregate may be treated as a mixture of two separate phases, solid particles and a cement paste, see figure 1. Solid particles consist of well graded aggregate usually separated into two categories, coarse and fine. The main purpose of aggregate is to work as a filling material, reducing the cement content in the concrete mix. It also serves as a structure for the paste to fix during hardening. The amount of aggregate used depends on the application and workability requirements. Concrete mixes produced for heavy construction may contain coarse large stone aggregate, i.e., dams and bridge foundations. When self leveling properties are required finer aggregate are utilized.

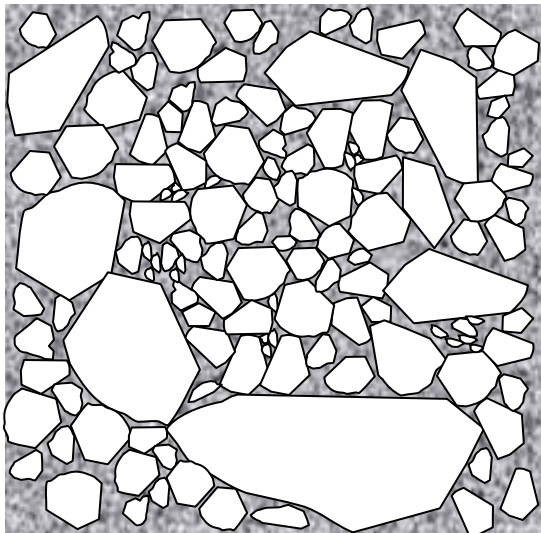


Figure 1. Illustration of concrete divided into two phases, white polygons and shaded area representing aggregate and cement paste respectively.

The cement paste is a mix of water and cement. Many different properties of cement paste and hardened concrete is affected by the mass ratio between water and cement, W/C-ratio. This ratio quantifies the density of cement grains in the cement paste, see figure 2. The W/C-ratio affects pouring related properties important in fresh concrete, i.e. workability, stability and

setting. In the hardened state other properties are affected, i.a., pore size distribution, porosity, permeability, and diffusion coefficients, moisture content in relation to relative humidity, the sorption isotherm.



Figure 2. Illustration of a high water cement ratio to the left and a low water cement ratio to the right. Water, reaction products, CSH-gel, and cement grains are represented by the white area, lighter and darker shaded polygons respectively.

When cement and water are mixed chemical reactions initiate. The reaction occurring when water becomes chemically bound to the crystal structure of cement is called hydration. These reactions are strongly exothermal, which means that energy is released and the temperature increases. At an early stage the hydration rate is high as there are a lot of available unhydrated cement grains surrounded by liquid water. The rate accelerates with the temperature increase and is also influenced by the W/C-ratio, cement composition and the cement fineness. The process slows down when the amount of available water and unhydrated cement decrease. This results in a temperature decrease, eventually leveling with ambient temperature.

Needle shaped reaction products, Calcium-silicate-hydrates, CSH, start growing from the cement grains surfaces instantly after mixing, see figure 3. As they multiply and grow the needles soon bridge the water filled gap between cement grains and aggregate. The CSH-gel connects the solid particles forming a complex fine lattice, the concrete hardens. Needle growth continues as long as the available water volume exceeds about 2 times the volume needed for the reaction product [2]. Eventually the grain becomes completely covered with CSH-gel, which turns into a barrier that diminishes the water supply to the grain core. Cement in the grain core stays unhydrated until additional water diffuses through the barrier. Further core grain hydration takes place at a very low rate as the thickness of the barrier increases.

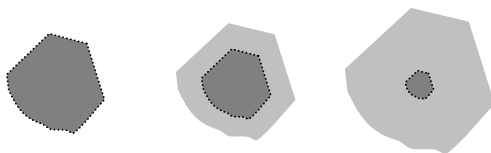


Figure 3. Polygons representing from left to right unhydrated, partly hydrated and almost completely hydrated cement grains. The hydration of a cement grain, the CSH-gel and the unhydrated core are shown as a lighter and darker shaded area respectively.

During hydration water becomes a part of the solid material. This bound water occupies about 75 % of its unbound volume. This reduction of water volume turns into small interconnected air voids in the cement paste, often classified as gel pores and capillary pores the former being smaller [3]. Larger pores originate from the mixing and pouring procedure. These pores altogether forms a system in which a liquid or gas may permeate.

All pores in the CSH-gel are irregular as they are made of needle shaped building blocks, their true shape has not yet been revealed. Many shapes have been presented throughout history in efforts to explain experimental data, one accepted model is the ink-bottle theory [4, 5]. This theory describes the pores as inkbottles with a narrow neck. Pictures taken with electron microscopy bear evidence that pores more likely should be treated as slit pores [6].

Theoretically, a pore may be identified as an empty space able to hold one atom. This definition however becomes impractical as such a small pore size is not measurable. A more practical definition for a pore could be a space able to withhold one or a few water molecules. The size of a free water molecule is about 3.5 Å. Pores in concrete vary in size from nanometers found in the CSH-gel, to centimeters, air voids remaining after pouring and compacting.

Some of these pores are partly filled with water, some are emptied as the water chemically binds in the lattice and some still remain water filled. Among others pore size distribution determines the concretes ability to bind water from the surrounding atmosphere, it also influence capillary suction. A large proportion of small pores increase the binding capacity at low RH-levels. Capillary suction is improved by smaller pore size but to a limited extent. When pores become too small, forces from the walls and flow resistance limits the maximum suction height.

2.2 Moisture fixation in cement based materials

This section presents two types of moisture binding in concrete and cement based screeds, chemical and physical fixation. Moisture becomes chemically fixed in the solid because of the cement/water reactions taking place during hydration. Moisture from residual water, exterior liquid sources, and surrounding air becomes physically fixed on material surfaces and in capillary pores by forces originating from molecular attraction, such as cohesion, adhesion, and adsorption.

In the surrounding air, which is a mixture of different gasses, moisture appears as vapor. The amount of water molecules in air is dependent on environmental conditions. Air above a plane water surface is for example completely saturated, see figure 4, meaning that the maximum water vapor content is reached. The water vapor content is exerting a partial pressure on the air, expressed in Pascal. At atmospheric pressure and temperatures the saturation vapor content is mainly dependent on the temperature.

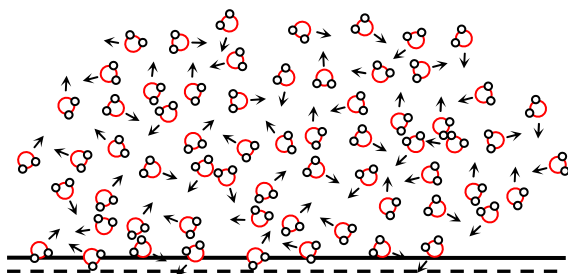


Figure 4. Illustration of water molecules in air moving randomly above a flat water surface.

A practical way of defining the amount of humidity in air is to relate it to the saturation vapor content. This relation is often called the relative humidity, RH, and is expressed as a ratio

between actual and saturation vapor content in percent RH (% RH). A proper definition of the moisture content in air includes both relative humidity and temperature. For example air containing 0.0086 kg/m^3 at $20 \text{ }^\circ\text{C}$ is equal to a relative humidity of 50 % RH at $20 \text{ }^\circ\text{C}$. The relative humidity is calculated using equation 1.

$$RH = \frac{v}{v_s} \quad (1)$$

The vapor content in indoor air is usually limited to about $0.004 - 0.020 \text{ kg/m}^3$. Vapor will condense on material surfaces and become a liquid if the saturation vapor content is exceeded. This limit is called the dew point and is also referred to as the saturation vapor content, e.g. 0.0173 kg/m^3 at $20 \text{ }^\circ\text{C}$ at sea level. The RH level in indoor air has been demonstrated to fluctuate between some 30 - 70 % RH [7]. Higher RH levels are frequently reached on a short time basis for instance in bathrooms when a resident takes a hot shower. RH below 30 % RH is also reached, for example, in hot indoor premises during winter time when the outdoor air moisture content is low.

2.2.1 Chemical moisture fixation

Moisture becomes a part of the solid structure as it reacts chemically with the cement grains. This moisture, referred to as chemically bound moisture, becomes bound to the material by strong ionic bindings as the concrete hardens. It takes a lot of energy or very low vapor pressures to break such bindings. Chemically bound moisture is released gradually as the temperature rises. Investigations on cement paste have shown a release of what is considered to be chemically bound moisture when subjected to increasingly lower RH levels, especially below 10 % RH [8, 9].

Removal of chemically bound moisture has been interpreted as breaking the structural solid. The amount of chemically bound water in concrete is strongly dependent on the amount of cement used in the concrete mix but also on the cement content alone.

Chemically bound moisture is moisture remaining in the sample after applying a particular drying method, various methods generate different results. In this work, water remaining after drying in air at $20 \text{ }^\circ\text{C}$ at 10 % RH has been considered to be chemically bound. This definition agrees well with observed RH levels in indoor premises.

2.2.2 Physical moisture fixation

Physical fixation of moisture vapor on a material surface is linked to the RH in adjacent air. Putting a completely dried well hardened concrete on a balance in humid air and the mass will increase. Water molecules will become attached to it and accumulate on exterior and interior surfaces, see figure 5. The energy surplus exhibited by the dry material surface will decrease as vapor molecules exhibiting energy deficit attach on the surface. This will happen as a result of the chemical potential difference of air borne water molecules and the water molecules attached to a material surface.

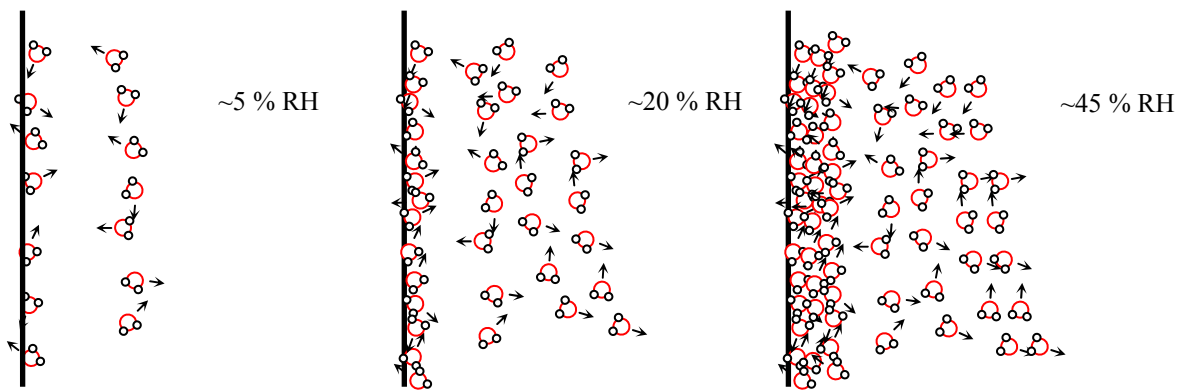


Figure 5. Adsorption of water molecules on a material surface, the adsorbate thickness increases from left to right with an increasing RH level.

Water molecules are merely momentarily attached to the surface on locations called adsorption places. Bindings forming between molecules and surfaces are usually weak hydrogen or van der Waals forces. In contrast to ionic bindings these bindings are easily broken. Molecules continue accumulating on the surface until reaching the lowest possible energy level. This new energy level is called the equilibrium state. At this state an equal amount of molecules attaches to and leaves the surface. As the RH increases further water molecules attach on the surface for a longer time, ultimately forming a thin water film on the surface.

The process when water molecules are accumulating on a surface is called adsorption and the thin film formed is called an adsorbate, see figure 5. The opposite process is called desorption, when water molecules are released from the surface to the dry air.

Porous materials like concrete exhibit both exterior and interior surfaces available to adsorption, e.g. edges and pore wall surfaces. The pore surface area in ordinary concrete is in the range of 20 - 40 m²/g. This comparably large area partly explains porous materials ability to adsorb substantial amounts of moisture compared to solid nonporous materials such as metals. Pure adsorption only includes moisture attaching to the surface as a consequence of chemical potential differences.

As the RH increases further water molecules attach to the adsorbate ultimately generating a more liquid like film on the surface. There are many theories explaining the nature of adsorption and binding forces between adsorbed molecular layers. One example of monolayer adsorption is the Langmuir theory [10], multilayer adsorption theories includes the BET [11] and Dent's to mention two of the theories. Dent's equation shows similarities with adsorption isotherms determined for concrete at a relative humidity below some 45 % RH [3]. In Dent's theory water molecules change their properties as they are absorbed on a surface. Adsorption on dry surfaces is believed to be stronger bound than on surfaces covered with water film. As more molecules become attached the thickness of water film increases, thus gradually decreasing the binding force.

Water surfaces in small pores will curve at the pore walls depending on surface tension forces acting between adsorbed moisture layers and the material. Suddenly at a certain RH a meniscus is created. This meniscus bridges the empty pore space separating the adsorbed

moisture layer, see figure 6 [12]. A hydrophilic, “water loving”, material such as concrete will exhibit concave water menisci. The concavity curvature at the pore wall becomes increasingly important as the pore size decreases, the capillary phenomenon exists at pore sizes between 1.4 nm - 0.1 μm. Below 1.4 nm the tensile strength of water is exceeded [3] therefore menisci are considered as nonexistent below this pore radius.

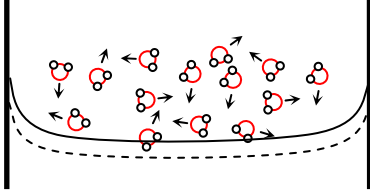


Figure 6. Illustration of water molecules moving above a curved water surface in a small pore in concrete.

Saturation pressure above a concave water surface is less than over a flat surface and also less over a flat surface than over a convex surface. The Young-Laplace equation defines the relationship between the pressure gradient across a closed elastic membrane or liquid film sphere and the surface tension in the membrane or film

$$p_a - p_b = \frac{2\gamma}{r_1 + r_2} \quad (2)$$

where p_a is the internal pressure and p_b is the external pressure, γ , represents the surface tension, and r_1 and r_2 is the radii of curvature. This formula was used by Thomson 1871, to derive an expression of the saturation pressure, p , above a curved surface,

$$p = p_{sat} - \frac{\gamma\rho_v}{\rho_l - \rho_v} \left(\frac{1}{r_1} - \frac{1}{r_2} \right) \quad (3)$$

where p_{sat} is the saturation pressure above a plane water surface, γ is the surface tension, ρ_v is the density of vapor, ρ_l is the density of liquid, r_1 and r_2 are representing the two radii in the principal sections of the surface bonding liquid and vapor, being positive when concave [13]. The original equation notation is changed to the notation used in this thesis.

A more common used form of the Kelvin equation is the familiar expression,

$$\ln\left(\frac{p}{p_{sat}}\right) = \frac{2\gamma V_m}{T \cdot R \cdot r_m} \quad (4)$$

where R is the gas constant, T is the absolute temperature, V_m is the molar volume and r_m is the mean radius of curvature of the meniscus, also known as the Kelvin radius. This means that water molecules in air above a concave curved surface exceeding saturation pressure will condense on the water surface until a new equilibrium is reached, thus enlarging the radius.

The conceived radius is also known as the Kelvin radius. This process when moisture from the air condenses on a curved meniscus is called capillary condensation adding to the already

adsorbed moisture. The capillary condensation phenomenon is believed to exist at RH levels exceeding some 45 % RH; above this level capillary condensation becomes the superior moisture binding mechanism.

The common term used for adsorbed and capillary condensed moisture put together is absorbed moisture. Concrete is able to absorb substantial amounts of moisture, over 100 kg/m³.

Putting a wet well hardened concrete on a balance inside a cabin ventilated with dry air and the mass will decrease. Completely filled pores at the surface will lose water molecules to the air and menisci will develop as a consequence of the dry atmosphere. The forming menisci decrease the hydrostatic pressure and as a consequence air bubbles will spontaneously form inside pores that are larger than the minimum critical stable radius. Water corresponding to the air bubble volume will be transferred to the surface [14]. These menisci will break when the saturation pressure above the concave pore radius defined by the Young-Laplace equation is less than the actual vapor pressure. However, this breaking of the meniscus corresponds to a lower RH level than for creating the menisci. All corresponding pores in connection to the surrounding atmosphere at an equal pore size will in due time release moisture to the air.

A sorption isotherm is a property that defines the mass of physically bound water held in a material with respect to RH at a specific temperature. It expresses the equilibrium moisture content in a material in relation to the corresponding RH. The equilibrium moisture content at a certain RH is higher for a saturated cement based material subjected to drying than for a completely dry material moistened to the same RH. The former process, drying of a saturated material sample, is called desorption and the latter absorption. If a process change occurs, for instance from drying to wetting, the RH increases corresponding to a scanning curve. Such an isotherm, crosses the area between the desorption and absorption isotherm, and has a considerably lower moisture capacity compared to the desorption isotherm. The low moisture capacity means that a comparably low increase in moisture content gives rise to a high RH increase.

The desorption and absorption isotherm branches for a w/c 0.65 concrete at 20 °C is shown in figure 7. These branches are boundaries showing the extremes of the moisture binding capacity in a drying and a wetting mode. For concrete the desorption isotherm is found above the absorption isotherm. Inside this area span by the two sorption isotherms every combination of moisture content and RH is obtainable depending on the preceding moisture history. The area span by the two boundary sorption branches will be referred to as the main boundary loop.

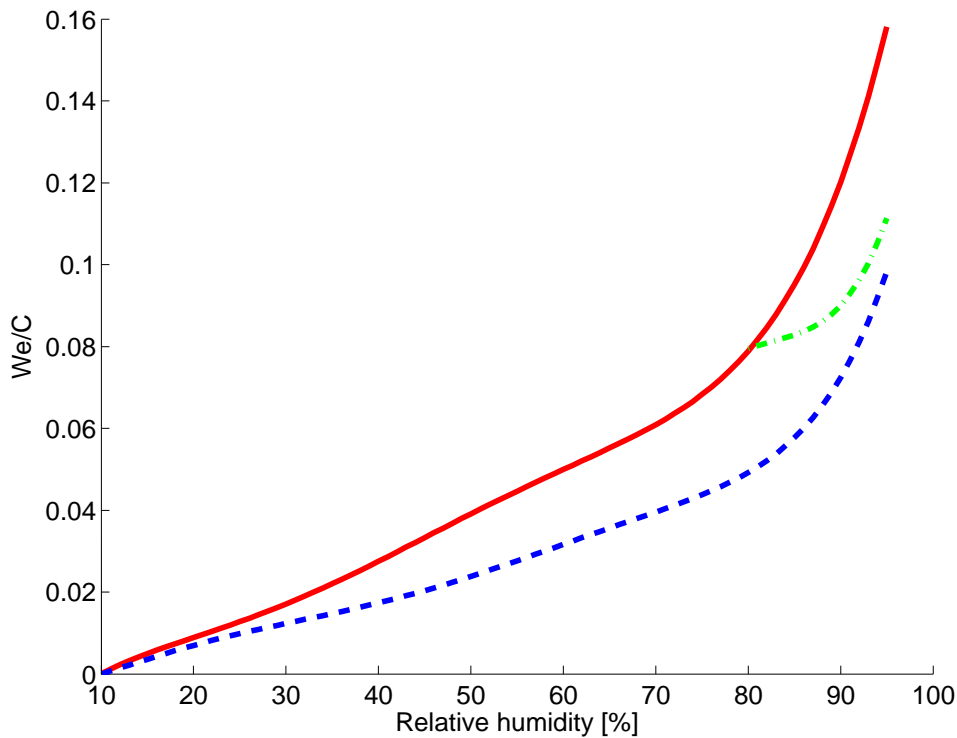


Figure 7. Sorption isotherm of a w/c 0.65 concrete between 10 - 95 % RH, including one absorption scanning curve determined from 80 - 95 % RH. The desorption isotherm is represented by the solid line, absorption scanning curve by the dash dotted line, and the absorption isotherm is represented by the dashed line.

When a material like concrete after initial drying is rewetted at some RH level the increase in RH will give rise to a new isotherm, scanning curve or scanning curve, see dash dotted line in figure 7. The moisture content will increase but at a lower pace compared to the reduction during desorption. The new isotherm will cross the main boundary loop and move toward the absorption isotherm. At first the path is more or less parallel to the x-axis and the moisture content slowly increases.

This slow increase in moisture content is suggested to be a consequence of adsorption occurring on the pore area set free at desorption. As wetting continues the main moisture binding mechanism will gradually change from adsorption on the available pore area to capillary condensation, hence the significant raise at an increasing RH level.

A material showing a desorption isotherm separated from the absorption isotherm is said to exhibit hysteresis. A general definition of the hysteresis phenomenon by Everett [15] states that

‘A process is said to exhibit hysteresis if, when the direction of change of an independent variable x is reversed, a dependent variable Y fails to retrace the values through which it passed in the forward process; the dependent variable “lags behind” in its attempt to follow the changes in the independent variable...’

In other words a material is said to exhibit hysteresis if the moisture content in a material during desorption fails to retrace its values back when absorbing moisture. The moisture content at a certain RH is dependent on the preceding moisture state in a material exhibiting

hysteresis. Cement based materials like concrete usually exhibit hysteresis to a variable degree.

There are a number of theories of why adsorption hysteresis occurs in a porous material like concrete. The classical ink-bottle theory developed from two articles by Kraemer [4] and McBain [5] is one example of a model which explains the hysteresis phenomenon. The ink bottle theory is based on the assumption that the pores are interconnected with varying sizes of radii and have the shape of ink bottles.

One key requirement for adsorption hysteresis to occur is that there is at least one spontaneous irreversible step change when shifting from a drying to a wetting mode. This irreversible step could be ascribed to exist in an open ended cylinder where the building of a meniscus does not happen at the same humidity as for breaking it, see figure 8. This means that the capillary condensation phenomenon on its own is not enough to achieve hysteresis. In a tapering pore, see figure 8, capillary condensation should occur reversibly, as capillary condensation during absorption occurs at the same RH level as it ceases during desorption.

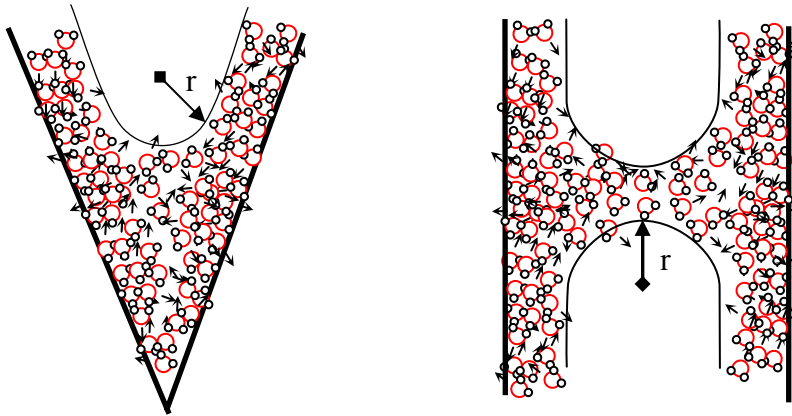


Figure 8. Illustration of a concave meniscus formed in a pore tapering pore and a cylindrical pore as a consequence multiple layers of water molecules and capillary condensation, r is equal to the Kelvin radius.

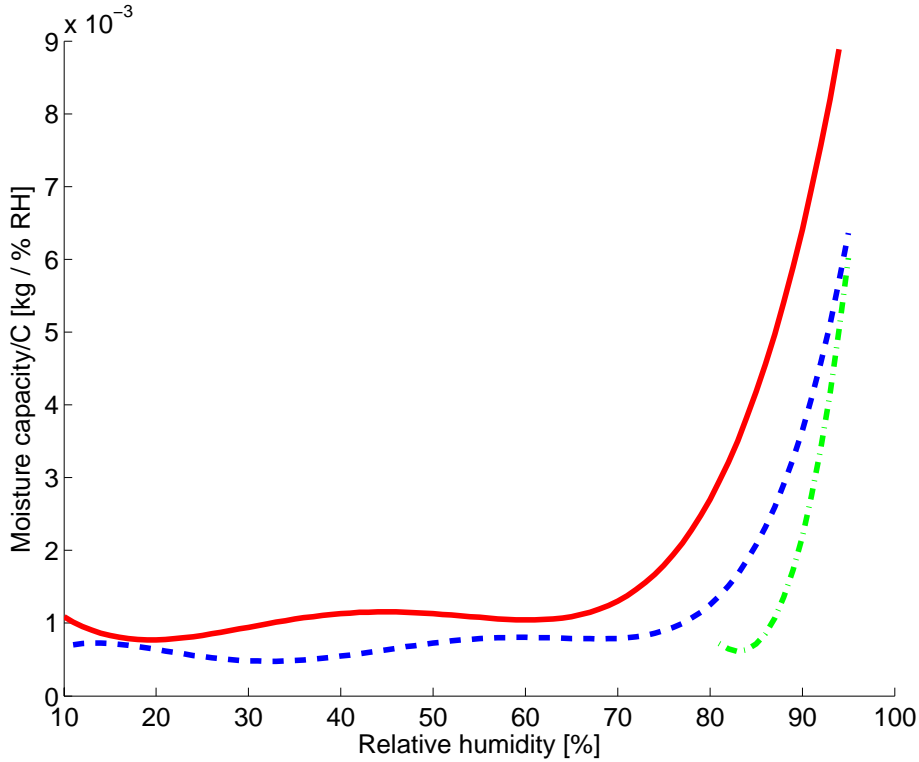


Figure 9. Illustration of the moisture capacity of a w/c 0.65 concrete including the moisture capacity of a scanning curve determined in the 80 - 95 % RH range. The moisture capacity of the desorption isotherm is represented by the solid line, absorption scanning curve by the dash dotted line, and the absorption isotherm by the dashed line.

The moisture capacity for a certain RH is determined by using equation 5,

$$\text{moisture capacity} = \frac{\partial We}{\partial RH} \quad (5)$$

where ∂We represents the difference in evaporable water in kg, ∂RH represents the difference in relative humidity in % RH.

This property shows how much a moisture content change is affecting the achieved RH. Figure 9 shows that a change in RH from 70 - 80 % RH does not change the moisture capacity as much as a change from 80 - 90 % RH does. In other words a steep sloping isotherm gives rise to a high moisture capacity and a gentle sloping isotherm gives rise to a low moisture capacity. This means that small moisture transfers from wet to dry regions in a concrete change the RH level according to the previous history for the moisture receiving region.

2.3 Moisture transport in cement based materials

There are three basic mechanisms governing moisture flow through a material viz capillary suction, diffusion and convection. Moisture flow through a cement based material like concrete is mainly governed by capillary suction and diffusion. Transport of moisture through gas convection, i.e. air, originating from external pressure difference is insignificant in this study.

Diffusion is defined as transport of matter through a fluid, air or liquid, due to differences in chemical potential, both occurring in cement based materials. The chemical potential may be described as concentration differences occurring from unevenly distributed molecules in a confined fluid volume. The molecules eventually become uniformly distributed with time because of diffusion. Such transport is spontaneous and comes from the random motion exhibited by all molecules immersed in a fluid.

The predominant diffusion in concrete takes place as water vapor transferred through air in the communicating pore system. Diffusion of entrained air through water also takes place in partly filled capillaries. Moisture diffusion also exists on a molecular level on the pore walls in the thin layer of adsorbed water molecules; such diffusion is insignificant from a macroscopic perspective.

The rate of diffusion in concrete is dependent on the porosity, moisture content and tortuosity of the concrete. The diffusion rate increases with porosity and decreases with moisture content and tortuosity.

One-dimensional diffusion through a slice of material, see figure 10, is described by Fick's first law.

$$J_v = -\delta_v \frac{\partial v}{\partial x} \quad (6)$$

where, J_v , represents the diffusion moisture flow, δ_v , represents the vapor diffusion coefficient, v , represents the vapor content, and x , represents the depth from surface.

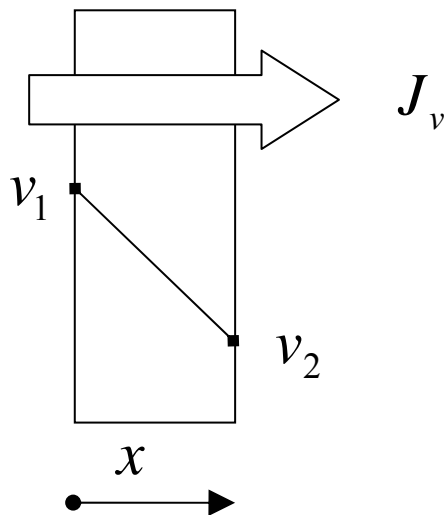


Figure 10. Diffusion through a slice of material governed by a vapor potential difference.

Diffusion through a pore, see figure 11, is limited by the pore area perpendicular to moisture transport. As the vapor pressure increases the accumulating moisture adsorbed on the pore walls reduces the available area and the moisture transport therefore decreases.

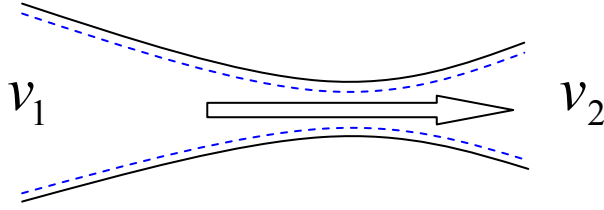


Figure 11. Illustration of diffusion through a pore, solid lines represent pore walls, dotted lines represent adsorbed water molecules, the arrow shows the direction of moisture flow, $v_1 > v_2$.

As the humidity increases further moisture will adsorb on the pore walls until capillary condensation occurs which fills the pore, see figure 12. At this point moisture transport as diffusion through the pore comes to an end. On the other hand, as continuous water paths develop in the pores the moisture flow increases by orders of magnitude due to capillary suction.

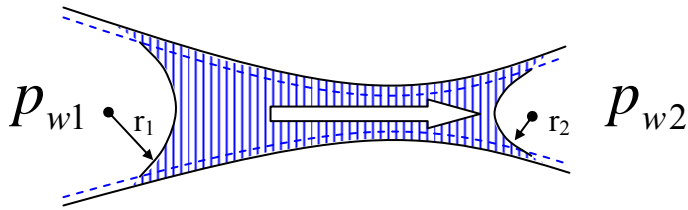


Figure 12. Moisture flow through a filled pore, shaded area represents fluid water, $r_1 > r_2$, flow direction is from p_{w1} to p_{w2} .

One-dimensional moisture flow due to capillary suction in a pore is derived from Poiseuille's equation describing laminar flow between two plates or in this case a cylindrical pore,

$$J_l = -\frac{k_p \cdot \partial p_w}{\eta \cdot \partial x} \quad (7)$$

where J_l represents moisture flow due to pressure differences, k_p represents permeability, p_w represents pore water pressure, η represents viscosity, and x represents the length.

The total flow is a sum of both diffusion and capillary suction given by equation 8.

$$J_{tot} = J_v + J_l \Rightarrow J_{tot} = -\delta_v \frac{\partial v}{\partial x} - \frac{k_p \cdot \partial p_w}{\eta \cdot \partial x} \quad (8)$$

However, it has up to this date not been possible to separate these two moisture flows. Diffusion and capillary suction are therefore usually treated as one, interpreted to one resistance coefficient, called the diffusion coefficient see figure 13.

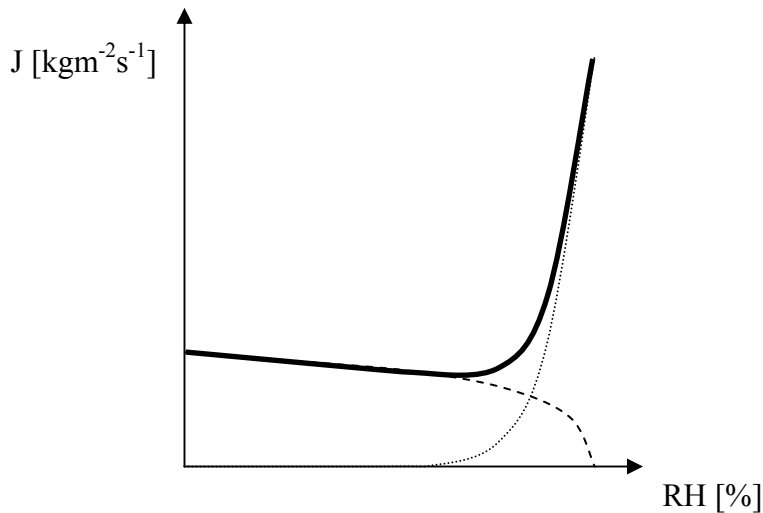


Figure 13. This is an illustration of the moisture flow in relation to relative humidity. The dotted line represents moisture flow as capillary suction, the dashed line diffusion and the thick solid line the total moisture flow.

Irregularities of the pore system are described by the tortuosity factor, see figure 14. The tortuosity factor, τ , indicates the distance a water molecule has to travel to flow through the material, a tortuosity factor of 1 indicating a straight path.

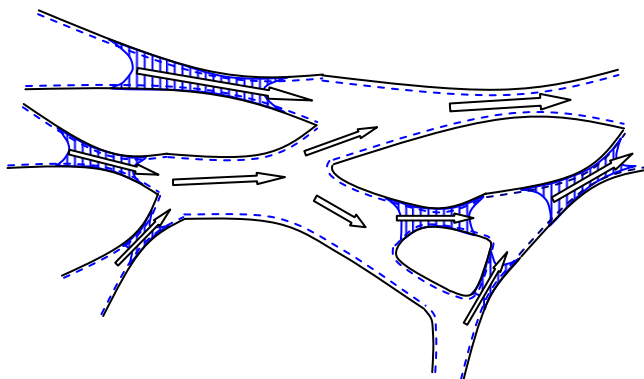


Figure 14. Principal figure of the tortuosity, some pores are filled with water. Solid lines represent pore walls and dashed lines represents adsorbed layer of water molecules. The arrows represent the direction of moisture flow.

3 Models

In this chapter the old model for residual moisture in homogenous slabs is presented in the first section. New models for residual moisture in screeded slabs are presented. The second and third section of this chapter presents a qualitative and quantitative model of moisture redistribution in screeded slabs.

3.1 Previous model

In 1978 a method was developed to determine the future maximum humidity obtained beneath flooring in a drying homogenous concrete slab [1]. This model is based on the assumption that no moisture leaves the slab after flooring, that the slab base is also sealed, and that isothermal conditions are valid. The residual moisture inside a sealed slab will redistribute until the RH level settles on a uniform vertical level, see figure 15.

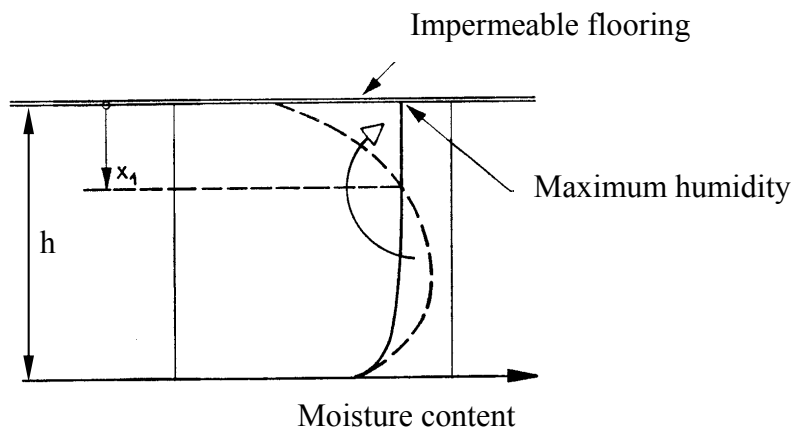


Figure 15. The depth x_1 , at which the RH level prior to flooring, corresponds to the maximum achieved RH level after flooring installation [1].

This method only gives a rough RH estimation as it is based on a computer simulation performed where a homogenous w/c 0.65 concrete slab is subjected to single sided drying. According to this model a standard depth of 0.4 h was decided as an equivalent depth where the humidity level is equal to the maximum RH later achieved beneath the flooring. This relation between RH before and after flooring is based on a computer simulation performed in the late 1970's, where a homogenous 100 mm concrete slab is drying from one side at 20°C and 40 % RH, [1]. Depending on the simulated drying time before flooring the depth from the surface varied between 0.35 and 0.42 of the slab thickness. The simulations are based on the simplification that the RH and moisture content may be described in one single equation. The relationship between RH and moisture content, sorption isotherm, is far more complex.

A sorption isotherm for a single concrete mixture was used in the simulation, without considering hysteresis. This left out hysteresis may have an impact on the estimated RH obtained from the simulation.

The method is not applicable to screeded floors. A new method is therefore needed in order to estimate the maximum humidity in such floors, a common construction today. This method is also applicable on homogenous floor slab constructions and is an improvement to the current

model. In the next section moisture redistribution is described qualitatively. In section 3.3 a proposed quantitative model is described.

3.2 Qualitative model

In this section a qualitative model is presented which describes the RH distribution for a two material combination, e.g., a screeded concrete slab. Three distinctive phases, drying of slab, screed application and drying, and Redistribution after flooring, illustrate important stages from a moisture distribution perspective in the production of a screeded floor. These phases are presented together with a corresponding sorption isotherm in figure 16.

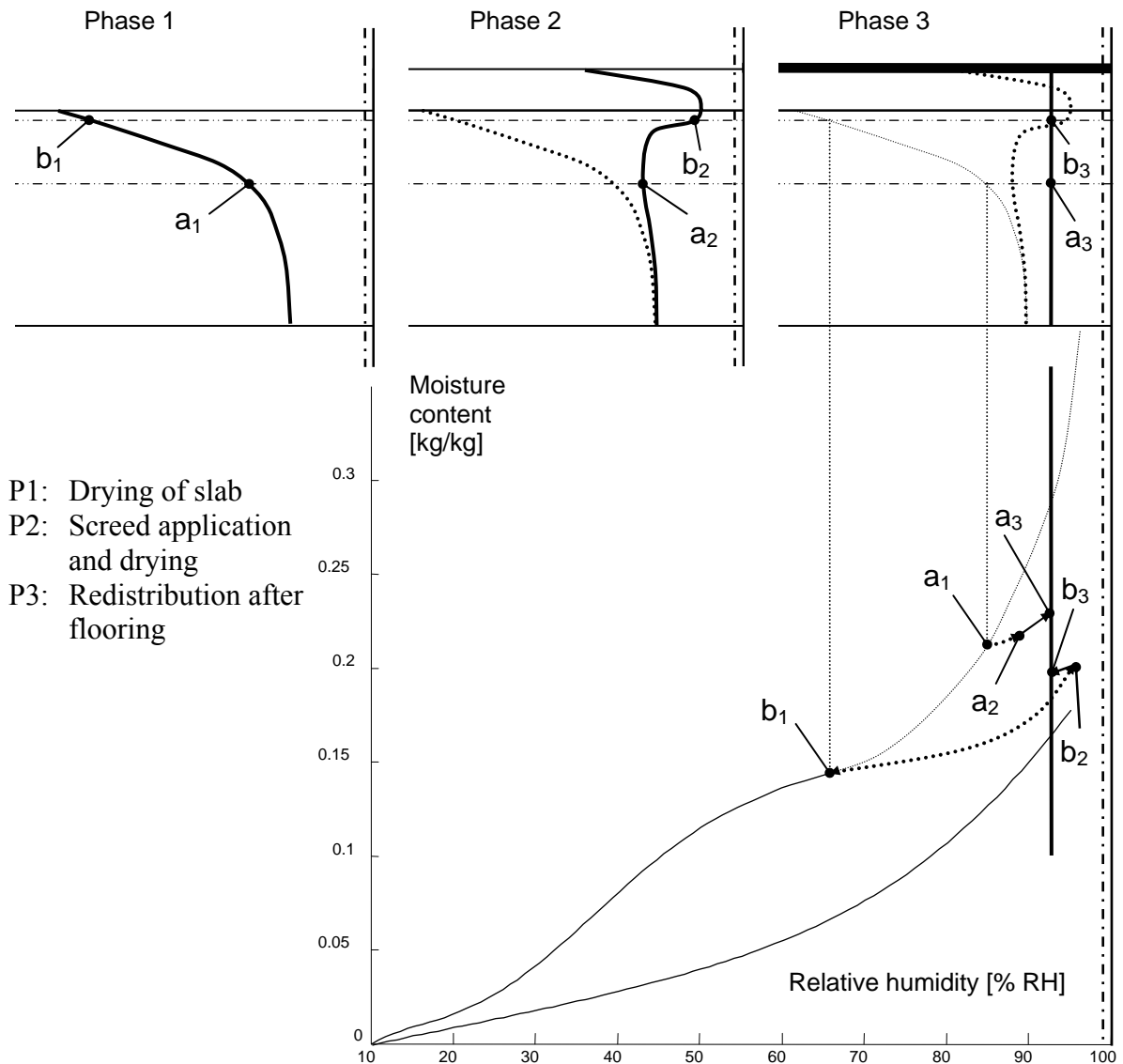


Figure 16. Phase 1 shows the distribution of residual moisture in a concrete slab. A wet screed is applied in phase 2 and subjected to drying, and finally moisture redistributes after flooring. Underneath a typical sorption isotherm is shown where a_i and b_i indicate two material sections and index indicates the corresponding phase number.

The slab represents a homogenous slab sealed at the base drying upward. Thick dotted lines show the starting moisture distribution in each phase and solid thick lines represent the moisture distribution just before entering the next phase. The moisture distribution in phase 1 is included as a thin dotted line in phase 3 to facilitate comprehending of the overall moisture redistribution changes and corresponding changes in the sorption isotherm. These changes are indicated for two slab sections, a_{1-3} and b_{1-3} , which are particularly interesting from a moisture redistribution perspective.

In the first phase a single sided drying concrete slab is shown, the moisture distribution clearly demonstrates a high slab base humidity and a lower slab surface humidity. A wet screed is applied on the semi dry concrete slab in the second phase. This wet screed dries through the top surface simultaneously moisture penetrates through the slab top. Later, some of the moisture redistributes toward the slab base. In addition the screed top dries as shown before leaving the second phase. Finally, the third phase shows the moisture distribution when leaving phase 2, and after flooring when internal moisture redistribution is completed.

In figure 16 letters (a) and (b) represent material sections where moisture content follows a particular path in the typical sorption isotherm diagram displayed in the same figure. Letter (a) corresponds to a section somewhat above the slab center. In the first phase the moisture content decreases, following the desorption isotherm down to point a_1 . Subsequently, after screed application, this section's moisture content increases, following an absorption scanning curve up to point a_2 and finishes at point a_3 . Letter (b) illustrates a material section where the moisture content decreases to point b_1 , following the desorption isotherm. In phase 2 the moisture content increases by following an absorption scanning curve up to point b_2 and finally decreases finishing at point b_3 by following a desorption scanning curve.

3.3 Quantitative model

A theoretical model is proposed, that suggests how to estimate the future moisture distribution in a screeded slab occurring after flooring is applied. The following simplifications are made:

- no further drying of the slab will occur
- isothermal conditions
- moisture transport is not considered
- residual moisture at the time of flooring becomes equally distributed through the slab

If a screeded slab is sealed the residual moisture will redistribute ultimately attaining a uniform vertical RH distribution, RH_{∞} , see figure 17. The moisture content change in each section is given provided each section's moisture history, RH change, and moisture capacity are known. As the moisture content will be maintained in the sealed slab it is possible to calculate the uniform RH level. This is done by adding all sections' change of moisture content. As no moisture is lost this sum is zero. The solution to this problem is obtained by iteration.

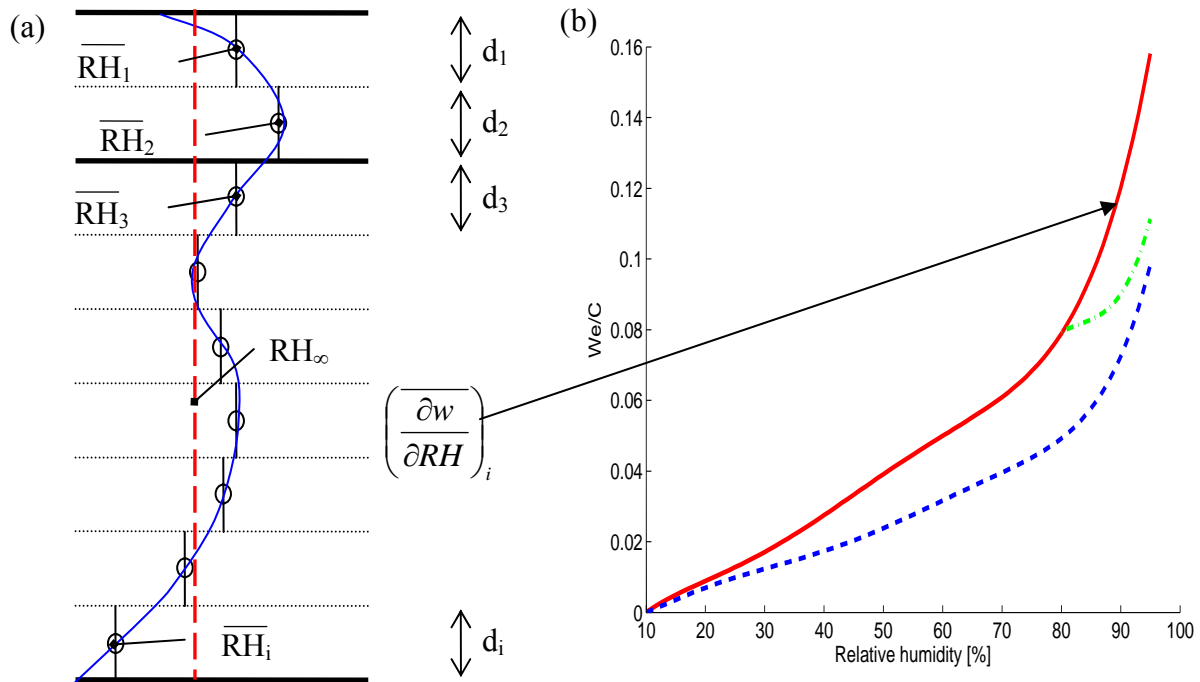


Figure 17. (a) Illustration of the RH distribution, solid line, in a screeded slab before flooring. The dashed line illustrates a possible uniform RH distribution after sealing. Illustration (b) shows a typical sorption isotherm including one scanning curve.

Based on the assumption that no moisture will escape from the screeded slab, the uniform RH level will settle somewhere in between the extremes of the RH distribution prior to sealing. A reasonable initial guess would end up in the midpoint of the two extremes. Next step will be to determine the moisture history of each section in order to assign a realistic moisture capacity.

Judging from the qualitative model both the slab base and screed sections have only experienced drying prior to flooring. Therefore they must be assumed to have reached their moisture content and corresponding RH level by following the desorption isotherm. Top slab sections, on the other hand, have experienced both drying and wetting prior to flooring, thus obtaining their moisture content and RH level by following a scanning curve. The above qualitative analysis is of great importance when determining the future redistribution of moisture.

The future moisture content in each section is determined from the preceding drying-wetting history as well as expected moisture gains or losses to adjacent sections in the future. If a section following a desorption isotherm will lose moisture to attain the guessed RH level its moisture capacity will be determined from the desorption isotherm. If on the other hand a section follows the desorption isotherm and suddenly starts to gain moisture, the moisture capacity is obtained from a scanning curve. And finally, sections already following an absorption scanning curve will in the future either continue to follow the absorption scanning curve or if losing moisture following a scanning desorption isotherm.

Applying the assumption about no further drying, the moisture content of the screeded slabs, per square meter, is constant before and after the flooring.

The above reasoning taken together with the above simplifications could be interpreted to an arithmetic expression equation 9,

$$\sum_{\Delta x_i} (\overline{RH}_i - RH_\infty) \cdot d_i \cdot \left(\frac{\partial w}{\partial RH} \right)_i = 0 \quad (9)$$

where \overline{RH}_i [% RH] represents the average RH level determined in segment d_i [m]

w [kg/m³] represents the section's moisture content,

$\left(\frac{\partial w}{\partial RH} \right)_i$ [kg/(m³ % RH)] represents the average moisture capacity of section d_i

obtained from the sorption (scanning) isotherm at current RH.

Equation 9 shows the change in moisture content with respect to each section's change from \overline{RH}_i to RH_∞ . As the slab is assumed sealed no moisture is lost, thus the sum of all sections moisture content changes is 0 (zero). By rearranging equation 9, equation 10 is obtained.

$$\sum_{\Delta x_i} \overline{RH}_i \cdot d_i \cdot \left(\frac{\partial w}{\partial RH} \right)_i - \sum_{\Delta x_i} RH_\infty \cdot d_i \cdot \left(\frac{\partial w}{\partial RH} \right)_i = 0 \quad (10)$$

or

$$\sum_{\Delta x_i} \overline{RH}_i \cdot d_i \cdot \left(\frac{\partial w}{\partial RH} \right)_i = \sum_{\Delta x_i} RH_\infty \cdot d_i \cdot \left(\frac{\partial w}{\partial RH} \right)_i \quad (11)$$

As the uniform RH, RH_∞ , is constant throughout the slab it may be moved outside the summation mark.

$$\sum_{\Delta x_i} \overline{RH}_i \cdot d_i \cdot \left(\frac{\partial w}{\partial RH} \right)_i = RH_\infty \sum_{\Delta x_i} d_i \cdot \left(\frac{\partial w}{\partial RH} \right)_i \quad (12)$$

Finally the sum of left side of equation 12 is divided by the sum of section thickness multiplied by moisture capacity leaving the uniform RH, RH_∞ , alone on the right side resulting in equation 13.

$$RH_\infty = \frac{\sum_{\Delta x_i} \overline{RH}_i \cdot d_i \cdot \left(\frac{\partial w}{\partial RH} \right)_i}{\sum_{\Delta x_i} d_i \cdot \left(\frac{\partial w}{\partial RH} \right)_i} \quad (13)$$

The resulting RH_∞ is thereafter compared to the initial guess. If the difference is large then a new calculation needs to be performed by replacing the initially guessed RH_∞ with the resulting RH_∞ as the moisture capacities for each section changes accordingly.

4 Experimental

In this chapter the performed experimental works are presented. The manufacturing of a number of screeded floor slabs and different materials used in this work is presented in section 4.1. The sorption measurements used to determine sorption isotherms of the used materials is described in section 4.2 including results obtained from the performed measurements. Two methods to determine both absorption and consecutive desorption scanning curves, a comparison between the two and results from used methods are presented in section 4.3. Finally, section 4.4 presents a method to evaluate moisture transport properties together with obtained results from measurements performed on the some of the used materials.

4.1 General description of experimental works

The conducted experimental works has followed two basic courses. First of all, test specimens in three batches were manufactured aiming to replicate the essential character of three common screeded concrete floor constructions. Secondly the material properties were investigated on samples continuously extracted from the floor constructions in order to seize possible property transformations.

Batch 1 was intended to replicate a homogenous slab on ground, Batch 2, a level separating floor construction, and finally Batch 3 an end point hollow core slab. These batches were produced in full scale regarding thickness, covering an area of 0.5 - 1 m², see figure 18.



Figure 18. Left picture shows one floor construction in batch 1 prepared for screed application, one corner was spared for sample extraction. Right picture shows four floor constructions from batch 2 vertically tilted in climate conditioned room not yet covered with screed.

In total nine concrete floor slabs were produced in this research. Eight homogenous slabs were manufactured at the laboratory and one hollow core slab was delivered from a factory. The homogenous slabs were prepared to reproduce two different screed application scenarios, application on a slab subjected to a short period of drying and application on a slab subjected to a longer period of drying. The hollow core slab was prepared to reproduce a situation, where a centre hollow core is filled with concrete at the slab end prior to screed and flooring application.

Four cement based materials were used to manufacture the screeded slabs, see table 1. The homogenous structural slabs were manufactured by using a w/c 0.65 concrete, C. Cement mortar w/c 0.55, M, and Floor 4310 Fibre Flow, SFC were used for screed application. Both

- 4 Experimental -

the concrete and mortar was mixed and poured at the laboratory. The flooring compound was delivered as a dry power mix from the factory. Water was added to the dry powder and mixed in the laboratory according to instructions from the manufacturer. Finally, the hollow core slab was manufactured in a factory by using a w/c 0.4 concrete, C_{HCS} .

Table 1. Mixture for each used material. Quantities are presented in kg/m³.

Material	C	M	C_{HCS}^*	SFC[*]
w/c ratio	0.65	0.55	0.4	
CEM II/A-LL 42,5 R	250	400		
CEM I 52,5 R			390	
Portland Cement				1-5
Aluminous cement				5-20
Gypsum				2 -10
Water	162	220	147	20
Dolomite 0.002-0.1 mm				31
Sand 0.1-1 mm				47
Sand 0-8 mm	976	1672	973	
Sand 6-13 mm			851	
Sand 8-12 mm	489			
Gravel 8-16 mm	489			
Polymer				1-5
P30			1.2	
Glenium 51	1.5	2.9		

* Mixture according to manufacturer mass-% of dry powder, density~1900 kg/m³

All slabs were subjected to certain drying times in suitable climate rooms before and after screed application. Then a PVC flooring, 2 mm Tarkett Eminent, was installed all nine slabs by using an adhesive, CascoProff Solid. Material combinations and application sequences are described in detail in table 2.

Table 2. Slab material combination, application sequence, and drying plan.

Batch No.	1				2				3
	1	2	3	4	5	6	7	8	9
Material	C	C	C	C	C	C	C	C	C_{HCS}
1 st Drying [days]	105	105	110	110	9	11	408	408	28 ¹
Screed	SFC	SFC	M	M	M	SFC	M	SFC	SFC
2 nd Drying [days]	48	96	98	90	261	259	40	40	138
Adhesive [m ² /l]	3.6	3.6	3.5	4.3	3.1	3.0	3.3	3.0	3.0
Flooring	PVC	PVC	PVC	PVC	PVC	PVC	PVC	PVC	PVC
Redistr.[days]	206	158	149	157	269	269	91	91	273

¹ Initial drying time of the C filling of the mid core, the HCS is cast approx. 60 days earlier.

The humidity distribution was determined in each slab prior to floor application on samples obtained by using a core drill, see figure 19. Subsequent to floor installation the slabs were put back into the climate room. The moisture distribution was determined once more after a certain time of moisture redistribution, see table 2. These moisture distributions are shown in chapter 5. A detailed description of slab preparation, material application and used climate conditions is found in paper IV, appendix.



Figure 19. The remaining hole from \varnothing 90 mm core drill, after extracting samples to moisture distribution determination before flooring. Drilling was performed from the top in a homogenous slab from Batch 1. Note the clear breaking zone separating the mortar screed from the concrete material.

4.2 Sorption measurements

Several sorption measurements were performed on a number of small material samples, 20 - 100 mg, which were obtained from the floor constructions. All but two material samples were chiseled out from the material top surface at a depth of about 20 - 25 mm. The two other samples were taken from 200 mm depth of one of the concrete slabs. To avoid carbonated material 10 - 15 mm of the surface material was cut off. The samples were mainly removed from material subjected to a certain drying time in a 60 % RH at a temperature of 20 °C. Details of the sorption isotherm evaluation are presented in paper III together with results.

A gravimetric vapor sorption balance, DVS, was used for all sorption isotherm determinations. Its key component is a balance, Cahn D-200 that continuously determines the mass of a sample subjected to a sequence of well defined constant or variable RH levels. These RH levels are generated from a mixture of dry and saturated nitrogen gas. The generated humid gas stream is split in two before one half passes the reference and the other passes the sample pan. In order to achieve stable conditions the balance is installed inside a climate controlled cabinet. For a detailed description of the sorption balance see paper II, appendix.

Desorption, absorption and scanning curves were determined by changing the RH in the sorption balance stepwise in a certain sequence. The measurements always started with a saturated specimen. Typical RH sequences are shown in figure 20 and 21. The difference between the two sequences is the RH-changing during scanning where drying is followed by wetting or wetting is followed by drying. In figure 20 it is done with a gradual RH-change with time. In figure 21 it is done stepwise.

- 4 Experimental -

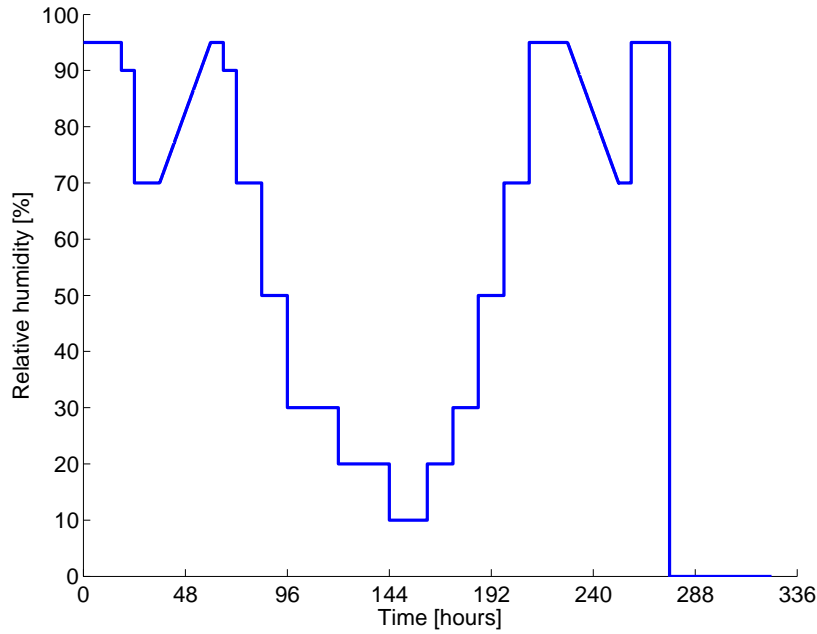


Figure 20. Illustration of a typical RH test sequence used in paper III, where an absorption and desorption scanning curve is determined by using a linearly increasing and decreasing RH.

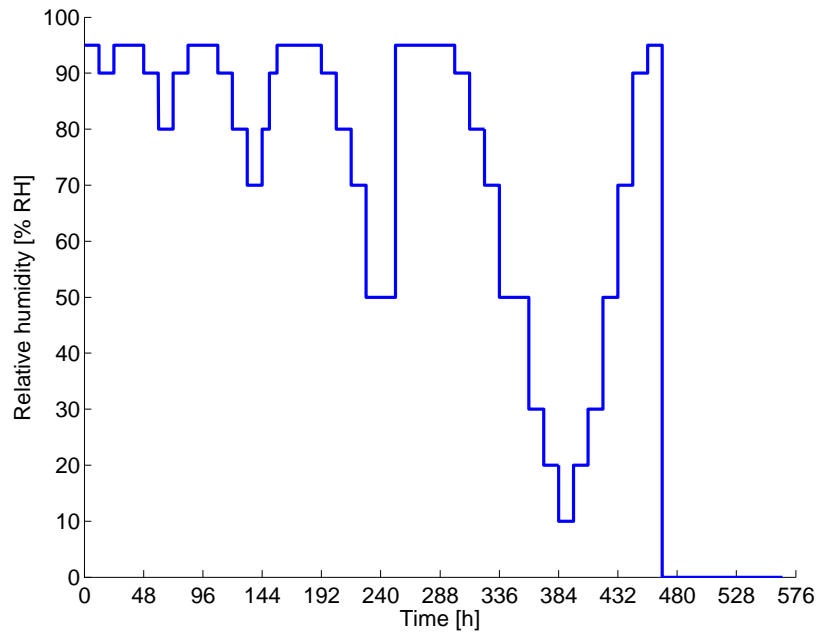


Figure 21. Illustration showing a typical test cycle for determining the boundary sorption isotherm loop including inner scanning curve loops by using the most recent method, where RH step changes are used, instead of linearly increasing/decreasing RH.

Each sample was put on a saturated piece of cloth inside a sealed glass container minimum 24 hours prior to the test, in order to become capillary saturated. Subsequently it was loaded into the sorption balance and subjected to the test sequence.

In order to obtain the asymptotic mass corresponding to each RH level, see figure 22, each RH step was evaluated by curve fitting according to equation 14,

$$m(t) = m_f - (m_f - m_0)e^{-k(t-t_0)} \quad (14)$$

where $m(t)$ represents the sample mass at the time t , m_0 is the initial mass for each curve fitting, m_f represents the asymptotic final mass, k is a curve fitting constant and t_0 is the initial time for each curve fitting. The best fitting curve was obtained by the least squares method. This curve fitting is further explained in paper III, appendix. Note that the sample was not subjected to 0 % RH until the final step of each test sequence, see figure 20 and 21. This arrangement of the 0 % RH step was decided based on the hypothesis that chemical moisture may be released at RH levels below 10 % RH, thus destroying the material structure, see section 2.2.1. The dry mass was therefore obtained from the curve fitted asymptotic mass at 10 % RH.

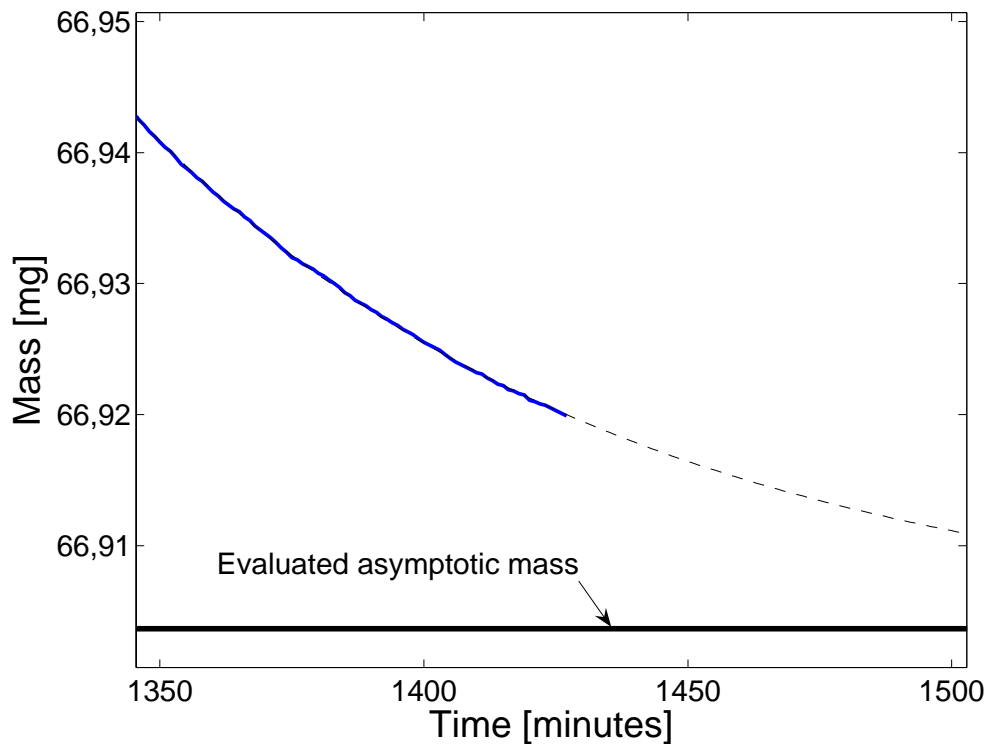


Figure 22. Curve fitting of the recorded mass in an RH step to determine the asymptotic final mass for each RH step.

Sorption isotherms were determined for four different materials, two concretes, C and C_{HCS} , cement mortar M, and one flooring compound, SFC. The moisture content is quantified as the evaporable moisture content, w_e , divided by cement content, C, for material C, C_{HCS} , and M. The cement content was estimated by first quantifying the Ca content in each C, M, and C_{HCS} sample. This was accomplished by using inductively coupled plasma atom emission spectroscopy, ICP-AES, for a detailed description see paper III, appendix. For material SFC the moisture content per mass of material is represented as a fraction of mass at 10 % RH.

Desorption and absorption isotherms for the four materials are shown in figures 23 – 27, where the results in paper III are compared with data for new samples. For concrete C

different sorption isotherms were obtained depending on the depth where the sample originated. The other materials showed a smaller deviation.

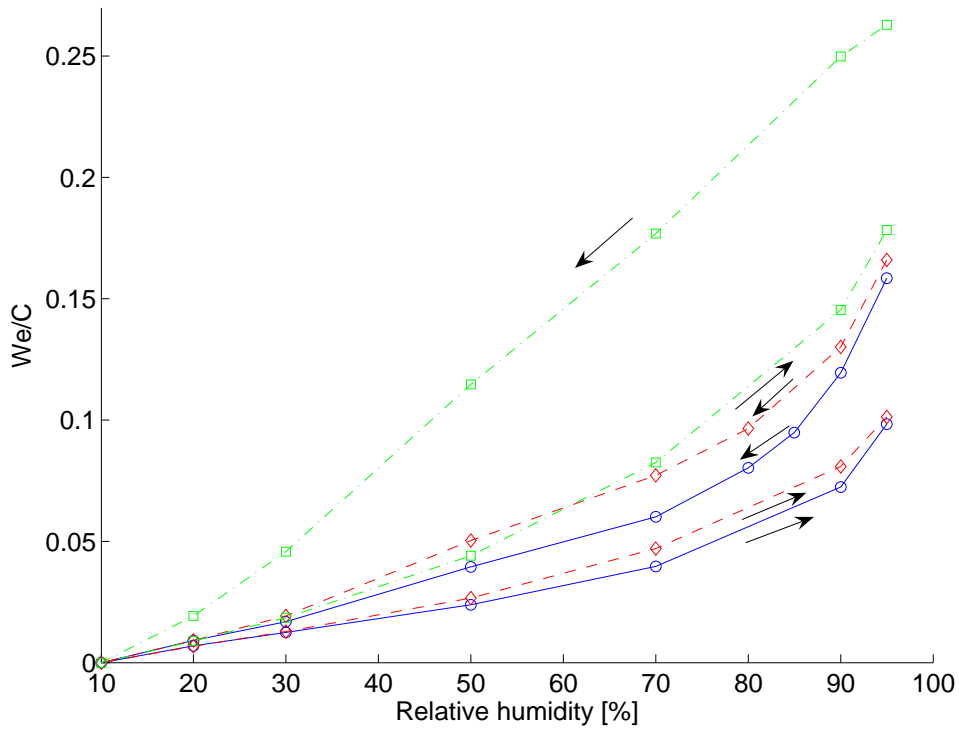


Figure 23. Sorption isotherms determined for three samples of material C. One sample, 16 months old, represented by the dash dotted line is removed from the upper corner edge part of a slab about 2 cm from the surface facing air. The other two samples, 9 and 12 months old, are removed from central parts 2 cm from the base surface.

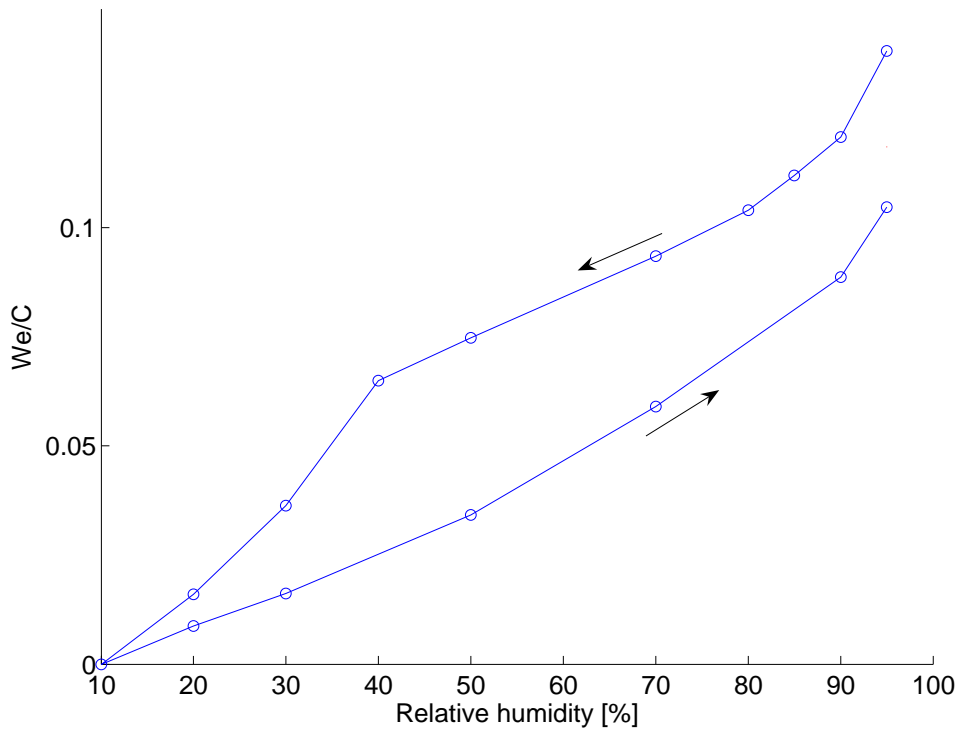


Figure 24. Sorption isotherm determined for one sample of material C_{HCS} .

- 4 Experimental -

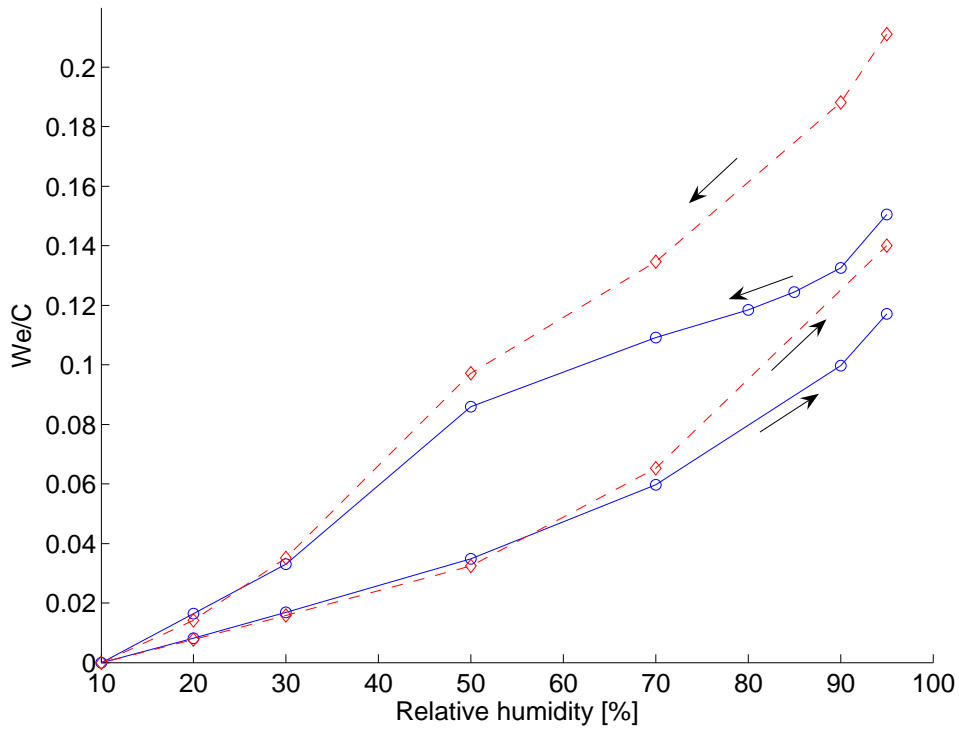


Figure 25. Sorption isotherms determined for two samples of material M, w/c 0.55 cement mortar. The dashed line represents a sample subjected to drying for 1 month in 60 % RH and the solid line 12 months of drying at the same conditions.

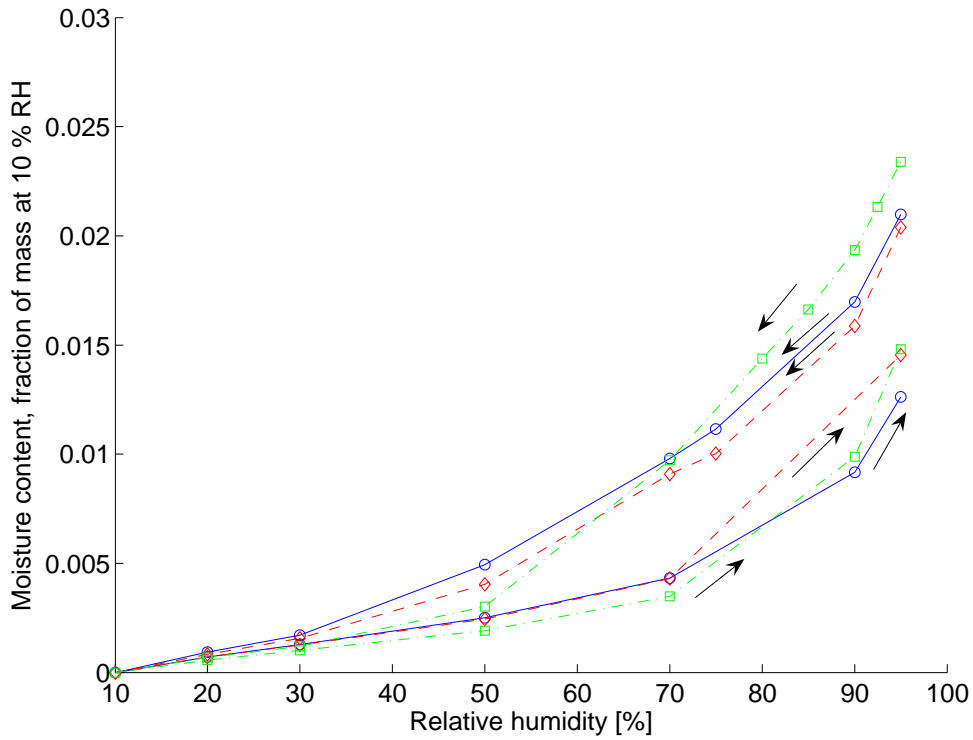


Figure 26. Sorption isotherms determined for three samples of material SFC, Floor 4310 Fibre Flow.

4.3 Scanning curves

In each of the first test series, two scanning curves were obtained by two sections of linearly increasing/decreasing RH, ramp, one commencing from the desorption isotherm and the other from the absorption isotherm. This method was previously used for determining scanning curves for self leveling flooring compounds [16]. The RH level was kept constant for a certain time before and after the scanning determination sequence, in order to achieve sample mass equilibrium. However, as equilibrium, in a strict sense, was not obtained from the prior RH level no matter how long RH was kept constant, the scanning ramp initially became disturbed by a mass loss/gain, see figure 27.

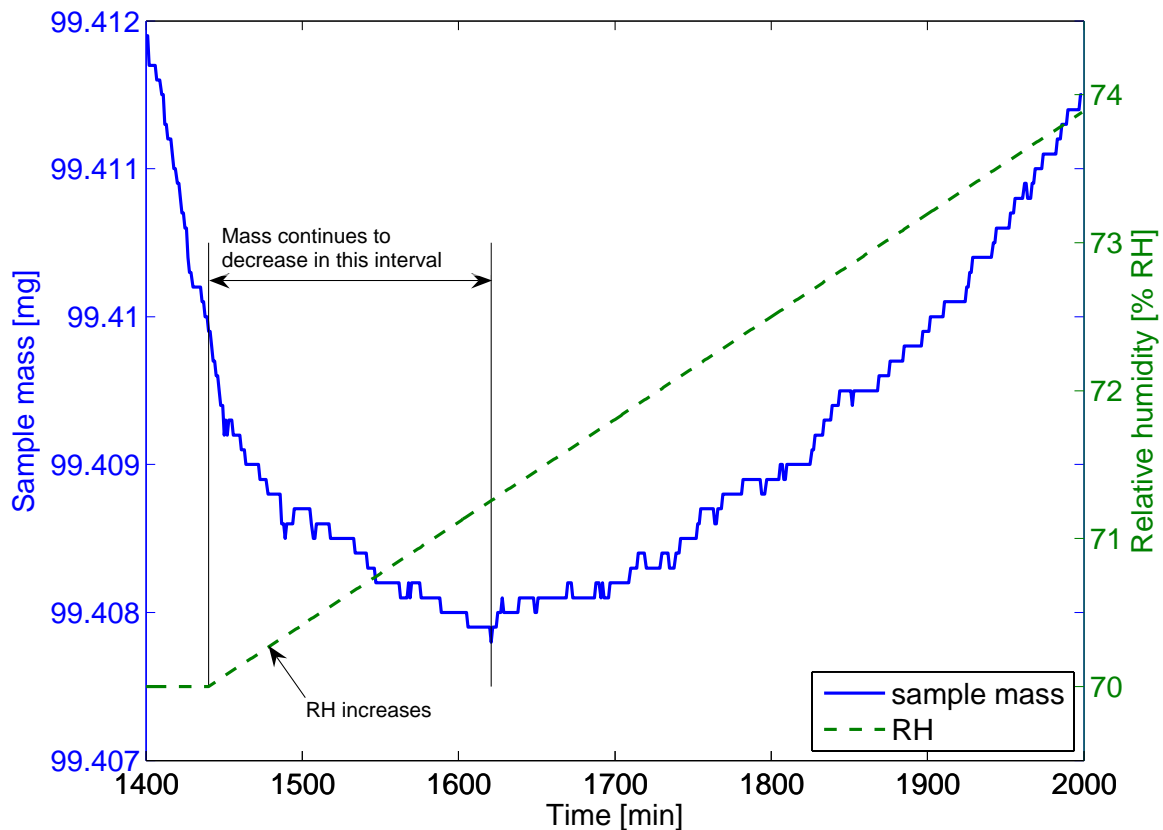


Figure 27. Equilibrium is not obtained before the RH ramp starts at 1440 min and 70 % RH.

In figure 27 the x-axis represents time in minutes, the left hand y-axis represents sample mass in mg and the right hand y-axis represents RH in % RH. As can be seen in figure 27 the sample mass, solid line, still decreases beyond 1440 minutes, even though the generated RH increases, dashed line. Therefore a time lag effect was achieved. In addition, the achieved error increased even more as the curve fitted asymptotic mass was used.

This effect was compensated by linearly super imposing the achieved difference between the recorded and asymptotic mass thereby reducing the error. Unfortunately, it was not feasible to apply curve fitting according to equation 14 on scanning sections determined from a linearly increasing/decreasing RH. Instead a calculation was performed to compensate the obtained time lag effect, by linearly superimposing the achieved difference between recorded and

asymptotic mass. The curve fitting method, time lag compensation, and obtained sorption isotherms are presented in detail in paper III, appendix.

The test sequence for scanning curve determination was modified by inserting a step wise RH change before the gradual RH change see figure 28. In this way it was possible to compare a scanning curve evaluated by using equation 15 with a scanning curve obtained by using the time lag compensation evaluation.

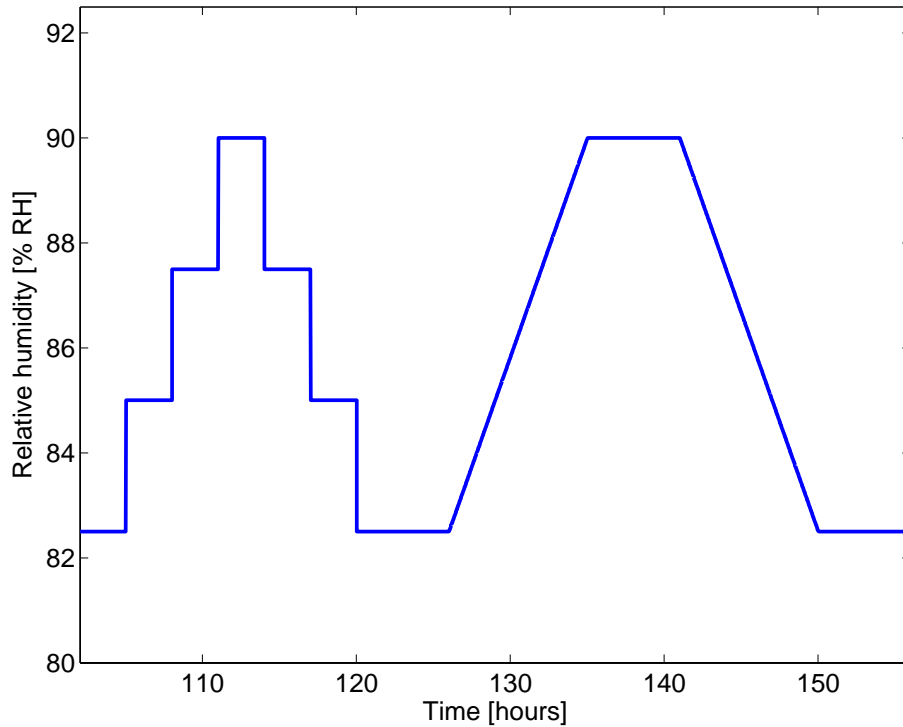


Figure 28. Detail of test sequence for comparing one scanning curve obtained by stepwise RH-changes with a scanning curve obtained by gradual RH-changes.

Results from this investigation clearly show that the scanning curve slope increases faster by using the stepwise RH-changing method, see figure 29. The scanning curve obtained by using the recorded sample mass, dashed line, contain less moisture compared to the scanning curve obtained by using the time lag compensation, solid line. In turn, the scanning curve obtained from stepwise changing the ramp, dash dotted line, contains more moisture compared to the time compensated scanning curve obtained from the ramp.

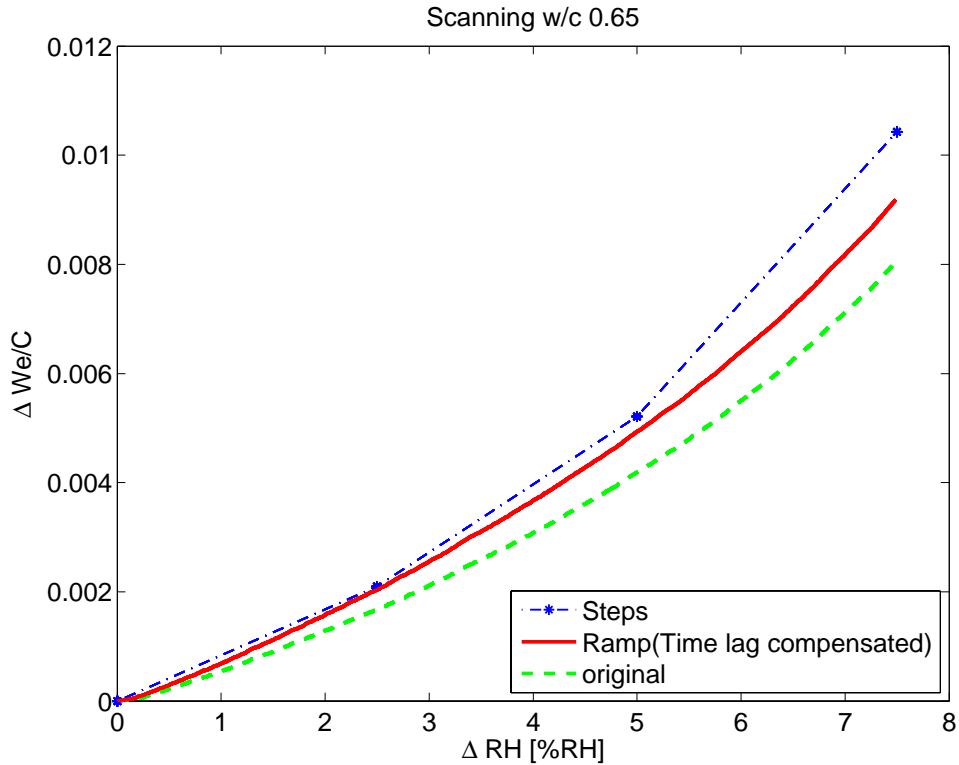


Figure 29. A comparison of the absorption scanning curves determined by using original data, a gradual RH-change (time lag compensated), and a stepwise RH-change, dashed, solid, and dash dotted line respectively. The point of origin represent the starting points at the desorption isotherm where scanning starts.

In order to decrease possible remaining time lag effects, the previous method was further developed in the later test series. By substituting the RH ramps in the test sequence with a sequence of small discrete RH steps potential time lag effects were minimized see figure 21 in the previous section. Thus the attained scanning curves were less affected by the non existing equilibrium caused by earlier RH steps.

These new set of scanning curves were solely starting from the desorption isotherm. In addition, the scanning absorption curves were directly followed by a desorption scanning curve, thus forming a small loop inside the main boundary loop. This approach was chosen, as such a sequence of moisture changes may occur in a concrete slab top surface when a screed is applied.

Figure 30 gives an example that illustrates where the different scanning curves are located in reference to the sorption isotherm.

- 4 Experimental -

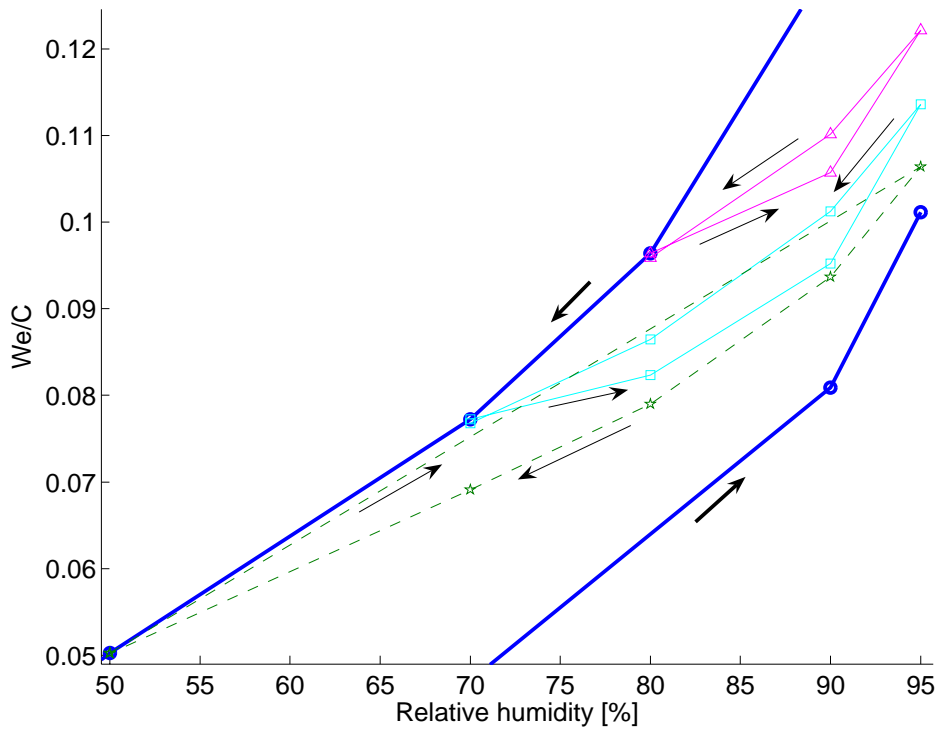
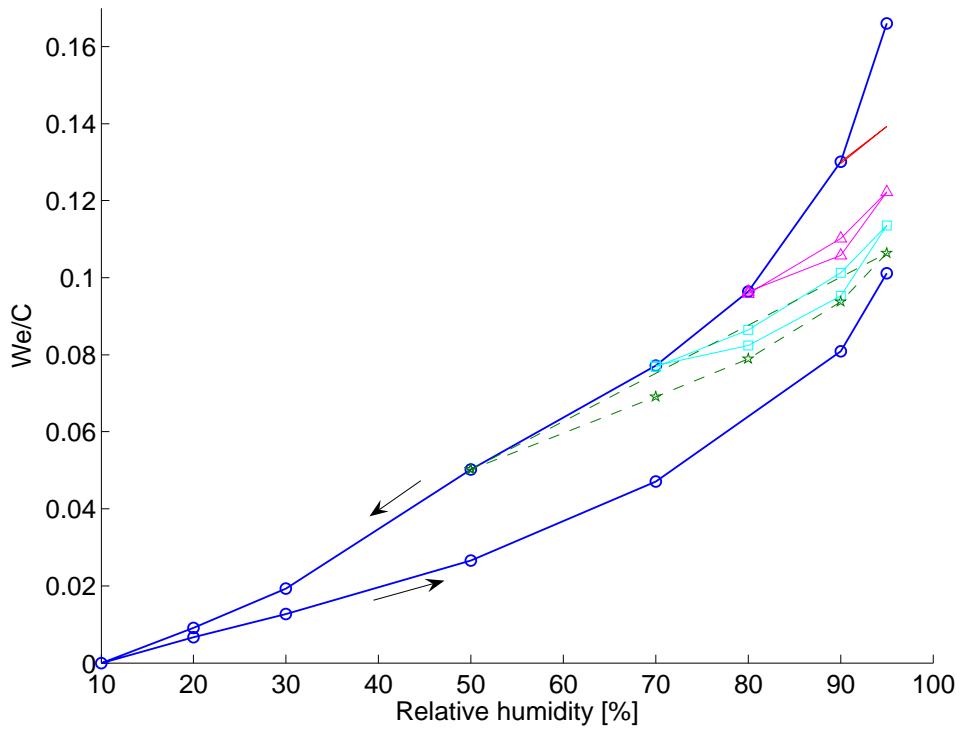


Figure 30. The top diagram shows the absorption and desorption isotherm of a w/c 0.65 concrete including a number of sequential scanning curves starting at different RH, 90, 80 and 70 % RH. This sample is taken 20 mm from the slab base. The bottom diagram shows a detail of the achieved scanning curves where arrows indicate if absorption or desorption scanning are determined.

4.3.1 Absorption scanning curves

To be able to show the scanning curves in detail, curves for different starting points on the desorption isotherm have been combined into one diagram from the starting point at the desorption isotherm.

Figures 31 - 34, display absorption scanning curves starting from RH_0 on the desorption isotherm for each separate material. Curves marked $RH_0 = 82.5$ are not “pure” absorption scanning curves. Originally they started scanning at 80 % RH, but experienced a number of inner absorption/desorption scanning cycles before starting at 82.5 % RH, inner scanning.

The x-axis in figures 31 - 34, represents the change in RH. The y-axis in figures 31 - 33, represents the change in We/C , in figure 34, the y-axis represents the change in moisture content. The starting point of each scanning curve is indicated as RH_0 at the end of each displayed absorption scanning curve, line markers indicate the determined $\Delta We/C$ with reference to the starting point. The dashed line in figure 31 suggests an estimated absorption scanning curve beginning from 50 % RH, since the moisture content was not determined on intermediate RH steps.

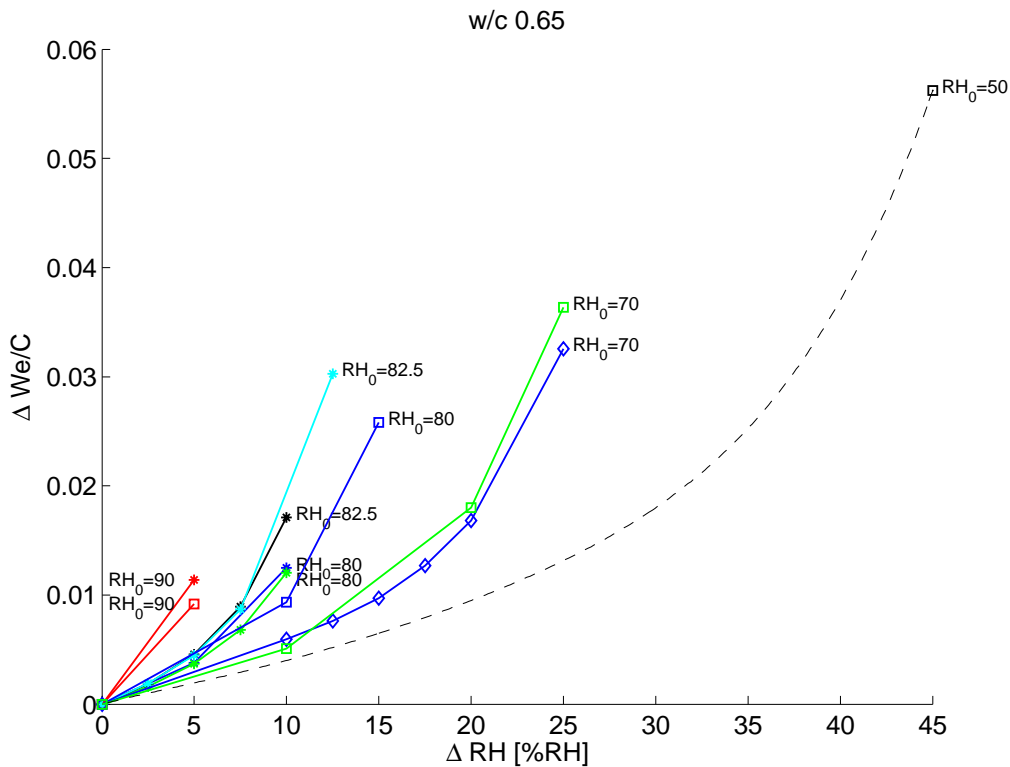


Figure 31. Absorption scanning curves for three samples of w/c 0.65 concrete, material C, expressed as changes of We/C and RH from the starting point RH_0 of the desorption isotherm. The three line markers stars, squares, and diamonds represent three separate samples.

- 4 Experimental -

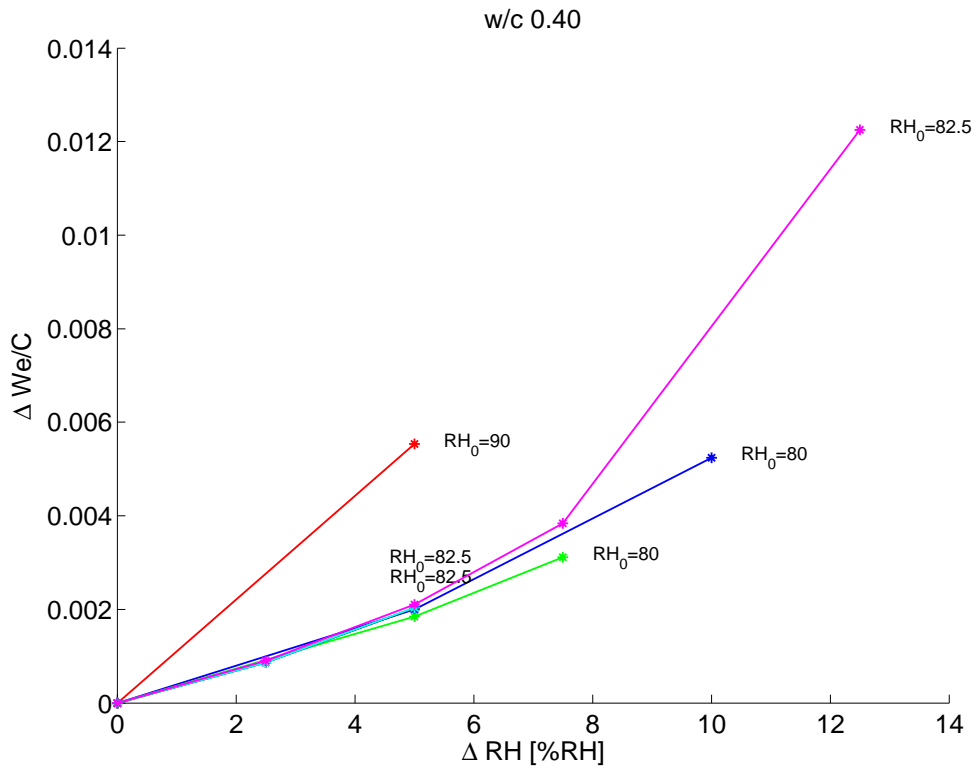


Figure 32. Absorption scanning curves determined for one sample of w/c 0.40 concrete, material C_{HCS} .

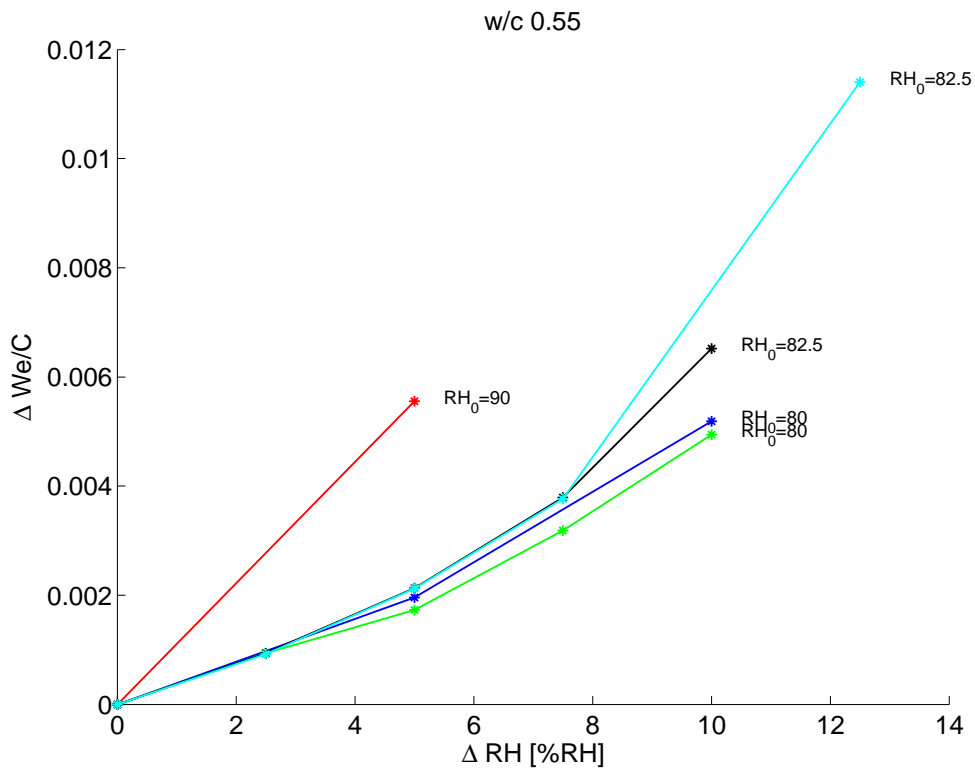


Figure 33. Absorption scanning curves determined for one sample of w/c 0.55 cement mortar, material M.

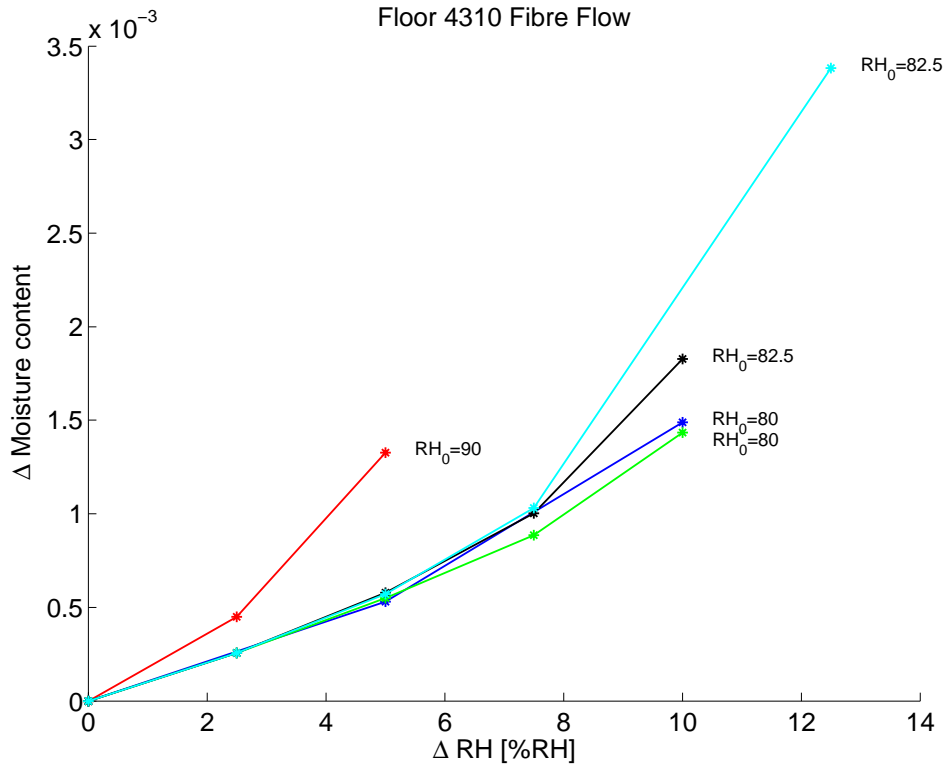


Figure 34. Absorption scanning curves determined for one sample of Floor 4310 Fibre Flow, material SFC.

There is a clear relationship between the achieved absorption scanning curves and the starting point on the desorption isotherm. The slope of an absorption scanning curve starting at a lower RH increases at a lower rate than a slope starting from a higher RH level. In addition the spread of the achieved absorption scanning curves spread is low.

The absorption scanning curves achieved at a starting point of 90 % RH appear to be linear, in figures 31 - 33. Such results were obtained since the moisture content was not determined for intermediate RH levels.

4.3.2 Desorption scanning curves

Desorption scanning curves are shown in a similar way as the absorption isotherm with the starting point of the absorption scanning curve as a common reference.

Figures 35 - 38, display desorption scanning curves starting from the end point of a prior absorption scanning curve. The x-axis in figures 35 - 38, represents the change in RH. The y-axis in figures 35 - 37, represents the change in We/C, in figure 38, the y-axis represents the change in moisture content. RH_0 defines the starting point on the preceding absorption scanning curve, line markers indicate the obtained $\Delta We/C$.

- 4 Experimental -

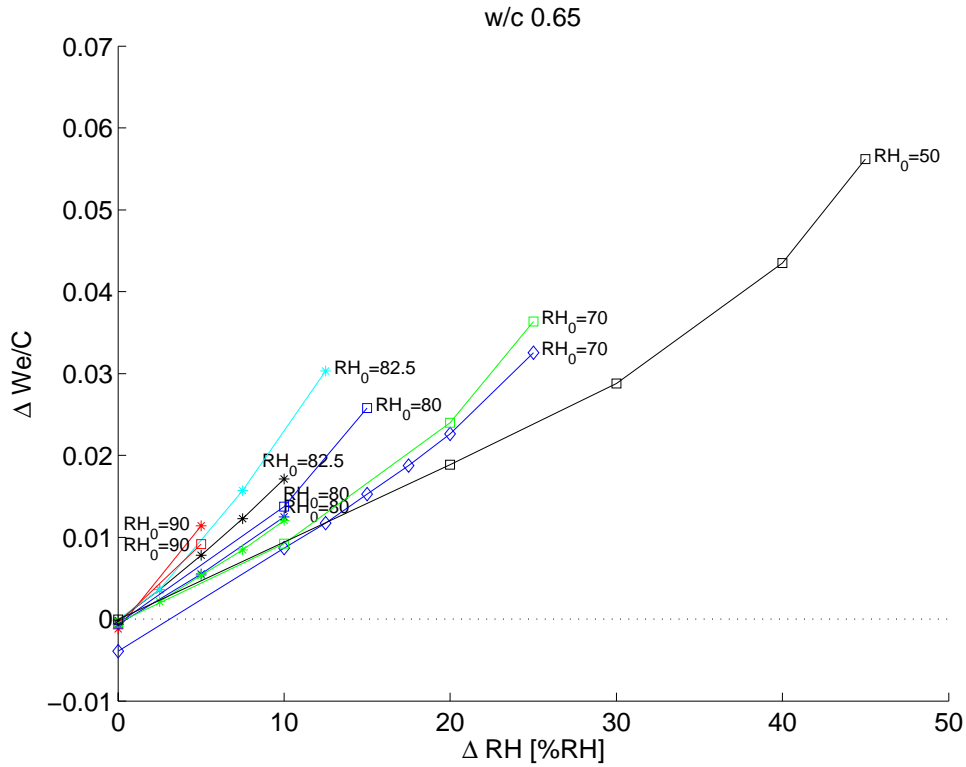


Figure 35. Desorption scanning curves starting from the absorption scanning curve for w/c 0.65 concrete, material C, expressed as changes of We/C and RH from the starting point RH_0 of the absorption scanning curve.

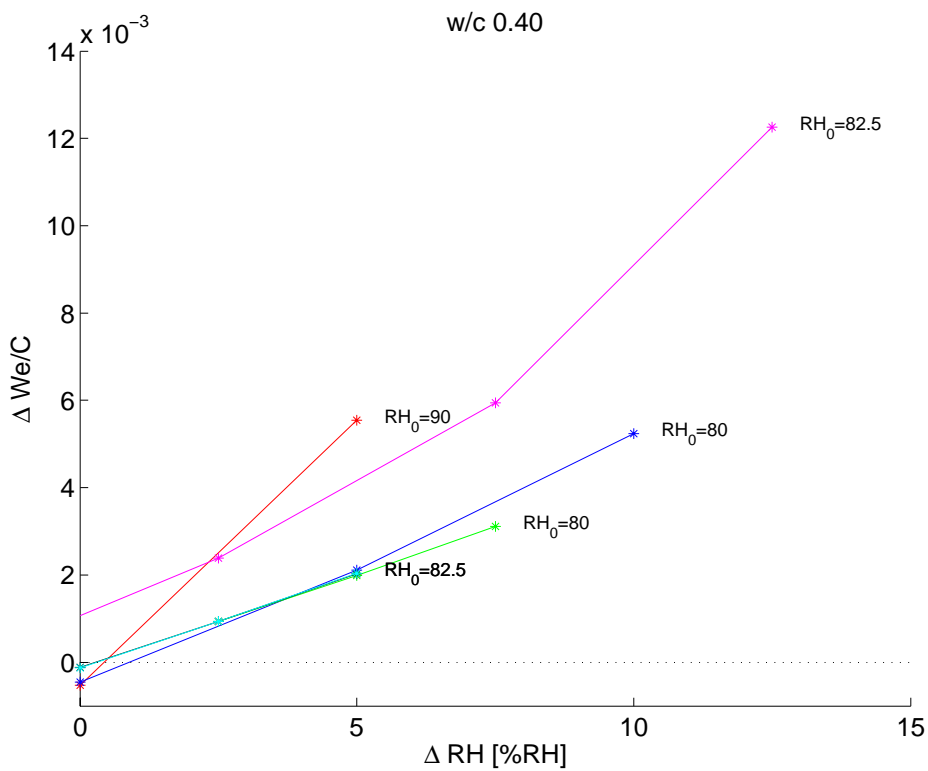


Figure 36. Desorption scanning curves starting from the absorption scanning curve for w/c 0.40 concrete, material C_{HCS} .

- 4 Experimental -

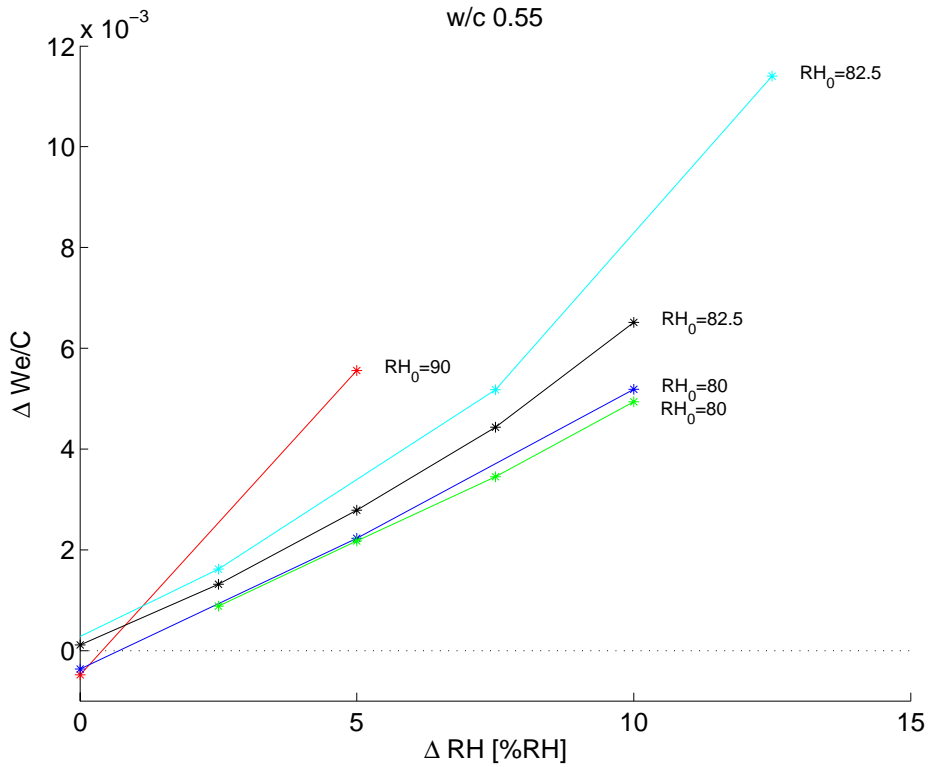


Figure 37. Desorption scanning curve starting from the absorption scanning curve for w/c 0.55 cement mortar, material M.

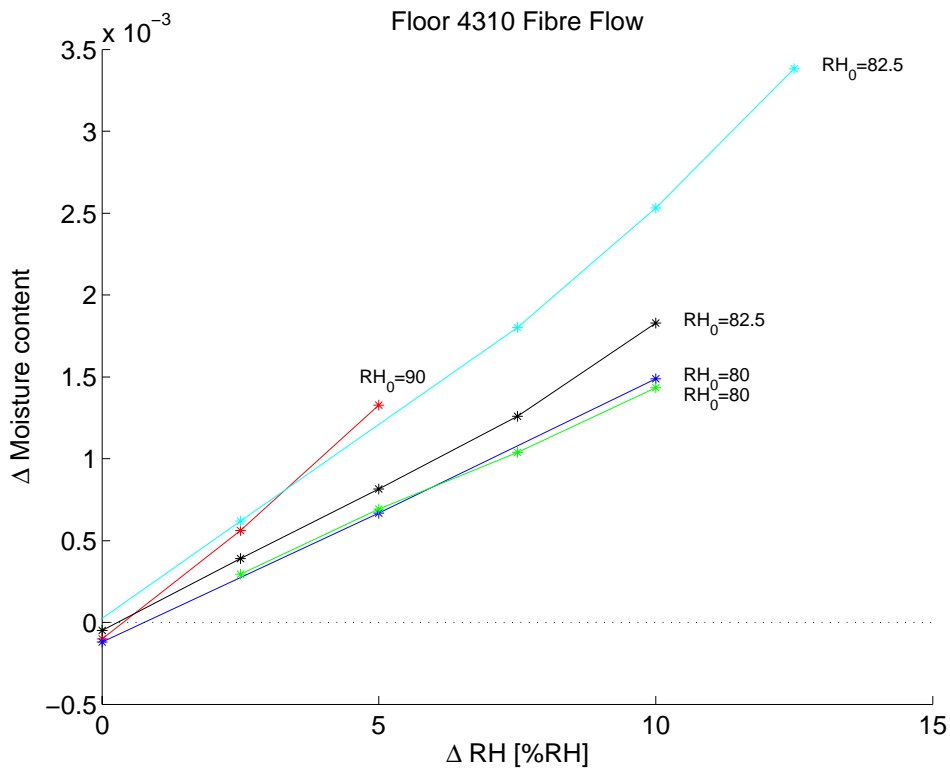


Figure 38. Desorption scanning curve starting from the absorption scanning curve for Floor 4310 Fibre Flow, material SFC.

The determined desorption scanning curves clearly show that they are dependent on the starting point RH, RH_0 . In addition the larger part of the desorption scanning curve

approximately ends on the starting point. This suggests that an absorption scanning curve taking off from the desorption isotherm at a particular moisture content returns to the starting point thus closing the loop. The path back is dependent on where the absorption ends and desorption starts. The above may imply that if a complete saturation would occur when absorbing moisture, then the desorption scanning curve would follow the desorption isotherm when returning to the starting point provided no change in material characteristics, i.a., hydration would occur throughout the saturation procedure.

4.4 Moisture transport properties

Moisture redistribution through a screeded concrete slab is slow. Therefore it may take a long time to reach a complete redistribution. When flooring is applied early on a humid screed, thus achieving an uneven moisture distribution, the model may underestimate the actual humidity obtained beneath the flooring, because the “local” redistribution in the screed is much faster than the over all redistribution in the whole slab. To be able to quantify these effects moisture transport properties must be known. However, such considerations was not included the quantitative model described in chapter 3. Measurements on moisture transport coefficients were determined in order to illustrate possible differences of the used materials and to be used if such considerations should be included in future model development.

Moisture transport coefficients were determined for C, M, SFC, and coated plywood by using the cup method. This method is based on moisture loss determinations performed on closed impermeable vessels, where the top is “sealed” with the investigated semi-permeable material. The cup is stored in a climate room where the surrounding climate is kept constant at 55 % RH and 20 °C.

A small container of saturated salt solution is put inside the vessel, see figure 39. The mass of each vessel is determined on a calibrated balance, hence monitoring the expected mass loss. Several humidity levels may be achieved inside the vessel by using a number of different salt solutions. In this study maximum five different salt solutions were used to generate a specific RH at 20 °C [17], see table 3.

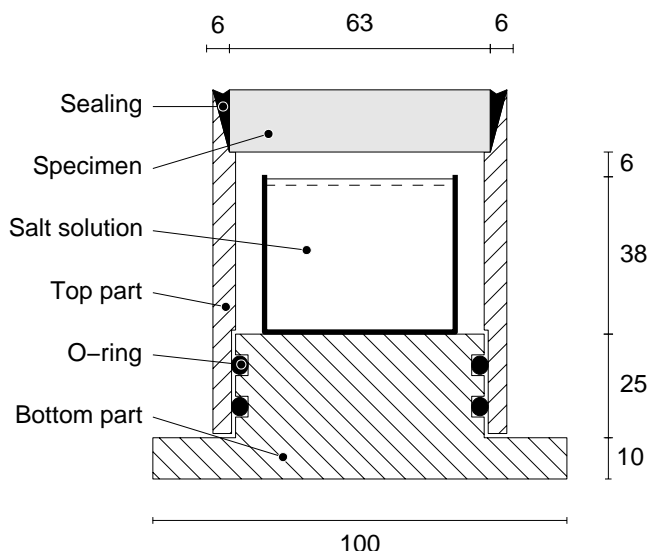


Figure 39. Illustration from [18] displaying the cup used to determine diffusion coefficients on material C, M, SFC and coated plywood. Figures in mm.

Table 3. Five different salt solutions and deionised water and corresponding generated RH.

Salt solution	NaBr	NaCl	KCl	KNO ₃	K ₂ SO ₄	H ₂ O
RH [% RH at 20 °C] ¹	59.1	75.1	85.1	94.6	97.6	100

Cylindrical samples of w/c 0.65 concrete, w/c 0.55 cement mortar, and Floor 4310 Fibre Flow, were extracted from Batch 1 by using a water lubricated core drill. These cores were subdivided into 13 - 20 mm thick discs by using a wet saw, in order to separate screed from concrete material and to obtain smooth specimen surfaces. Mean diffusion coefficients for w/c 0.65 concrete were determined by using four to nine discs per each salt solution. Mean diffusion coefficients for the two screeds were determined by using one to two discs per each salt solution.

The mean diffusion coefficients for plywood were determined on three discs per each salt solution. Mean flows were calculated and used to calculate the air layer between the salt solution surface and the base of the specimen, thus achieving the actual boundary RH. The final evaluation of average diffusion coefficients were performed by using a method described in [18].

Diffusion coefficients for the flooring material, Tarkett Eminent, were determined on one sample per each RH level, by using glass cups with a larger diameter, 183 mm, to reduce possible edge effects.

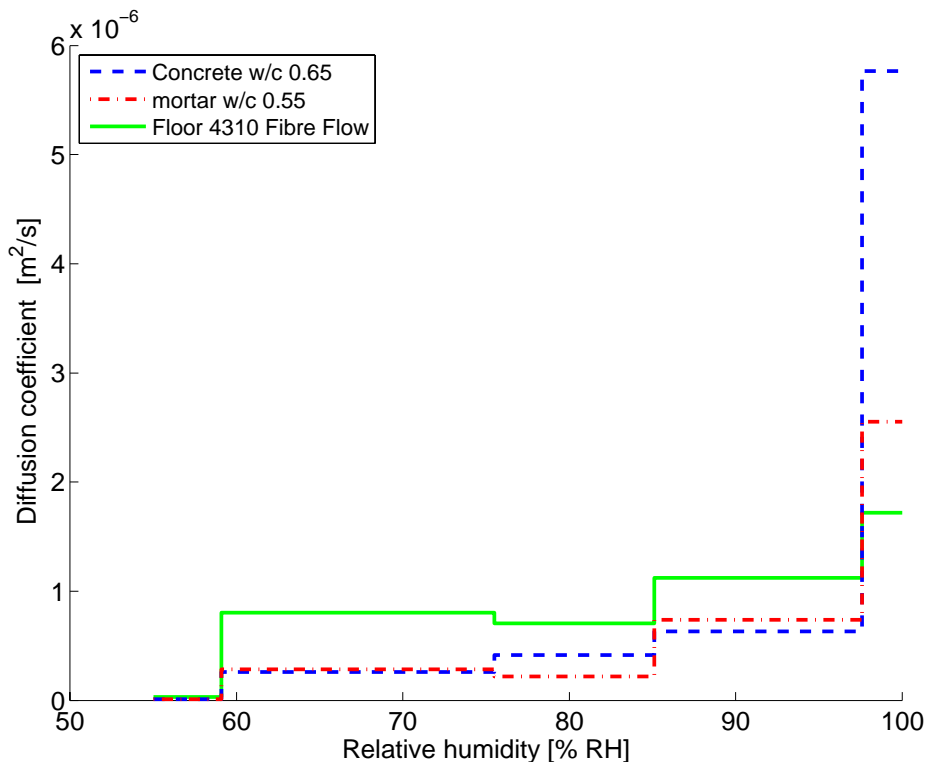


Figure 40. Mean diffusion coefficient of material, C, w/c 0.65 concrete, M, w/c 0.55 cement mortar, and SFC, Floor 4310 Fibre Flow. The diffusion coefficient was determined in the interval 55 - 100 % RH.

- 4 Experimental -

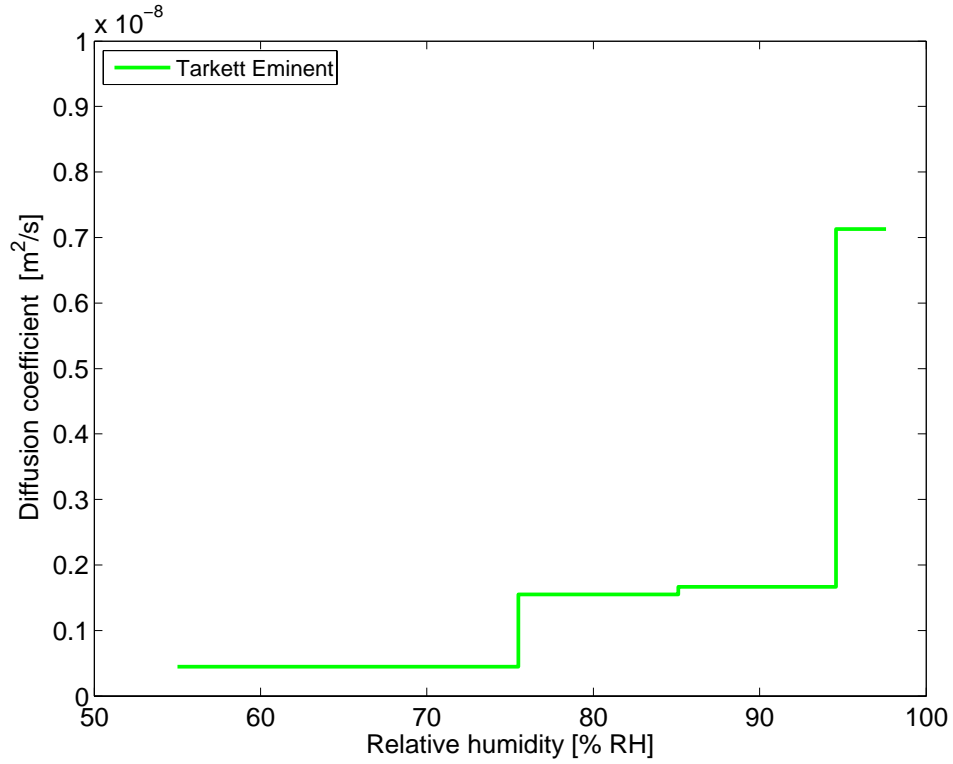


Figure 41. Mean diffusion coefficient of a Tarkett Eminent, 2 mm, homogenous PVC flooring. The diffusion coefficient was determined in the interval 55 - 97.6 % RH.

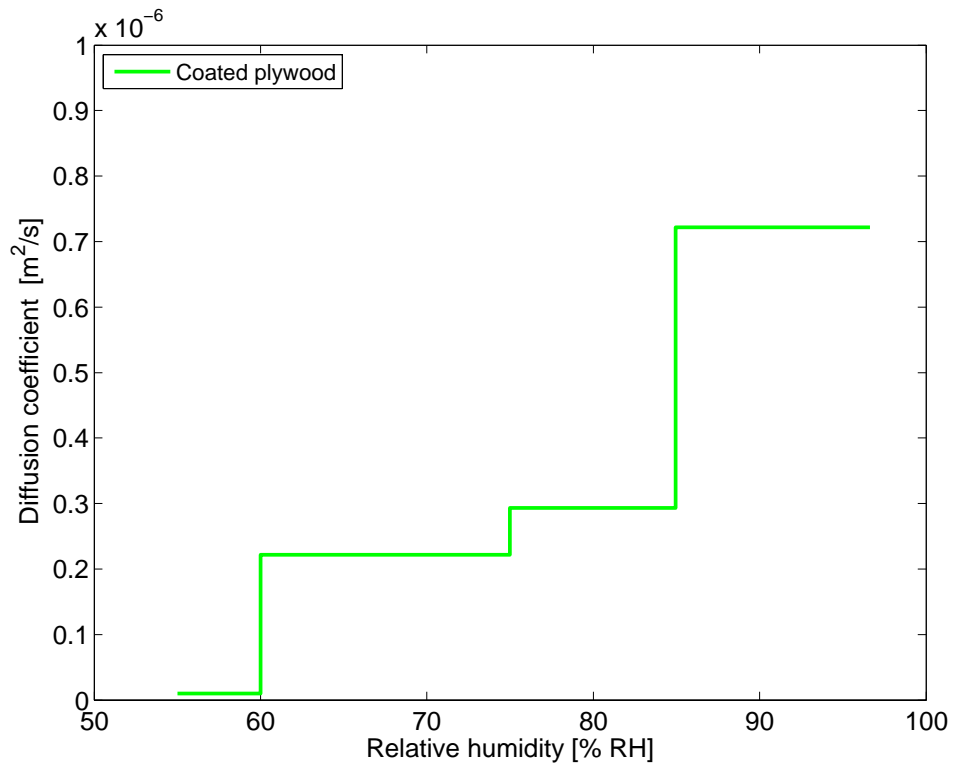


Figure 42. Mean diffusion coefficient for coated plywood 13 mm, used as formwork. The diffusion coefficient was determined in the interval 55 - 97.6 % RH.

- 4 Experimental -

The results of the evaluated mean diffusion coefficient for the w/c 0.65, see figure 40, shows the most reliable results, since it was determined on several discs per each salt solution. The results from the w/c 0.55 cement mortar and Floor 4310 Fibre Flow were determined material on a few discs per each salt solution thus the uncertainty increases. The mean diffusion coefficient between 55 % RH and 60 % RH seems too low in comparison to the higher levels. This is possibly either a consequence of the low difference between the outside and the inside climate or an error in the generated 55 % RH climate.

The mean diffusion coefficient of the PVC flooring material shown in figure 41 is two orders of magnitude lower than for the cement based materials, thus it is less permeable than those materials.

Mean diffusion coefficients for coated 13 mm plywood, determined on three discs per salt solution shown in figure 42, are of the same magnitude as for the cement based materials. The mean diffusion coefficient in the 55 - 60 % RH range is unexpectedly low. The plywood sample cups were stored in the same climate room as the concrete sample cups, thus the low mean diffusion coefficients may be explained correspondingly.

5 Model validation

Moisture distributions were determined for nine screeded slabs at several occasions before and after flooring, see paper IV, appendix. The future moisture profiles were evaluated by using the proposed method in chapter 3. Each diagram in figures 43 - 47 shows the screeded slab's moisture distribution before flooring, dashed lines, and after a certain time of redistribution, solid lines. In addition, the evaluated uniform RH level is shown as a thick dashed line in each diagram.

The complete iteration procedure is shown in table 4, where slab 4 serves as an example.

Table 4. The calculation of the future uniform moisture distribution inside a screeded concrete slab is performed according to the quantitative model presented in section 3.3.

Depth	d_i	\overline{RH}_i	1:st iteration			2:nd iteration		
			$\left(\frac{\partial We}{\partial RH}\right)_i$	$d_i \cdot \left(\frac{\partial We}{\partial RH}\right)_i$	$d_i \cdot \left(\frac{\partial We}{\partial RH}\right)_i \cdot \overline{RH}_i$	$\left(\frac{\partial We}{\partial RH}\right)_i$	$d_i \cdot \left(\frac{\partial We}{\partial RH}\right)_i$	$d_i \cdot \left(\frac{\partial We}{\partial RH}\right)_i \cdot \overline{RH}_i$
[m]	[m]	[% RH]	[kg/m ³]	[kg/m ²]	[kg/m ²]	[kg/m ³]	[kg/m ²]	[kg/m ²]
0.00-0.02	0.02	75.5	0.06	0.0012	0.0906	0.08	0.0016	0.1208
0.02-0.04	0.02	82.5	0.42	0.0084	0.693	0.13	0.0026	0.2145
0.04-0.06	0.02	85	0.78	0.0156	1.326	0.25	0.005	0.425
0.06-0.08	0.02	86.5	0.8	0.016	1.384	0.8	0.016	1.384
0.08-0.10	0.02	86.5	0.8	0.016	1.384	0.8	0.016	1.384
0.10-0.12	0.02	86.5	0.8	0.016	1.384	0.8	0.016	1.384
$\Sigma=$				0.0732	6.2616		0.0572	4.9123
$RH_\infty=$		81		$Eq.13 \Rightarrow$	$\frac{6.2616}{0.0732} = 85.5$		$Eq.13 \Rightarrow$	$\frac{4.9123}{0.0572} = 85.9$

Judging from the determined moisture distribution the maximum RH, 86.5 % RH, is found in the 0.06-0.08 m section and the minimum RH, 75.5 % RH, is found in the 0.00-0.02 m section. Therefore an initial guess of the uniform moisture distribution RH_∞ according to the model should be the midpoint in that interval, 81 % RH. The moisture capacity in each section is calculated by using the desorption isotherms for sections where the determined RH is above 81 % RH and absorption scanning curves where the RH is below 81 % RH. These moisture capacities are derived from the results presented in section 4.2 and 4.3.

The desorption isotherm moisture capacity is evaluated from the w/c 0.65 concrete, see figure 23, for one of the two samples removed 20 mm from the base surface. The moisture capacity for the screed is determined from the used screed, w/c 0.55 cement mortar, see figure 25. The moisture capacity from the absorption scanning curves for w/c 0.65 concrete and w/c 0.55 cement mortar are evaluated from figure 31 and 33 respectively.

Equation 13, section 3.3, gives an $RH_\infty = 85.5$ which is significantly higher than the initial guess of the uniform moisture distribution. Therefore a second iteration is performed where the uniform moisture distribution, RH_∞ , is assumed to be 85.5 % RH.

In the second iteration the moisture capacity in section 0.02-0.04 m is evaluated by using the absorption scanning curve diagram. In the first iteration the desorption isotherm was used, but since the RH level in this point, 82.5 % RH, now becomes less than the assumed $RH_\infty = 85.5$ % RH, the absorption scanning curve diagram is more appropriate to use. This change of the

assumed RH_{∞} also affects the moisture capacity evaluation for section 0.04-0.06 m, where the RH level is less than 85.5 % RH. Thus the absorption scanning curve should be used instead of the desorption isotherm.

The second iteration gives an RH_{∞} = 85.9 % RH. A better precision is not obtainable.

In each diagram the RH is found on the x-axis and the vertical distance in mm from the slab surface is shown on the y-axis, positive figures for increasing depth. The line markers represent the obtained RH level in each section. Flooring installation is defined as day 0 (zero) and each legend states when the profile was obtained in relation to flooring.

The different materials used for each screeded slab is indicated in the diagrams, C representing w/c 0.65 concrete, C_{HCS} representing w/c 0.4 concrete, SFC representing Floor 4310 Fibre Flow, and M representing w/c 0.55 cement mortar.

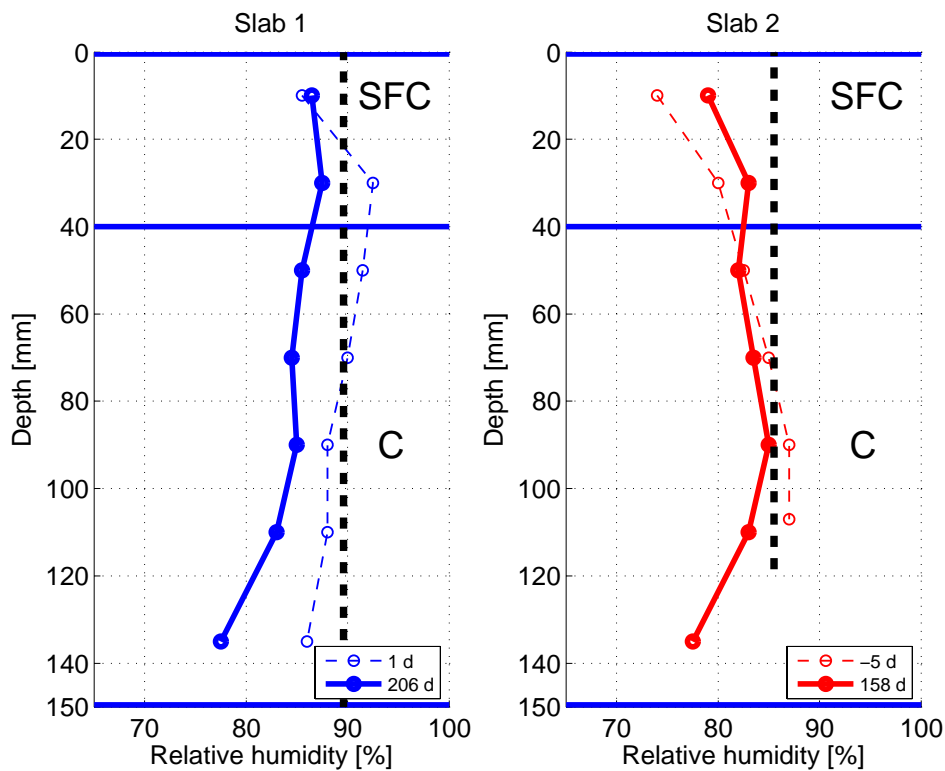


Figure 43. Moisture distribution determined for two SFC screeded concrete slabs on plywood at the time of flooring, thin dashed line, after complete redistribution predicted by the model, thick dashed line, and after x days of redistribution, thick solid line.

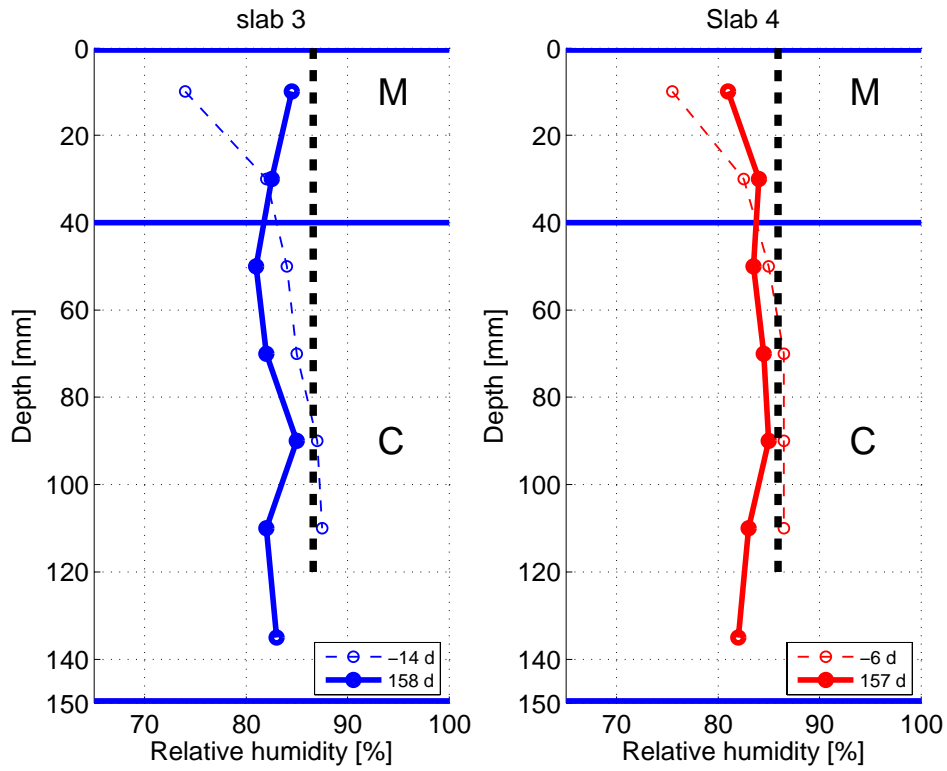


Figure 44. Moisture distribution determined for two M screeded concrete slabs on plywood.

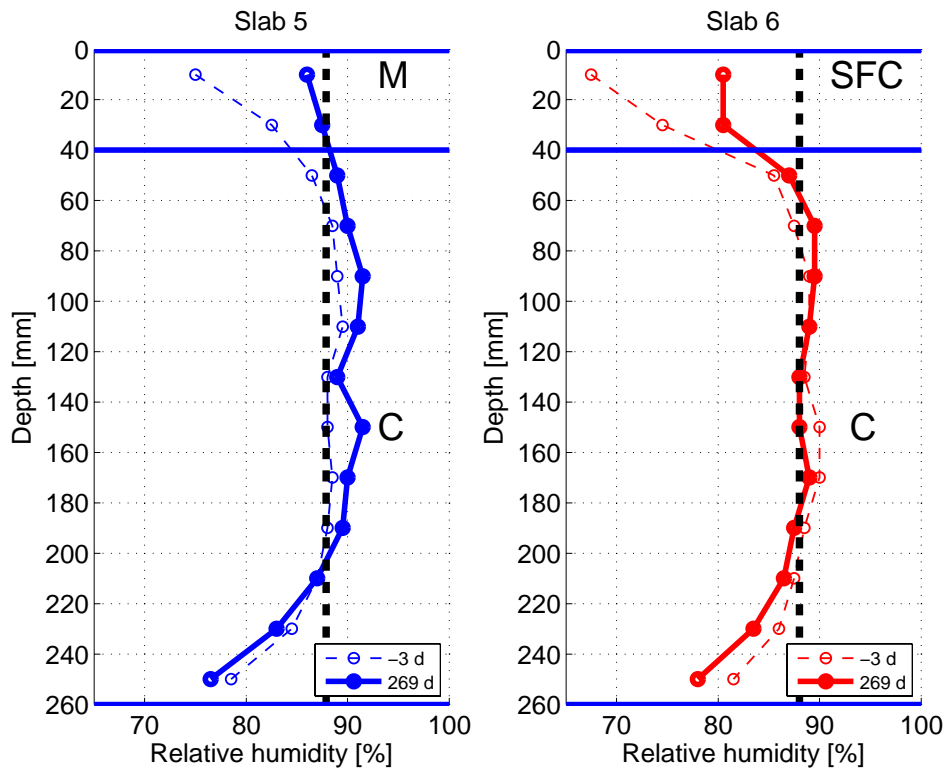


Figure 45. Moisture distribution determined for the M and SFC screeded concrete slabs.

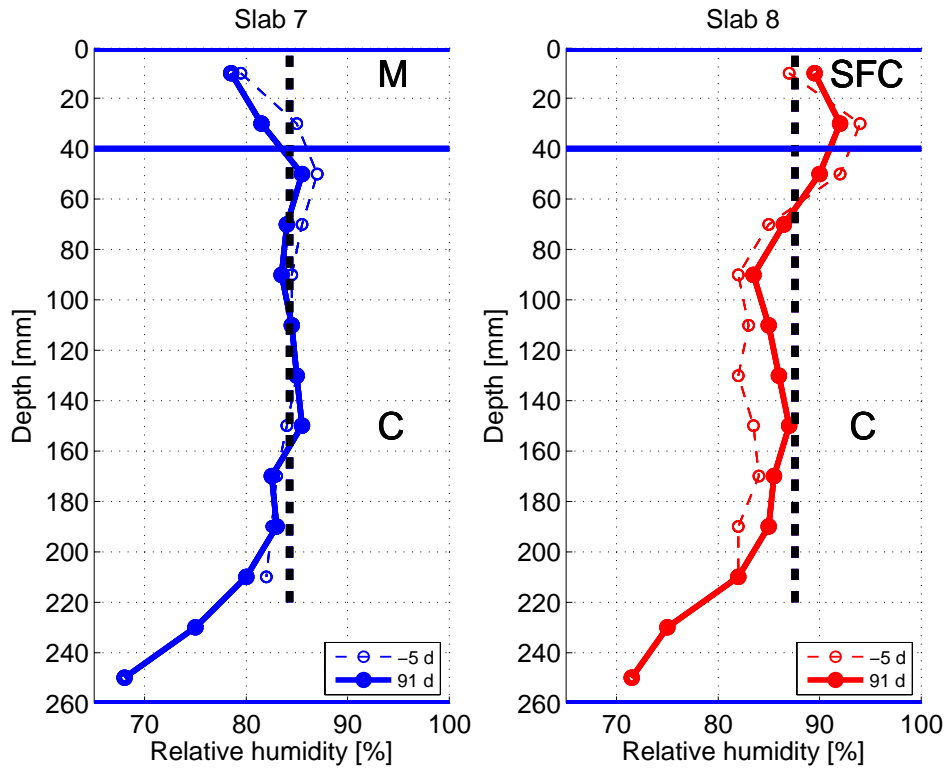


Figure 46. Moisture distribution determined for the M and SFC screeded concrete slabs.

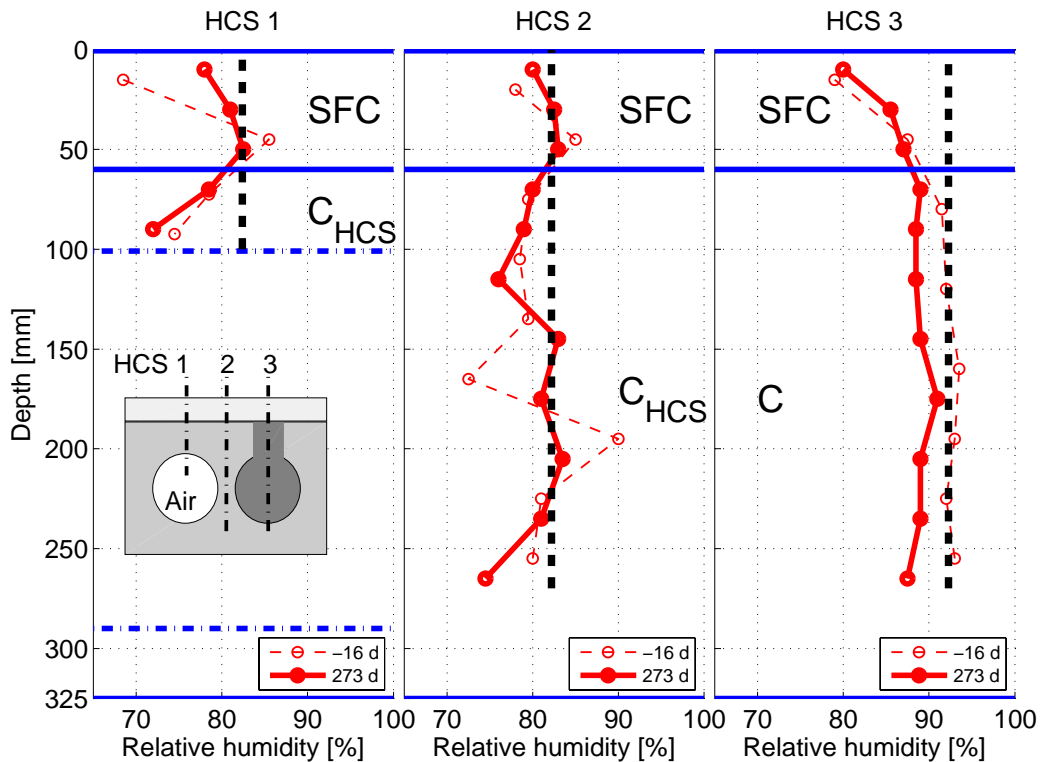


Figure 47. Moisture distribution determined for three separate sections of the SFC screeded hollow core slab, with one core hole filled with material C. Section 150-180 and 180-210 in vertical section HCS 2 were judged as outliers and therefore excluded from the estimation of future RH distribution.

6 Discussion and conclusions

The model is dependent on the initial moisture distribution through the screeded slab. Determination of such a distribution is performed before flooring either in situ or in a laboratory on extracted samples. A detailed description of this distribution may reduce the uncertainty. Dividing each material into a larger number of sections may be beneficial as the higher resolution may reveal unexpected moisture level changes, thus enhancing the knowledge about the moisture history. The knowledge of the slabs' internal moisture distribution scatter increases by performing multiple moisture distribution sampling.

The current status of the floor construction should be described as detailed as possible in terms of comprising materials, layer thicknesses and moisture distribution. A rough description may give rise to a large uncertainty.

The moisture distribution is determined on representative sections. The total thickness of each material limits the number of feasible subdivisions. Each material should be treated separately, meaning that mixtures of materials are unfavorable. Determination of RH on thin material layers, below 10 mm may be difficult both because of possible moisture losses when sampling and equipment installation requirements.

The screeded slab is divided into separate vertically discrete sections of a certain thickness. As the initial moisture distribution in the slab is unknown it may be determined on sections equally thick. However, as the moisture profile is very steep in certain sections the determined profile may be misleading, especially in sections close to the surface.

Due to limitations of the employed measurements a certain section size may be required to minimize uncertainties. Individual section depths could be assigned if the over all distribution is known from former measurements. If the moisture distribution is determined on material samples, these should be collected in a way that enough material from each depth is obtained. If the moisture distribution is determined in situ using drilled in sensors, each sensor should determine the RH in the vertical mid point of each section.

The proposed qualitative model for estimating the moisture distribution in a screeded concrete slab fits the verifying experiments and serves as an illustration of how moisture may redistribute inside such a slab. The quantitative estimations of moisture distribution after flooring indicate a similarity to the results obtained from the performed experiments. However, the humidity in the verifying screeded slabs has not yet been completely redistributed given the limited redistribution time.

The humidity distribution determined 206 days after flooring in slab 1 indicates that the maximum RH is not yet reached, see figure 43. The higher RH level obtained at the 30 mm level indicates that additional moisture will be transported upwards thus increasing the level about 1 % RH. The results obtained from slab 2 and 4 clearly demonstrate that moisture will redistribute from the 30 mm level to the 10 mm level, see figures 43 and 44. It is very likely that the future RH level beneath flooring will increase about 3 - 5 % RH compared to the obtained top RH levels.

The determined RH distribution in slab 3 shows a higher RH level in the 0-20 mm section than in the 20-40 mm section, see figure 44. This may be a consequence of measurement

uncertainty as such an increase most likely could not be explained by moisture redistributing from deeper laying sections. Disregarding this possible future humidity increase, raise the proposed quantitative model gives results about 1 - 8 % RH on the safe side judging from slab 1 - 4. However, including the expected future raise for slab 1, 2 and 4 the overestimation shrinks to about 1 - 3 % RH.

Applying the quantitative estimation on slab 5 and 6 results in a 2 - 7 % RH higher humidity at the 10 and 30 mm level determined 269 days after flooring, see figure 45. However, based on this moisture distribution a further increase in humidity is very likely to occur. Judging from the determined moisture distribution the screed RH may increase about 3 - 8 % RH. Including this future suggested increase the quantitative model underestimates the screed humidity of about 1 - 2 % RH.

Applying the quantitative model on slab 7 and 8, the screed humidity estimation is higher than that obtained for slab 7 and slightly lower for slab 8, see figure 46. However, neither of the screeds maximum humidity is reached yet. It may be expected that the humidity may increase about 6 - 7 % RH for slab 7 and about 2 - 3 % RH for slab 8. Incorporating these expected increases the future screed humidity in slab 7 will be underestimated by 1 - 2 % RH and about 3 - 4 % RH in slab 8.

Comparing results from humidity distribution measurements with the estimated future uniform RH, the filled core, HCS3, shows about 5 - 10 % RH higher humidity level at the 10 - 30 mm level, see figure 47. However, considering future upward moisture redistribution the final humidity level in the screed may increase to about 90 % RH, thus reducing the apparent overestimation to some 2 - 3 % RH. The moisture profiles determined for vertical sections HCS 1 and 2 are in addition to vertical moisture redistribution also affected by horizontal moisture redistribution. The quantitative model is not designed to be used in such cases and therefore the estimated future moisture distribution is uncertain in those two vertical sections.

Neither the time aspects nor possible drying is included in the model. This may be beneficial when the screed is very dry at the time of flooring. On the other hand when the screed humidity is high, the time needed for redistribution has a negative impact of the achieved humidity below flooring, it will be higher than expected. The slow moisture transport in concrete is the key factor reducing the speed of moisture redistribution. Drying from the floor construction through both flooring and slab base will favorably affect the obtained screed humidity level as the average humidity decreases, thus reducing the maximum humidity beneath flooring.

In addition an uneven temperature distribution may affect the moisture distribution. Measurements performed on site that shows that the temperature on average is higher on the slab base than on the slab top, the report also shows that irregular temperature fluctuations are common on a construction site [19]. The lower average temperature in the floor top may have a negative effect on the humidity distribution as moisture then is transferred to the colder upper side, thus increasing the humidity.

The model uses an average moisture capacity to calculate the new moisture content at the estimated future RH distribution, see figure 48.

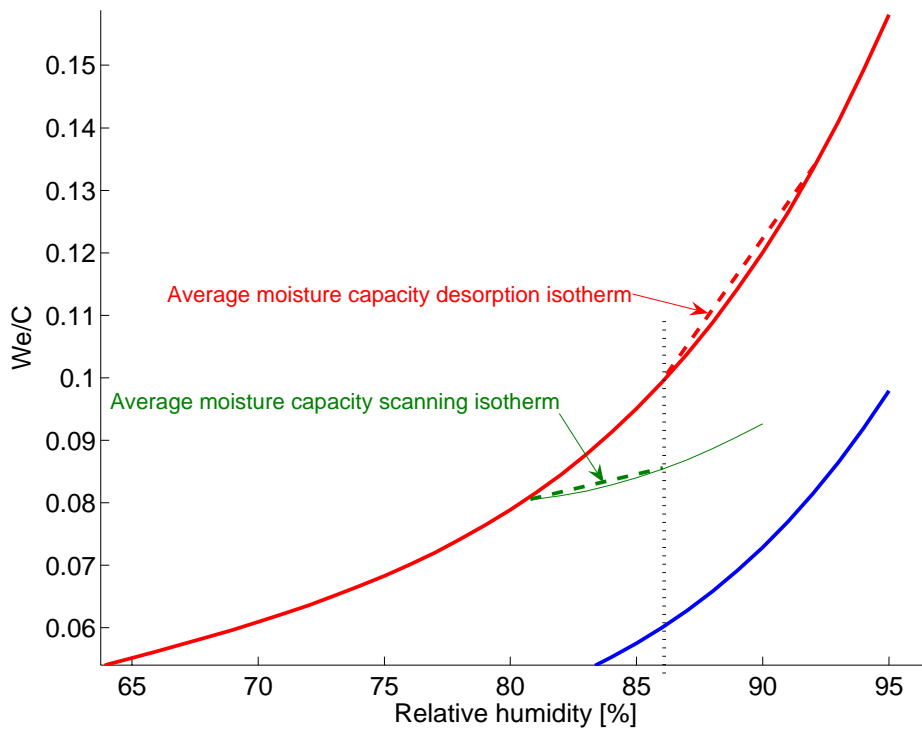


Figure 48. The average moisture capacity shown for two separate sections of a screeded slab, one for the desorption isotherms and one for the scanning curve. The uniform RH after redistribution is shown as a vertical dotted line.

It is possible to develop software which is able to estimate the moisture distribution underneath flooring according to the proposed quantitative model. However, additional data on isotherms for concrete mixtures and screed compounds, not included in this research, needs to be further investigated. The software would require a model for estimating scanning curves for different materials as such isotherms are not available for all expected conditions.

The sorption balance used for determining sorption isotherms is very useful for cement-based materials [20-22]. Besides reduced labor costs, the speed of determining one desorption and absorption isotherm is increased by a factor of 10 compared to the previously used climate chamber method [23, 24]. Such high speed isotherm determination is beneficial as uncertainties arising from hydration are reduced. In addition, sorption balances are accurate enough to perform scanning curve investigations. Testing is undertaken in a carbonate free environment thus preventing carbonation. However, one drawback is the high initial cost of the sorption balance.

In paper III, several scanning curves were presented for concrete, mortar and one self leveling flooring compound. All these scanning curves were investigated by subjecting the material sample to a linearly increasing/decreasing RH in a sorption balance. This method has previously been used in [20]. However, small but significant time lag effects were achieved as a consequence of the slow moisture exchange between the passing gas stream and the samples. These were minimized by linearly distributing the error originating from the start and the ending levels on the scanning curve. After this linear error distribution the time lag effects were reduced.

The small time lag effect may be further reduced by using an RH step change sequence for evaluating scanning curves. In this way there is a possibility to extrapolate each step's final mass instead of using linearly distributed errors, thus further reducing possible time lag effects.

Results from the repeated scanning sorption isotherms investigations indicate that the moisture content is recovered when returning to the desorption isotherm after performing one scanning curve loop.

7 Future research

The results from this research have raised a number of questions that needs to be investigated to develop the model further.

Additional inputs, such as sorption isotherms including scanning curves for other concrete mixtures and screeds is needed to decrease uncertainties of the proposed model. Desorption isotherms determined for samples extracted from shallow parts of concrete showed a decrease with time to bind moisture by absorption. Samples extracted from deeper lying parts also showed a decrease in the ability to bind moisture by absorption. These two findings may have an impact on moisture redistribution.

Moisture flow is temperature dependent and variable thermal conditions were not investigated in this thesis. Future research should investigate if there is and how large impact a non uniform temperature distribution has on initial and future moisture redistribution in screeded slabs. A few measurements have been presented in a short report where the temperature was higher in the slab base than on the top of a storey separating slab. Such a temperature difference would increase the upward moisture flow thus increasing the achieved maximum humidity beneath flooring.

As the sorption isotherm is temperature dependent and low temperatures regularly occur during construction, additional sorption isotherms should be determined for temperatures other than 20 °C.

The model does not take into consideration time lag effects and possible drying through the flooring material and an open base surface. Drying will decrease the achieved humidity beneath flooring, thus reducing the risk of moisture related damages.

A detailed analysis of the involved uncertainties and how it may affect the estimated maximum humidity level is not performed in this work. However, uncertainties originating from a lot of sources are briefly mentioned in the next four paragraphs.

First of all the, the uncertainty involved in RH determinations of each section will affect the over all achieved uncertainty. However, when determining a complete distribution throughout an entire screeded slab the over all moisture distribution uncertainty decreases. Sections may be regarded as outliers, disqualifying them from further analysis.

Secondly, by performing a detailed moisture distribution determination throughout the entire slab by subdividing it into many horizontal sections, a lower uncertainty may be obtained. The adverse, a higher achieved uncertainty, will follow if performing a non sufficient, poor, low resolution, or incomplete moisture distribution determination. In such a case it is not possible to disregard outliers.

Thirdly, possible non uniform temperature distributions occurring may also add to the uncertainty, since such are not included in the model. Such a non uniform temperature distribution will redirect moisture flow from warmer towards colder sections inside the screeded slab, thus reaching a non uniform moisture distribution.

- 7 Future research -

A fourth uncertainty source is possible drying occurring through the slab base and flooring. Further drying will reduce the achieved humidity level underneath the flooring and will reduce the maximum achieved humidity beneath flooring.

The magnitude of the mentioned uncertainties needs to be further investigated in future research. Some of the above stated sources of uncertainty affect the achieved maximum humidity more than others. Some may even possibly be disregarded.

8 References

1. Nilsson, L.-O., *Moisture measurements, Excess moisture in concrete slabs on grade. Drying and measurement methods (in Swedish)*. 1979, Div Building Materials, Lund Institute of Technology, Lund University: Lund.
2. Powers, T.C. *A discussion of cement hydration in relation to the curing of concrete*. in *Proceedings 27*. 1947. Washington, D.C.: Highway Research Board pp. 178-188.
3. Powers, T.C. and T.L. Brownyard. *Studies of the physical properties of hardened portland cement paste*. in *Journal of the American concrete institute*. 1948. Chicago, Illinois.: PCA Research Laboratories.
4. Kraemer, E.O., *Treatise on Physical Chemistry*, ed. H.S. Taylor. 1931, New York: Van Nostrand.
5. McBain, J.W., *An explanation of hysteresis in the hydration and dehydration of gels*. *Journal of American Chemical Society*, 1935. **57**: pp. 699-700.
6. Diamond, S. and K.O. Kjellsen, *Resolution of fine fibrous C-S-H in backscatter SEM examination*. *Cement and Concrete Composites*, 2006. **28**(2): pp. 130-132.
7. Lü, X., *Modelling of heat and moisture transfer in buildings: II. Applications to indoor thermal and moisture control*. *Energy & Buildings*, 2002. **34**(10): pp. 1045-1055.
8. Feldman, R.F. and V.S. Ramachandran, *Differentiation of interlayer and adsorbed water in hydrated portland cement by thermal analysis*. *Cement and Concrete Research*, 1971. **1**(6): pp. 607-620.
9. Feldman, R.F. and V.S. Ramachandran, *A study of the state of water and stoichiometry of bottle-hydrated Ca_3SiO_5* . *Cement and Concrete Research*, 1974. **4**(2): pp. 155-166.
10. Langmuir, I., *The constitution and fundamental properties of solids and liquids. Part I. Solids*. *Journal of the American Chemical Society* 1916. **38**(11): pp. 2221-2295.
11. Brunauer, S., P.H. Emmett, and E. Teller, *Adsorption of gases in multimolecular layers*. *Journal of the American Chemical Society*, 1938. **60** (2): pp. 309-319.
12. Young, T., *An Essay on the Cohesion of Fluids*. *Philosophical Transactions of the Royal Society of London*, 1805. **95**: pp. 65-87.
13. Thomson, W. *On the Equilibrium of Vapour at a Curved Surface of Liquid*. in *Proceedings of the Royal Society of Edinburgh*. 1871.
14. Fagerlund, G., *Om hysteresis mellan porvattentryck och fukthalt (in Swedish)*. 1999, Div Building Materials, Lund Institute of Technology, Lund University: Lund.
15. Everett, D.H., *Adsorption hysteresis*, in *The Solid-Gas interface Vol. 2*, E.A. Flood, Editor. 1967, Marcel Dekker: New York. pp. 1055-1113.
16. Anderberg, A., *Moisture properties of self-levelling flooring compounds in Division of building materials* 2004, Lund University: Lund. pp. 40.
17. Greenspan, L., *Humidity Fixed Point of Binary Saturated Aqueous Solutions*. *Journal of research of the national bureau of standards - A. Physics and Chemistry*, 1977. **81** A(1): pp. 89-96.
18. Anderberg, A. and L. Wadsö, *Moisture in self-levelling flooring compounds. Part I. Water vapour diffusion coefficients*. *Nordic concrete research*, 2004. **32**(2): pp. 3-15.
19. Åhs, M. *Remote monitoring and logging of relative humidity in concrete*. in *Proceedings of the 7th symposium on building physics in the nordic countries* 2005. Reykjavik, Iceland: The Icelandic building research institute pp. 181-187.
20. Anderberg, A. and L. Wadsö, *Moisture in self-levelling flooring compounds. Part II. Sorption isotherms*. *Nordic concrete research*, 2004. **32**(2): pp. 16-30.

- 8 References -

21. Johannesson, B. and M. Janz, *Test of four different experimental methods to determine sorption isotherms*. Journal of Materials in Civil Engineering, 2002. **14**(6): pp. 471-477.
22. Espinosa, R.M. and L. Franke, *Inkbottle Pore-Method: Prediction of hygroscopic water content in hardened cement paste at variable climatic conditions*. Cement and Concrete Research, 2006. **36**(10): pp. 1954-1968.
23. Baroghel-Bouny, V. and T. Chaussadent. *Pore structure and moisture properties of cement-based systems from water sorption isotherms*. in *Microstructure of Cement-based systems*. 1994. Boston: Materials research society pp. 245-254.
24. Ahlgren, L., *Fuktfixering i porösa byggnadsmaterial (in Swedish)*, in *Division of building technology*. 1972, Lund University, Lund. pp. 197.

I

Remote monitoring and logging of relative humidity in concrete

*M Åhs, Ph.D. student, Div. of Building Materials,
Div. of Building Materials, Lund University, Lund, Sweden;
magnus.ahs@byggtek.lth.se
http://www.byggnadsmaterial.lth.se*

KEYWORDS: *relative humidity, concrete, remote monitoring, in-situ measurements.*

SUMMARY:

It is important to measure the relative humidity, RH, level in a concrete slab before applying semi permeable flooring to the surface. If the moisture level in the concrete is too high when the flooring is applied the high alkali level in combination with the moisture will degrade the adhesive.

This paper describes a new system used to continuously measure and monitor RH in situ during the construction stage. The paper includes descriptions of the method, an authentic measurement, and also how to evaluate results given by the measuring equipment. The presented results are taken from measurements performed on a construction site where the RH has been monitored, via the mobile phone network.

1.Introduction

Drying of concrete is a slow process and frequent measurements appear redundant. However, there are benefits to be achieved from frequently measuring RH. First of all frequently performed measurements make it possible to follow how fast the concrete is drying in existing climate and secondly it is possible to estimate the remaining drying time until the flooring may be applied.

This paper describes a newly developed system for logging and monitoring in-situ measurements of RH. The system is called Betongdatorn Fukt 5.0. In short, an RH sensor, Humi-Guard, is installed in a hole drilled into the concrete slab. When the RH sensor is installed it is connected to an instrument that transmits readings to a data logger. Measurements from both temperature and RH are stored at an optional rate in the data logger which is located indoors on the building site. The data logger is connected to a GSM-link. The software Betongdatorn Fukt 5.0, is installed on a computer with a modem. The modem is used to connect to the data logger via the GSM-Link. Data from the data logger is accessed and transmitted to the computer via the mobile phone network. Evaluations of the measurements are performed on a specially designed Excel spread sheet. Calculations of the uncertainties involved when measuring are performed for each in-situ measurement individually in the specially designed Excel spread sheet.

There are many different methods for measuring RH in concrete in-situ, e.g. measurements in drilled holes using instruments from Humi-Guard, Vaisala, Testo, RBK (2001), e.g. measurements in drilled holes using a metal rod with wood and metal discs to measure a complete RH profile through a slab, Sjöberg (2004). Today in Sweden, the main part of RH measurements in concrete are performed manually. RH is, in best cases, measured about once or twice each month about two months before the flooring is applied. More commonly RH measurements are carried out about one week or less before the flooring. The actual measurements are carried out either as in-situ measurements or as measurements on samples removed from the concrete.

Measuring RH of a concrete slab in-situ is rather time consuming. When measurements are performed in situ, the RH sensor needs up to 4 days after installation to reach equilibrium according to RBK (2001). However, after this initial phase of reaching equilibrium, the RH and temperature can be measured anytime. In Sweden building companies purchase these measurements from other companies. In order to get a regular day-by-day follow up of the drying process of a concrete slab a computerized data acquisition system was developed by Skanska Sweden AB in 2002, Åhs (2002).

Today the high rate of construction demands carefully planning of forthcoming activities as accurately as possible in order to optimize construction. When planning applying semi-permeable flooring, e.g. PVC, to a concrete slab, time for drying needs to be taken into account, since time is often a critical parameter during construction. Very often construction time is limited and drying of concrete is slow, this makes it important to be able to estimate the time needed for the concrete to reach a certain level of RH.

If the RH is too high, there is a risk to create future moisture related problems. The adhesive may degrade due to the high moisture and alkali levels and create harmful emissions Sjöberg (1999, 2001a). These emissions are believed to have an essential role in the sick building syndrome Kumlin *et al* (1994), Sjöberg (1999, 2000), Hall (2003).

The common way to determine RH in concrete slabs is to measure RH just before attaching flooring. If requirements are not fulfilled the contractor often has no time to let the concrete dry further and the flooring is applied anyhow.

This may cause problems in the future since the moisture redistributes after flooring is applied. Moisture moves from areas with high moisture content to areas with lower moisture content and thus increases RH in the former dry areas. This process continues until equilibrium is established, if ever, and takes many months or even years. Underneath the flooring, the RH increases until it reaches a maximum level. The adhesive will degrade if the obtained RH level is too high. The problem is hidden on a short time basis since the problem with degrading adhesive does not occur until about 1 or 2 years.

If the RH on the other hand would be measured frequently, starting a long time before applying PVC flooring, then the contractor can take measures to speed up the drying process. This could lead to a faster and more reliable prognosis making of when the earliest possible date of flooring could be identified.

One other problem when measuring RH in-situ is the temperature stability during construction. In many cases temperature stability during construction is very poor because the building is not finished yet. Often doors, windows and insulation in walls and roof are not installed when the measurements are to be performed. The unstable temperature results in very uncertain measurement results. If the temperature has recently been very high and suddenly decreases fast, the reading shows to high RH and vice versa.

The newly developed system of logging RH has revealed unknown behaviour of how the Humi-Guard RH-sensor is working and how the actual temperature in concrete changes in time.

2.Method

This method for measuring RH in concrete is based on in situ measurements performed in a concrete slab.

A Ø16 mm hole is drilled in the concrete to a certain depth minimum 35 mm from surface. The depth of the hole is determined depending on the drying situation.

The depth of the hole is measured to ensure that you have reached the desired depth. Then the hole is carefully cleaned from concrete particles and dust using a vacuum cleaner or an air pump. A cylindrical brush is used to remove dust from the holes inner surface. A special manufactured measurement tube with a rubber sealing in the bottom is after cleansing inserted in the hole. The rubber sealing is open to the concrete surface and fitted tight to the sides of the hole. Sealing paste is put in between the measurement tube and the top of drilled hole to both fix the tube and also to prevent air movements from interfering with the measurements.

A leak detector is used to find out if the installation of the measurement tube is air tight fitted to the hole. If a leak is detected, the leak should be sealed and new tests are performed until no leak is detected.

After this a RH sensor, Humi-Guard shown in figure 1, is attached/fixes to a rubber plug contact, see figure 1, and promptly, approximately within 30 s, inserted in the measurement tube using a special rubber plug installing device. The RH sensor is read using a conductance meter shortly after installing it in the measurement tube. If the reading from the sensor is above 2 µS, the installation of the sensor has been carried out promptly enough. If the reading is below 2 µS then the sensor shall be replaced with a new sensor. After a successful sensor installation a rubber plug is inserted in the measurement tube to ensure that the whole installation is air proof.

The RH sensor is sensitive to RH changes and for one time use only. Its operating range in RH is (75 – 95) %. Sensors must be kept in a moisture controlled environment during storing. The RH sensor is sensitive to low RH, if the sensor has been exposed to below 75% RH for more than 30 seconds it may be damaged.

The RH sensor is constructed from two thin electrodes made of silver that are attached on the opposite sites of a small plastic core. The RH sensor is approximately Ø2 mm and 14 mm long. A fibrous body of polypropene containing a hygroscopic electrolyte is spun like a web close-coiled around both the plastic core and the two silver threads. The electric conduction of the hygroscopic electrolyte is dependent on the moisture and to some extent the temperature in the ambient air and the conductance between the two electrodes changes accordingly.

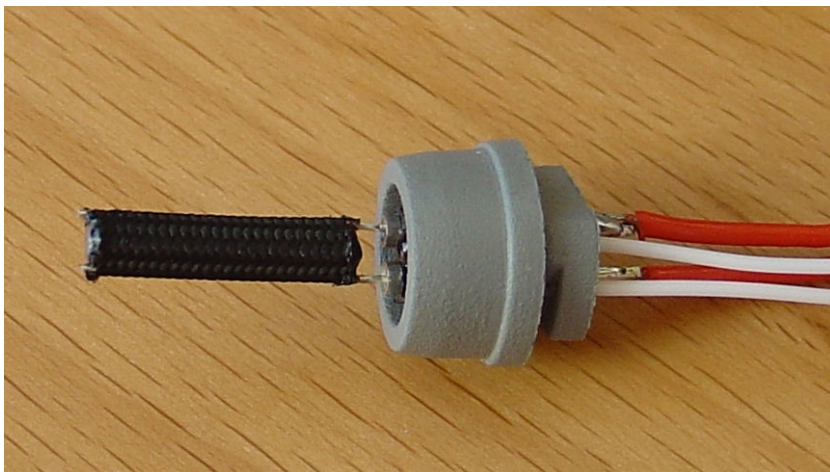


FIG. 1. Humi-Guard sensor attached on a rubber plug contact.

In close proximity to the RH sensor a temperature sensor is fixed on the rubber plug which is fitted into the measurement tube. The measurement tube and rubber plug contact, sealing, and concrete create an air tight space. Another rubber plug is inserted in the top of the measurement tube to prevent dirt and large air movements from interfering with the measurement. Four thin wires from the sensors are squeezed tight using the top rubber plug. The wires are connected to a specially designed transmitter, which is fixed on a steel frame next to the drilled hole, see figure 2.

The temperature sensor is a thermistor with an operating range between (0 - 40) °C.

Mineral wool with a thickness of about 70 mm covering (250*250) mm² is placed on top of the concrete as insulation to reduce temperature fluctuations from affecting the RH results.



FIG. 2. Transmitter and insulation on top of concrete at the measuring position

The instrument in the transmitter measures the conductance between the two silver threads and the temperature from the thermistor. The transmitter sends the data at an optional rate to the receiver via an antenna. It is able to transmit data to the receiver at a distance of 3 km if free sight in between the transmitter and the receiver. The data logger stores data at an optional rate ranging from 1 s up to once a month.

The software receives data from the data logger. The data is compared to data that is obtained from a reference system. The reference system is constructed from an insulated aluminium block. Inside the aluminium block 2-4 RH generating cells from a uniform batch are installed. The cells are made of a small glass container filled with a roll of cloth wetted in hygroscopic water solution. These cells generate a very accurate RH of about 85.1 %. Each batch of reference cells are inspected at an UKAS accredited laboratory. Above these cells RH sensors from the same batch are positioned. The software is used to calculate the RH values from the sensor in the concrete using a special algorithm that includes how the sensors from the same batch reacts to a known RH which is provided by the reference system.

3. Test results

In the in-situ measurement the RH and temperature were measured for a concrete layer cast on top of a hollow core slab. The top layer concrete was never subjected to any additional water in terms of rain since it was cast after the roofing was completed.

Data has been logged at an hourly rate during a period of 3.5 months starting from late April and ending in mid August 2004.

The RH (thick line) is represented on the left hand y-axis and the temperature (thin line) is represented on the right hand y-axis, see figure 3. The x-axis represents time.

During the first 5 weeks no insulation was on top of the concrete where the measurement was performed. In this period both the temperature and the RH fluctuates quite much and the mean RH is about 90% and the mean temperature is about 15 °C. The heating system was not running during this period. The drying rate is low during this period. A piece of mineral wool was put on top of the measuring point after 5 weeks and at the same time the heating system was turned on. The purpose of placing insulation on top of the measuring point was to reduce the amplitude of the fluctuations of the temperature. The amplitude of the temperature

and RH were both reduced very much and the insulation served its purpose. During the following 15 weeks the mean temperature was about 20 °C and the mean RH was about 85 % RH.

During the measuring period the RH in the concrete has varied between 83.9 % to 94.4 % RH and the temperature has varied between 8.5 °C to 24.7 °C

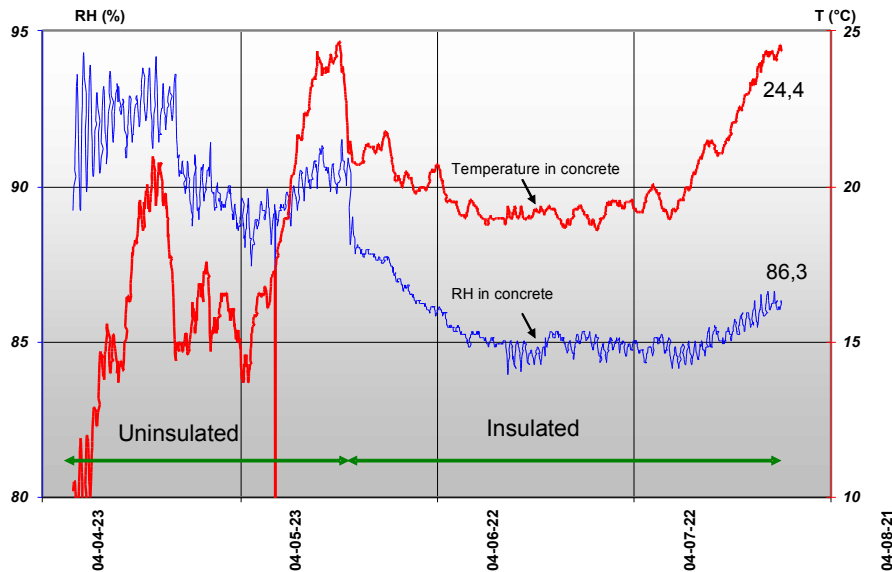


FIG. 3. Relative humidity (thick line) and temperature (thin line) measurements performed during a period of 3.5 months in a concrete slab w/c 0.38.

4. Discussion

The RH and temperature both fluctuate on a daily basis, see figure 3. This fluctuation is probably corresponding to the temperature outdoors, however the outdoor temperature was not measured during the period. During the first part when the measured spot is uninsulated both curves shows larger fluctuations than during the latter part.

During the first month with no insulation the RH sensor does not measure RH in the concrete accurately. The result is affected by the temperature changes to some extent. Since RH rises each time the temperature drops it is obvious that the RH sensor is affected by the surrounding air. When the temperature in air suddenly drops, the RH level increases instantaneously, a temperature drop of 1 °C in air leads to approximately a rise in RH of 5 % RH. In contradistinction to air, the RH in a material drops when the temperature decrease however the drop of RH is small, less than 0.3% RH, Nilsson (1980, 1987), Sjöberg et al (2002).

The amplitude of RH fluctuations declines from ± 2.5 %-units down to ± 0.5 %-units, when the measurement spot is insulated. The result is now in harmony with established theories for moisture mechanics in material and earlier research performed in laboratory. In laboratory it has been shown that the RH rises between 0.1 – 0.5 %-unit/°C depending on w/c-ratio and RH level. The insulation is interfering with the drying process. The insulation put on top acts as an additional obstacle for the water to pass through when the concrete slab is drying. The resistance for the water to pass through the mineral wool insulation corresponds to about 2-3 mm of extra concrete put on top.

It is possible to explain the behaviour in the uninsulated period in two different ways.

The materials in the drilled hole i.e. air, concrete, plastic tube, RH sensor, temperature sensor, sealing paste and rubber plug absorb moisture at different rates. When the temperature suddenly drops in the system the equilibrium is no longer present. The RH in the air instantly increases and the materials in the system suddenly all has a lower RH than the air. The materials respond to this increase of RH by absorbing surplus moisture from the air by diffusion. The rate of absorption is both dependent on the geometry of the

measurement system and how quick the materials absorb water. The concrete at the bottom of the hole is quite slow to absorb water both because of a small exposing area and because of the concrete's moisture properties. The RH sensor, however, which both has a larger exposing area and absorbs water quicker than concrete, reacts immediately and therefore a rise in RH, is measured. Another possible explanation is that differences in temperature or differences in how fast the temperature changes in concrete, air, temperature sensor and RH sensor affects the results.

The newly developed system of logging RH has enlightened this behaviour of the measuring sensor and how the actual temperature in concrete changes in time.

To detect fast changes of a studied parameter a high frequency in data acquisition is required. On the other hand long term measurements produce large amounts of data if the frequency is high.

One advantage of logging data from an RH sensor is that when measuring RH manually you are not able to determine if you have measured during a time when the RH is increasing or if it is decreasing. When logging data you may notice fluctuations.

The data acquired in many cases gives a better view of changes which is not possible to detect manually. Slow changes on the other hand are also hard to monitor if the changes are too small to determine on a day by day basis. Unexpected events are also much easier to detect when the measurements are performed by an automatic system.

5. Conclusion

Betongdatorn Fukt 5.0 logging system compared to manually performed measurements gives a better view of how the drying process is proceeding in a concrete slab, e.g. on a construction site.

The system presents both temperature and RH in a diagram and this makes it easy to follow how the drying in the concrete is progressing. The diagram also shows if the temperature is stable enough to make a reading of RH. The drying rate of concrete is clearly shown in the diagram and this gives you an instrument to evaluate if the existing drying climate conditions are satisfactory.

The diagram also makes it quite easy to make a prognosis of when the RH is low enough to apply the flooring.

There is a risk that manually performed measurements are made when the temperature has recently peaked, e.g. when the sun has warmed the measured spot. Measurements performed just after a temperature peak shows a much lower RH than the actual RH. Betongdatorn Fukt 5.0 makes it possible to distinguish misleading results of this kind.

6. References

- Hall T. 2003. The physical status of an existing building and its components – special emphasis on future emissions. Chapter in “Improving Construction Competitiveness”. Blackwell Science, Oxford, England
- Kumlin A., Åkerlind L-O., Hall T. 1994. Method to solve indoor air quality problems: a practical Swedish strategy. Proceedings of Indoor Air – An Integrated Approach '94. Gold Coast, Australia. 27 Nov – 1 Dec 1994. Vol 1. pp 329-332.
- Nilsson L-O. 1980. Hygroscopic moisture in concrete – Drying measurements & related material properties. Report TVMB-1003, Lund Sweden 1980, pp 24 – 37.
- Nilsson L-O. 1987. Temperature effects in RH measurements on concrete – some preliminary studies. Proceedings of the Symposium and day of Building in Lund Sweden, August 24 – 27, 1987 pp 456-462
- RBK, 2001. Manual for measuring moisture in concrete (in Swedish), third edition 2001, The Swedish Council for Building Competence.

- Sjöberg A. 1999. Transport Processes in covered concrete floors. Proceedings of the XVII Symposium on Nordic Concrete Research. Reykjavik, Iceland. 4 – 6 August 1999. pp 122-124.
- Sjöberg A. 2000. Concrete floors as secondary emission source. Healthy Buildings 2000. Espoo, Finland. 6-10 August 2000.
- Sjöberg A. 2001a. Secondary emission from concrete floors with bonded flooring materials. Department of building Materials, Chalmers University och Technology, Göteborg, Sweden. Publication. P – 01:2. www.bm.chalmers.se/research/publika/p012.htm
- Sjöberg A., Nilsson L-O., Rapp T., 2002. Measuring relative humidity in concrete slabs with floor heating system Stage I, (in Swedish). Publication P – 02:1 Göteborg 2002. www.bm.chalmers.se/research/publika/p021.htm
- Sjöberg A. 2004. A method for measuring moisture distribution in concrete structures. Experimental evaluation of the OE-method. (in Swedish) Report TVBM-3122, Division of Building Materials, Lund Institute of Technology, Lund 2004. www.byggnadsmaterial.lth.se/tvbm-3122.htm
- Åhs M. 2002. Remote monitoring of relative humidity in concrete. Betongdatorn 5.0 a new system for measuring relative humidity in concrete structures – evaluation of new system and methodology. SBUF Rapport 11105. Malmö 2002.

II



A METHOD FOR STUDY SORPTION PHENOMENA

M Åhs^{1,2,*}, A Sjöberg^{1,3} and A Anderberg^{1,4}

1 Division of Building Materials, Lund University, Lund, Sweden

2 Skanska Sverige AB, Malmö, Sweden

3 Fuktdimensionering AB, Malmö, Sweden

4 maxit Group, Stockholm, Sweden.

ABSTRACT

Sorption of humidity in surface materials is a crucial parameter for the moisture balance in the indoor air. In a similar way, sorption of indoor pollutants in surface materials is important for the level of, for example, VOCs and other compounds in the indoor air. Knowledge of sorption capacity and sorption rate is of fundamental importance when indoor air quality is modeled.

This paper describes studies of sorption phenomena made with a sorption balance. It includes descriptions of the method and one measurement, and it shows how the evaluation is performed. In the study, steady state sorption phenomena have been measured for a surface material used in furniture and clothes. The procedure for water vapor sorption has been studied.

INDEX TERMS

Sorption phenomena, sorption balance, steady state, dynamic state

INTRODUCTION

During the last decade, several models for simulating indoor air quality have been developed of different scientists all over the world, for example Damain *et al.* (2002) and Murakami *et al.* (2003). To imitate the reality as close as possible the user is in great need for material properties that are actually used in the simulating model.

These models require different input parameters like air flow, surfaces, dimensions of the room and the properties of the surface materials. In order to simulate the surface material interaction with the surrounding atmosphere and thus the indoor air quality, the materials ability to absorb, desorb and store substances from the air in the room has to be known.

One method to evaluate sorption phenomena for a material is described in this paper. This method, based on a sorption balance, has been used in pharmaceutical and food industry for organic materials for a long period of time. The sorption balance has in these cases been used to study sorption of water vapor on *e.g.* protein inhalation powders by Maa *et al.* (1998), morphine sulphate by Wadsö and Markova (2001), durum wheat semolina by Hébrard *et al.* (2003) Plant lipases by Caro *et al.* (2002). Inorganic materials used in buildings has also been studied such as, self leveling flooring compounds by Anderberg (2004), and the outcome has proved to be satisfactory. The method is fast in comparison to other methods and generates the important material properties involved when modeling indoor environments. In addition to studies made on water vapor, both absorption/desorption and the diffusion rate of volatile organic compounds (VOC) in surface materials are properties that can be studied in measurements performed with a sorption balance. Measurements on VOCs have been performed on polyurethane foam by Cox *et al.* (2001) and on vinyl flooring by Zhao *et al.* (2004).

This paper also presents how a sorption isotherm for water vapor in natural wool was achieved. Natural wool can be found in many applications *e.g.* as a part of a weave in furniture fabric or in clothes used in the indoor environment. The method described can easily be applied on VOCs and other volatile substances instead of water vapor, since the sorption balance used in this study is designed for organic compounds as well.

The content of for example moisture in a material depends, among others, on the vapor pressure of the substance in the surrounding atmosphere. The material has a certain content of the substance when in equilibrium with

* Corresponding author email: magnus.ahs@byggtek.lth.se

surrounding atmosphere. If the vapor pressure in the atmosphere surrounding the material changes, the equilibrium state is no longer present. The material responds either by an uptake or a loss of content of the substance to the surrounding atmosphere to reach equilibrium once more. This process is a continuously ongoing process. Therefore it is important to know the equilibrium content of a substance at a corresponding vapor pressure and how much and how fast it changes when modeling indoor air environments.

RESEARCH METHODS

The method described in this paper is based on a sorption balance. The sorption balance, figure 1, is a high performance balance arranged in a climate cabinet equipped with a stable and reliable climatic control unit. The temperature is adjustable well within a range that may be expected in an indoor environment *e.g.* 0-50 °C. Vapor pressure of a substance is generated by mixing different proportions of a saturated gas stream and a dry gas stream, and is adjustable between completely dry to completely saturated gas. The saturated gas is generated by bubbling dry gas through a liquid substance.

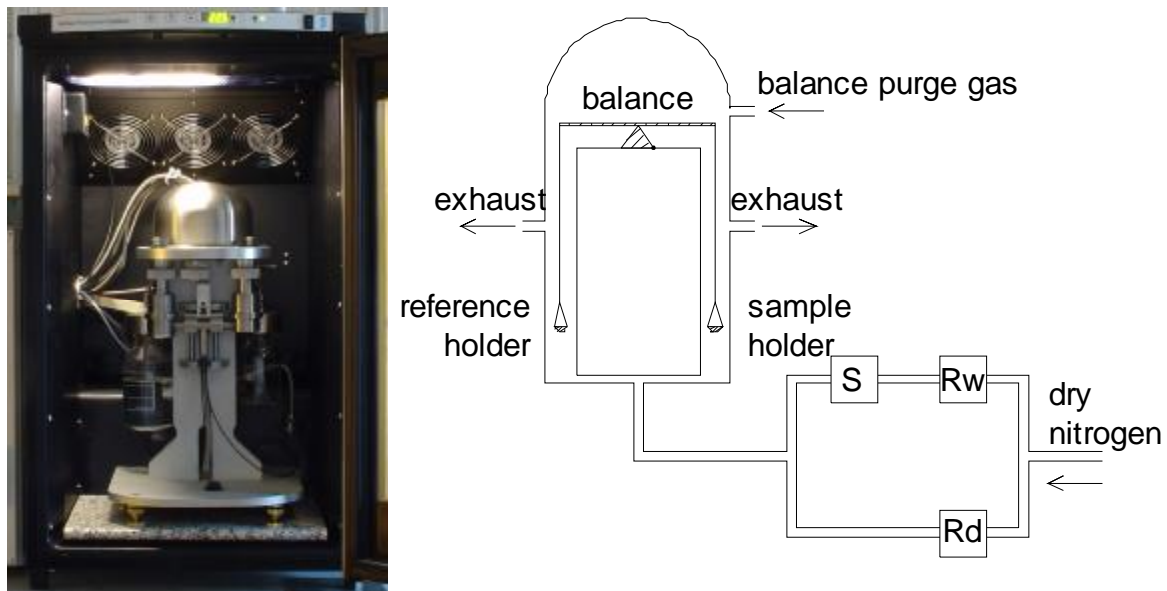


Figure 1. On the left side the sorption balance in a climate cabinet from Surface measurements System, SMS, is shown on the right side a sorption balance principle is shown

The balance, which is the key component in the system, monitors the sample mass as a function of time. It is continuously weighing the sample which is subjected to different vapor pressure levels of the active substance. The sample mass is digitally recorded on a computer at a predefined rate.

A carrying gas is conveyed through a mass flow control unit which distributes the gas in two separate tubes which are equipped with very accurate gas flow control meters. One gas tube runs through a glass vial which is filled with a liquid substance, *e.g.* water or VOCs that generates a saturated gas. The second gas tube works as a dry mixing gas which is mixed in different proportions with the saturated gas by the mass flow control unit to achieve the desired level of vapor pressure. The mixed gas flows past both the reference pan, (reference holder in figure 1), and the sample pan (sample holder in figure 1) at a constant speed.

Two identical glass pans hang in a symmetric microbalance which detects very small differences in sample mass, *e.g.* mass changes of as little as 0.1 µg is possible to recognize for sample sizes as big as 1.5 g. The material sample is put in one glass pan and the other one is empty called the reference pan. These pans should always be used in pairs to avoid systematical errors. The symmetric setup minimizes disturbances from absorbed substance on the glass pans.

The vapor pressure, in the gas stream passing the pans, is defined in a test cycle and runs in a predefined order, called a sequence. The level of vapor pressure is either set to a constant level, stepwise change or continuously increasing/decreasing level (ramping or sinusoidal). Each step runs for either a predefined time period or when a predefined maximum mass change per time unit is reached. A scanning curve is measured by ramping up or down from different levels at a low speed. This ramping application would result as a curve starting from either the

desorption or the absorption isotherm, reaching towards to the opposite isotherm.

The balance is placed in a temperature stable climate cabinet since partial pressure is strongly temperature dependent. If the substance used in the sorption balance is water a rise in temperature of 1 °C leads to a variation of up to 10% in saturated vapor pressure. Therefore fans are installed in the cabinet which circulates the air inside to prevent temperature gradients on the instrument from influencing the test.

RESULTS

In a study by Svennberg (2005) a sorption balance of the brand DVS 1000 from Surface Measurement Systems at Lund University, has been used. In that study the absorption and desorption isotherm on 100 % natural wool for water vapor was measured.

As the study was made for water vapor, de-ionized water was used for saturating the carrying gas, which in this case was N₂. The wool sample were exposed to step changes in vapor pressure ranging from 0 % relative humidity, (RH), up to 95% RH down to 0 % RH in 10 % RH steps and the equilibrium moisture content was determined for each step. The sorption isotherm for water vapor is shown in Figure 2.

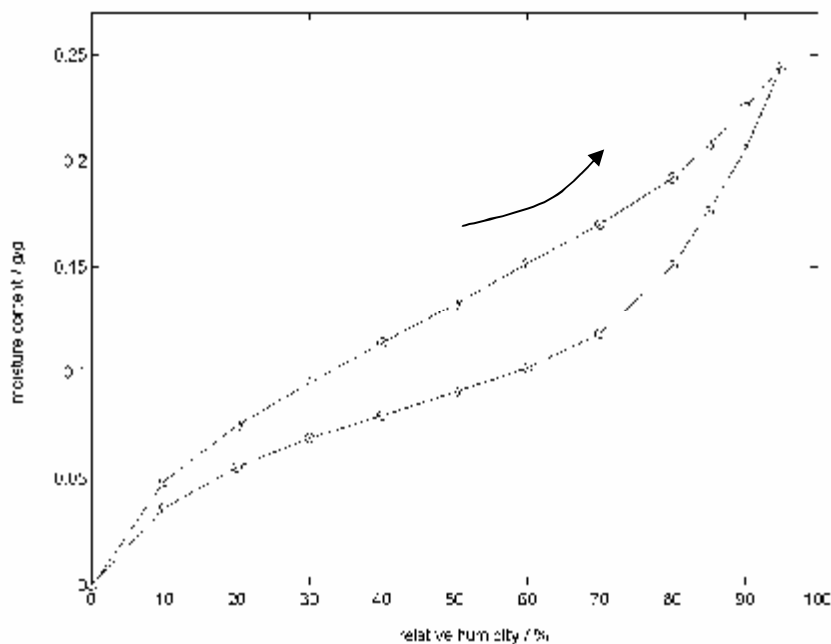


Figure 2. Water sorption isotherm for 100% natural wool (felt, density 176 kg/m³).

The rings in figure 2 shows the result from each step in the sequence and represent the ratio between equilibrium mass at a certain generated vapor pressure and the dry mass. In figure 2 it is possible to see the difference between the absorption and the desorption isotherm. If the desorption sequence is not followed through to the bottom but turns upwards again lets say from 70 % RH and slowly going up to 90 % RH, the curve would start from 70 % and finish at the 90 % RH level. This would result as a scanning curve, see arrow, figure 2.

DISCUSSION

The method is quite fast, for instance the whole sorption isotherm for wool fibers was measured during a time of approximately 72 hours. This makes it possible to run several tests after each other to make a statistical analyze of the material properties studied.

The time required for achieving one complete sorption isotherm lasts from a couple of hours for low density porous materials, such as glass wool insulation, up to about two weeks for high density porous materials such as concrete.

Comparing the obtained results with existing sorption isotherms shows that there is a strong reliability in the



material properties extracted through a sorption balance. However there are some requirements that must be met and errors to be aware of.

The sample size is limited due to two conditions, firstly the total maximum load of the sample is limited to a few grams and secondly the total mass change in the test cycle is limited to about a hundred milligrams. This makes it in some cases difficult to select a representative sample of a dense inhomogeneous material such as concrete.

The temperature in the climate cabinet is very stable. However it is possible that large and rapid fluctuations in the room temperature may influence the climate in the cabinet. This may in some cases have an effect on the results. Disturbances of this kind may be taken into account since the temperature of the climate cabinet is recorded in the data file.

The set point vapor pressure is controlled via the gas flow controllers which are very accurate. However there is a small potential error in the gas mass flows distributed. The volume of the gas is dependent on two factors, the actual vapor pressure level and the temperature. Both the vapor pressure level and the temperature dependencies are managed via a preset table which provides the correct mass flow settings. There is a possibility to validate the generated water vapor pressure by measuring the mass change of a saturated salt solution in the sorption balance. Ramping from a vapor pressure above to below the equilibrium vapor pressure level should validate that the requested vapor pressure level is the same as the generated vapor pressure level.

Other potential sources of error in this method are for instance those connected to the sample pans. It is of uppermost importance to clean the sample pans in between the tests *e.g.* by flushing the pans using de-ionized water. The results might otherwise be affected by the previous material. The cleaning of the sample pan also minimizes the build up of static electricity. Otherwise that will be shown as a slow but significant weight drift.

The sample pans and the reference pans should be kept in pairs to minimize errors due to different behavior during a test cycle. If sample and reference pan are made of glass they should be handled with care since glass easily cracks. If a small crack occurs, in the sample pan or the reference pan, it may be difficult to observe that with the naked eye however it may influence the result. If a crack is suspected then one way to detect it is to run a test cycle with clean empty pans and monitor the mass change. A feared crack in either of the glass pans will show as a substantial mass change during the test cycle with the empty pans.

The wire hanging down from the balance has to run free and the sample pan may not touch surrounding surfaces when in measuring position. The position of the wire may be disturbed when putting the sample pan on the hook of the wire. If the wire or sample pan touches a surface inside the instrument the balance readings are inaccurate and the mass of the sample is very unstable.

Another source of error occurs if the time defined for a vapor pressure step is too short. Then the sample mass increase/decrease per time unit at the end of the step has not yet reached a reasonably low level. If the time step at a certain vapor pressure is too short then equilibrium has not yet occurred. There is a possibility to extrapolate the results to evaluate the mass for the sample in equilibrium with belonging vapor pressure. The accuracy on the equilibrium mass is depending on many parameters *e.g.* how precise your extrapolation imitates the reality, how to choose sufficient number of values from the measuring for the extrapolation and so on. If the sample mass in a step has not leveled out at all it is not possible to make an extrapolation with a decent accuracy.

CONCLUSION AND IMPLICATIONS

The sorption balance has proved to be an important instrument to use when producing sorption isotherms, which is an important material property input in many applications regarding indoor air quality simulations.

This instrument has the potential to be widely used in future research on material properties regarding different compounds *e.g.* VOC's and others. This will be of great importance in order to achieve better input values in order to improve the accuracy in the results from the simulations.

With the sorption balance there is a possibility to measure the diffusion coefficient in the same measurement as the sorption isotherms are measured. The study of sorption kinetics is performed on a specimen with a well defined geometry. However this possibility has not been used very often yet.



In addition to this, details in the sorption phenomena such as the scanning curves may be studied by continuously increasing/decreasing the vapor pressure level, *i.e.* ramping. In certain sorption balances there is a possibility to make the vapor pressure perform a sinusoidal variation. This may also be used as an interesting tool to study how a material responds to continuously changing vapor pressures in the surrounding environment.

ACKNOWLEDGEMENTS

Funding was provided by both SBUF, the Development Fund of the Swedish Construction Industry and FORMAS, the Swedish Research Council for Environment, Agricultural Sciences and Spatial Planning.

REFERENCES

- Anderberg A. 2004. Moisture properties of Self-levelling Flooring Compounds. Report TVBM-3120, Lund 2004
- Caro Y., Pina M., Turon F., Gilbert S., Mougeot E., Fetsch DV., Attwool P. and Graille J. 2002. Plant Lipases: Biocatalyst Aqueous Environment and Enzyme Activity, *Biotechnology and Bioengineering*, Vol 77, NO. 6, March 20, 2002
- Cox SS., Zhao D. and Little JC. 2001. Measuring Partition and Diffusion Coefficients for Volatile Organic Compounds in Vinyl Flooring, *Atmospheric Environment*, Vol. 35, 2001, pp 3823-3830.
- Damain A., Blondeau P. and Tiffonet AL. 2002. Investigating the Influence of the Wall Materials and the Thickness on the Reversible Sink Effect, *Proceedings of the 9th International Conference on Indoor Air Quality and Climate- Indoor Air '02*, Monterey: Indoor Air '02, Vol 3, pp 564-569
- Johannesson B. 2000. Paper 4, A Test of Four Different Experimental Method to Determine Sorption Isotherms., Ph. D. Thesis, Lund University, Lunds institute of technology,
- Maa YF., Nguyen PA., Andya JD., Dasovich N., Sweeny TD., Shire SJ. and Hsu CC. 1998. *Pharmaceutical Research*, vol 15, NO. 5, 1998, pp 768-775.
- Murakami S., Kato S., Ito K. and Zhu Q., 2003. Modeling and CFD prediction for diffusion and adsorption within room with various adsorption isotherms, *Indoor Air 2003*, Vol 13, Supplement 6, pp 20-27.
- Svennberg K. 2005. Sorption isotherms for textile fabrics and foam used in the indoor environment. Report TVBH-7227, Lund 2005
- Wadsö L. and Markova N. 2001. Comparison of three methods to find the vapor activity of a hydration step. *European journal of Pharmaceutics and Biopharmaceutics* 51, 2001, pp 77-81.
- Zhao D., Little JC. and Cox SS. 2004. Characterizing Polyurethane Foam as a Sink for or Source of Volatile Organic compounds in Indoor Air, *Journal of Environmental Engineering, ASCE*, Vol. 130, 2004, pp 983-989.

III

Scanning sorption isotherms for hardened cementitious materials

Abstract

Drying of screeded floor slabs is an important issue for the building industry. However, virtually no attention is paid to the hysteresis of sorption isotherms in prediction models, mainly because of lacking data. Disregarding the hysteresis in prediction models will generate inaccurate predictions of future moisture distribution and remaining drying time. This paper presents a method for fast determination of scanning sorption isotherms and sorption isotherms by using a gravimetric vapor sorption balance. A sorption balance continuously determines the mass of a small sample subjected to a sequence of predefined vapor pressures and temperatures. Sorption isotherms and two examples of scanning sorption isotherms at 20 °C are presented. Results from three materials commonly used in screeded slabs are included, viz concrete W/C 0.65, concrete W/C 0.55, and a screed, Floor 4310 Fibre Flow. Absorption scanning curves obtained for concrete show a significant moisture history dependency as a consequence of the hysteresis of the desorption isotherm itself. Desorption scanning curves originating from the absorption isotherms indicates little influence of the moisture history.

Keywords:

Sorption isotherms
Scanning
Hysteresis

Introduction

Drying of residual moisture and moisture distribution in screeded floor slabs are important concerns for today's building industry. Residual moisture is here defined as water in a material above a threshold known to cause damage to an adjacent material. Moisture coming from different sources, e.g. mixing, screeds, adhesives, and air, influences the vertical moisture distribution in the floor slab. Estimations of moisture distribution therefore require, apart from initial and boundary conditions, determination of various moisture related properties. The amount of water physically bound in the pore system corresponding to the relative humidity, RH, in the surrounding air, sorption isotherm, play a significant role in estimations of moisture distribution. However, the moisture history dependence of sorption isotherms, hysteresis, is often overlooked when performing such estimations. Sorption isotherms are indeed central to estimating residual moisture and later drying-wetting processes, e.g. when screed and flooring are applied.

Estimation of moisture distribution in one layer concrete floor slabs [1] is rather well known, while moisture distribution in two-layer slabs is not, not surprisingly, since such combinations has not been thoroughly investigated. This lack of knowledge may result in moisture related material damages and combinations of material where residual moisture may be the key factor indirectly responsible for health problems. For example, adhesive may degrade, in moist and high alkali environments, and release volatile organic compounds, e.g 1-butanol and 2-ethyl-

hexanol. High concentrations of such VOC's are suspected to cause problems such as runny noses and eyes [2]. The residual moisture may also cause visual damage to the flooring, e.g. axial deformations, discolorations, and blisters.

Prediction models currently used to estimate drying and moisture distribution do not take into account the hysteresis phenomenon of the sorption isotherm [3-5]. Disregarding hysteresis will lead to inaccurate moisture distribution estimations, e.g. the RH level in the screed top layer adjacent to PVC-flooring. When screed and flooring are applied small amounts of water coming from the adhesive, will increase the RH substantially in the upper part of the floor slab. Underestimating this increase of RH in turn will amplify the risk of getting moisture damages. An increased awareness of this problem is needed, especially since a prolonged concrete drying time is unattractive to building contractors.

For modeling of two layer combinations, it is particularly important to recognize the hysteresis phenomena of the sorption isotherm, since scanning sorption isotherms profoundly affect the moisture redistribution. Prediction is straightforward for initial drying, when the moisture distribution follows the desorption isotherm at all depths of the slab. However, when a second layer is applied to the slab, e.g. screed, predictions of the future moisture distribution becomes more complex since hysteresis needs to be taken into account. Scanning sorption isotherms, commencing from the desorption isotherm will develop in the floor slab, e.g. when a screed is applied. These scanning absorption isotherms will start from low moisture content levels on the desorption isotherm (fig 1, curve 1 and 3) and end up at successively higher moisture content levels. When the screed eventually dries and moisture load in turn decreases, a new set of scanning desorption isotherms, (fig 1, curve 2 and 4) commencing from the endpoint of the absorption scanning isotherm.

Previous research determining scanning isotherms in cementitious materials is scarce [6-8]. Research by Ahlgren [8], was not systematically carried out and variations within a material were never investigated. In addition, the experimental set up using climate boxes as time-consuming, e.g. 1 year was needed to determine a complete isotherm. As a consequence of the long testing period significant hydration took place during the experiment and had to be considered. A detailed description of the climate box method is published in [9]. Sorption balances has been widely used in other research areas such as pharmaceutical and food industry for a long time [10-12]. The sorption balance was used on materials like sedimentary calcareous sandstone, porous glass by Anderberg and Wadsö [6] used a sorption balance to determine both sorption isotherms and scanning isotherms of self-leveling flooring compounds. An inkbottle pore-method to predict scanning was recently published [13].

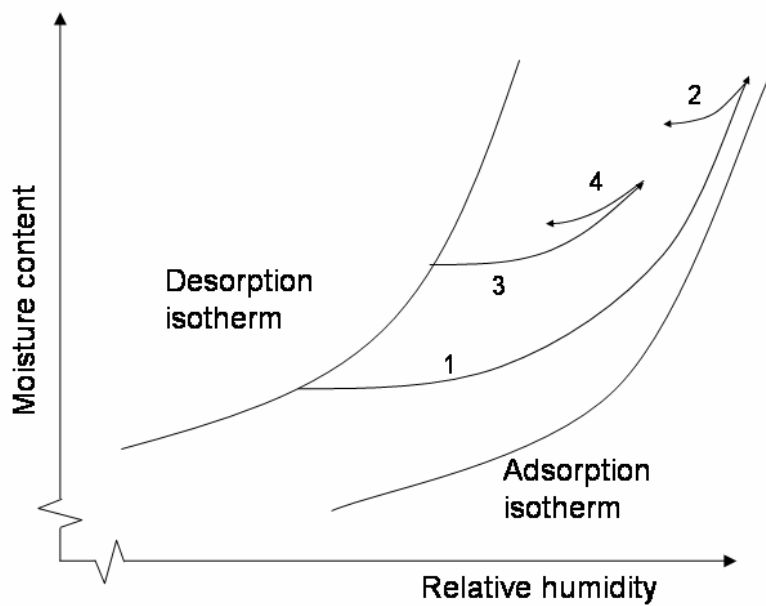


Figure 1. Illustration of scanning sorption isotherms. Adsorption scanning isotherms are marked 1 and 3 and desorption scanning isotherms marked 2 and 4.

This research has focused on experimental determination of isothermal scanning sorption isotherms for three different cement based materials, concrete W/C 0.65, concrete W/C 0.55, and a screed Floor 4310 Fibre Flow, SFC. A description of the method used and the investigated materials is presented as well as an estimation of the obtained accuracy of the performed measurements. Sorption isotherms have been obtained as well as two scanning sorption isotherms for each sample by using a sorption balance [14].

Material

Three cement-based materials were used in this study, two concrete mixes with a W/C 0.65 and W/C 0.55, and a screed, Floor 4310 Fibre Flow, SFC. Ordinary Portland cement was used in the two concretes tested. The basic binder of the SFC was aluminous cement. For a detailed description, see table 1.

Table 1. Mixture for each used material. Quantities are presented in kg/m³.

Material	w/c 0.65	w/c 0.55	Floor 4310, Fibre Flow*
CEMII/A-LL 42,5 R	250	400	
water	162,5	220	20
Sand 0-8 mm	976,4	1672	
Sand 8-12 mm	488,8		
Gravel 8-16 mm	488,8		
Portland Cement			1-5
Aluminous cement			5-20
Gypsum			2 -10
Dolomite 0.002-0.1 mm			31
Sand 0.1-1 mm			47
Polymer			1-5
Gelnium 51	0,214	0,292	

*Mixture according to manufacturer, mass-% of dry powder

All samples were obtained from a full scale floor construction at different stages drying in a room at 60 % RH and 20 °C. The samples were never subjected to RH levels below 60 % RH. To avoid effects of carbonation, at least 5 mm of the surface layer was chiseled off immediately prior to sampling. Samples were chiseled out from the floor construction at a specific time after casting about 1-7 days prior to testing. The actual RH level of the samples was not determined. However, the final RH levels reached prior to sampling were expected to decrease with time since samples were removed during a period of over year. Considering all samples were selected close to the surface and the youngest samples were older than one month the actual RH level of the samples should be closer to 60 % RH.

Sample mass varied within a range from 20 mg to 100 mg due to the limitations of the sorption balance. Concrete samples of this size may contain a comparatively large fraction of grits that are close to inert in sorption processes, apart from the interfacial transition zones, ITZ. The amount of sorped water in the ITZ of the larger grits is insignificant, when comparing the sorption isotherms. However, a grit fraction difference between samples significantly alters obtained sorption isotherm. In order to eliminate grit fraction differences, the cement content was determined for each sample, thus obtaining comparable sorption isotherms.

The cement ratio of the concrete samples was indirectly determined by analyzing the samples in an inductively coupled plasma atom emission spectroscopy, IPC-AES, thus obtaining the calcium content. The cement ratio, C_{ratio} , of each sample was calculated by using equation (1)

$$C_{ratio} = \frac{m_{Ca} \cdot M_{CaO}}{M_{Ca} \cdot 0.63} \quad (1)$$

where m_{Ca} represents the calcium content, M_{CaO} represents the molar mass of calcium oxide, M_{Ca} represents the molar mass of calcium, and 0.63 represents an assumed mass ratio of CaO

in the cement used. Two different batches of cement were used. Sorption isotherms for each sample were evaluated as mass of sorped water per mass of cement.

Method

Scanning curves and sorption isotherms were studied using a gravimetric vapor sorption balance. The balance continuously measures the mass of a material sample subjected to a test cycle of variable RH and temperature conditions. A mix of dry and saturated nitrogen, N₂, was used to achieve the set point RH level. Nitrogen, N₂, was used to prevent carbonation of the cementitious material. Data consisting of RH, temperature, and sample mass necessary for evaluating the samples sorption isotherms were recorded on a computer. The sorption balance inside the climate cabinet is symmetric with two glass pans suspended on hang-down wires from a balance arm. Linearly increasing and decreasing RH, ramping, was used in order to determine primary scanning curves of materials rewetted after initially being dried to some 60 % RH. Slow ramping, a linear increase of less than 1 % RH/50 minutes, increase the obtained degree of equilibrium at the current RH. The sorption isotherm was determined at the same time by step changes of RH during the test cycle. A detailed description of the sorption balance is found in [14].

Screeds may be applied on both dry and wet slabs with a unique moisture history. In order to capture data from multiple moisture histories, samples were removed from parts that dried in a 60 % RH climate for different time periods. Subsequently samples were put in a glass jar on a wetted cloth to soak in deionized water for minimum 6 hours to fill the capillary pores. However to achieve a sufficient degree of saturation for the concrete samples soaking continued for at least 48 hours. Soaking time could be reduced to about 6 hours for SFC samples. Immediately after soaking the sample was put on a sample glass pan and put in the sorption balance. Initial conditions in the sorption balance were set to 95 % RH and 20° C. As the balance was unstable a short while after loading, the test sequence was started after about 10-15 seconds, to avoid oscillating recordings.

Several test cycles all including constant RH levels and ramps were arranged in a sequence at a constant temperature of 20 ° C, fig 1. This test method has previously been used on screeds [6]. Test cycles were essentially based on constant steps starting from 95 % RH down to 10 % RH up to 95 % RH and finally a 0 % RH step at the end of the cycle. During this cycle two ramps were included, thus allowing investigation of the scanning phenomenon. Both absorption and desorption scanning were examined between 70 % RH and 95 % RH at a rate of 40 to 115 minutes per % RH. Absorption scanning started from an initial desorption phase and desorption scanning started after an initial desorption phase down to 10 % RH and a continuing absorption phase up to the start level at some 90-95 % RH. Before and after the scanning, constant RH steps were set in order to quantify the degree of equilibrium obtained from the sample. Test cycles to determine a complete sorption isotherm including two scanning curves lasted about 10-15 days.

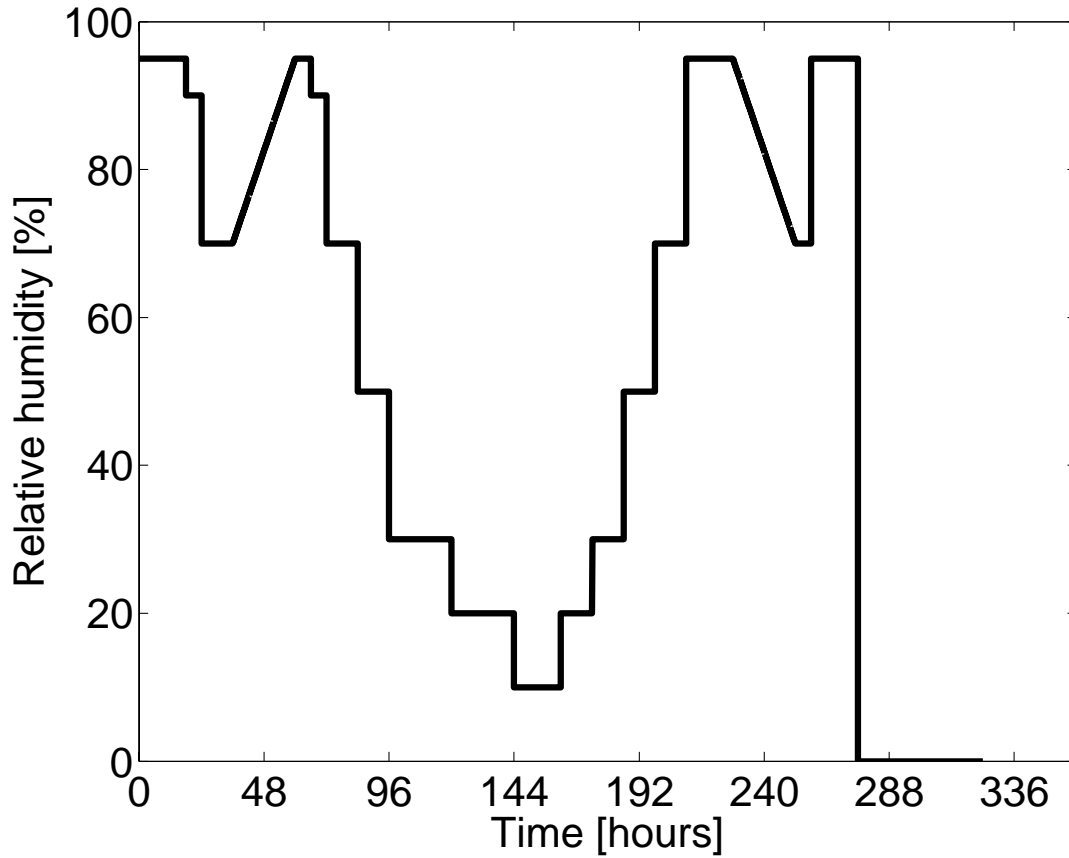


Figure 2. A typical test cycle for determining the sorption isotherm and scanning curve for the studied materials. The x-axis represents set point relative humidity in % RH and y-axis represents time in hours. The absorption ramp is located between 36 and 60 hours and the desorption ramp between 228 and 252 hours.

Mass equilibrium was almost reached for each RH step. The final part of each step was subjected to curve fitting using equation (2)

$$m_0(t) = m_f - (m_f - m_0(0))e^{-k(t-t_0)} \quad (2)$$

where $m_0(t)$ represents the recorded sample mass at the time t , $m_0(0)$ is the initial mass at time $t=0$, m_f represents the final mass, k is a curve fitting constant and t_0 is the initial time for each curve fitting. The best fitting curve was obtained by the method of least squares.

Two definitive points on the scanning curve, the beginning and the end, are determined by two constant RH steps before and after the ramp using equation (2). In between those points it is not possible to exactly calculate the equilibrium mass due to time lags effects. The difference between the last recorded sample mass and the extrapolated mass never exceeded 0.14 % of total mass change of each step excluding the step at 0 % RH.

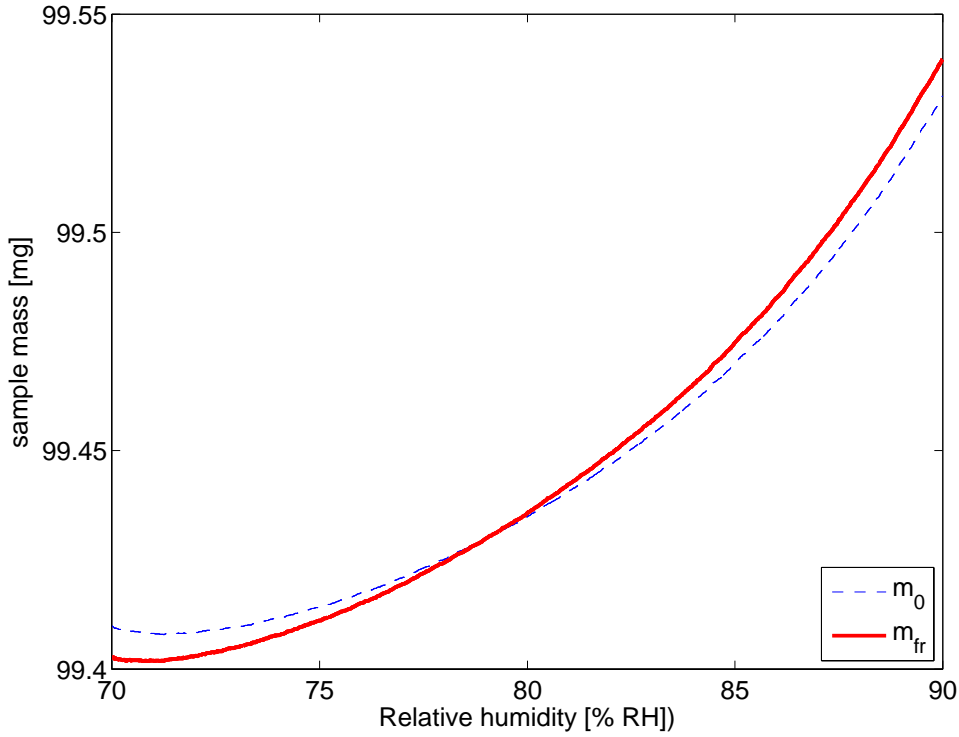


Figure 3. Illustration of the recorded sample mass m_0 (dashed line) in comparison with the m_{fr} (solid line) obtained by using equation 3 and 4.

This difference was evenly distributed, see fig 3, to the recorded mass with maximum difference in the beginning and zero in the end, using equation (3)

$$m_1(t) = m_0(t) - \frac{(m_0(0) - m_f) \cdot (t_{end} - t)}{t_{end}} \quad (3)$$

where $m_1(t)$ represents the resulting sample mass with the evenly distributed difference added, $m_0(t)$ represents the recorded mass, $m_0(0)$ represents recorded mass at the beginning of the ramp, m_f represents the extrapolated final mass before the ramp and t_{end} represents the ramp's ending time point, and t represents time.

Finally, the resulting mass of the scanning m_{fr} have been adjusted using equation (4)

$$m_{fr} = m_1(t) + \frac{(m_{fe} - m_0(t_{end})) \cdot t}{t_{end}} \quad (4)$$

where m_{fr} represents the resulting sample mass with the evenly distributed difference added, $m_1(t)$ from equation (3), m_{fe} represents the extrapolated equilibrium mass in the end of the step succeeding the ramp, $m_0(t_{end})$ represents the recorded mass at the end of the ramp, t represents time, and t_{end} represents the ramp's ending time point.

The difference between the recorded and the extrapolated final mass is calculated using equation (2). This difference has the largest impact at the beginning of the scanning curve due to time lag effects. However, the difference at the end of the scanning curve is most affected

by difference between the recorded and the extrapolated final mass at the end of the scanning curve. To minimize the time lag effects eq. 3 and 4 were used.

Results

Results of this study are divided into two parts. The first part, fig 4-6, presents sorption isotherms of W/C 0.65, W/C 0.55, and SFC respectively. The second part, fig 7-9, shows sorption isotherms of individual samples including adsorption and desorption scanning curves and the difference in amount of sorped water depending on when the samples were removed from the slab.

The x-axis in figures 4-9 represents the relative humidity in % RH. The y-axis in fig 4, 5, 7, and 8 represents the moisture content, quantified as the evaporable moisture content, W_e , divided by cement content, C . The y-axis in fig 6 and 9 represents the moisture content per mass of material as a fraction of mass at 10 % RH.

Sorption isotherms are presented for both concrete and SFC, fig 4-6. The results clearly show a hysteresis between desorption and absorption isotherms in all investigated materials. The obtained absorption isotherms show a significantly lower scatter than the obtained desorption isotherms.

One remarkable finding is the significant history dependency, hysteresis, in the desorption isotherm itself. Desorption isotherms for concrete W/C 0.65, determined 2 months after the casting are significantly higher, between 45 - 95 % RH, than subsequently removed samples, fig 4. This is also the case for the W/C 0.55 concrete, fig 5.

An important remark regarding the results of the 1.5 months and one of the 2 months old W/C 0.65 samples has to be pointed out. Their moisture contents at saturation are significantly lower than the remaining three samples showing a W_e/C of about 0.22 and 0.35 compared with 0.43-0.45.

Desorption curves for the SFC indicate minor time dependency. The hydration degree does not increase much between 1 and 9 months since the main binder component in the SFC is aluminous cement.

All materials are regarded as dry at 10 % RH. Markers on the sorption isotherms represent the extrapolated water gain at each RH step. The solid lines represent a general polynomial curve fit of the markers for each sorption isotherm.

Four scanning curves for each material are presented in fig 7-9. Two obtained absorption scanning curves are shown for each material, these mainly start from the desorption isotherms at 70 % RH. Two obtained desorption scanning curves are shown for each material; these mainly start from the absorption isotherms at 95 % RH.

All measurements are performed at 20 °C.

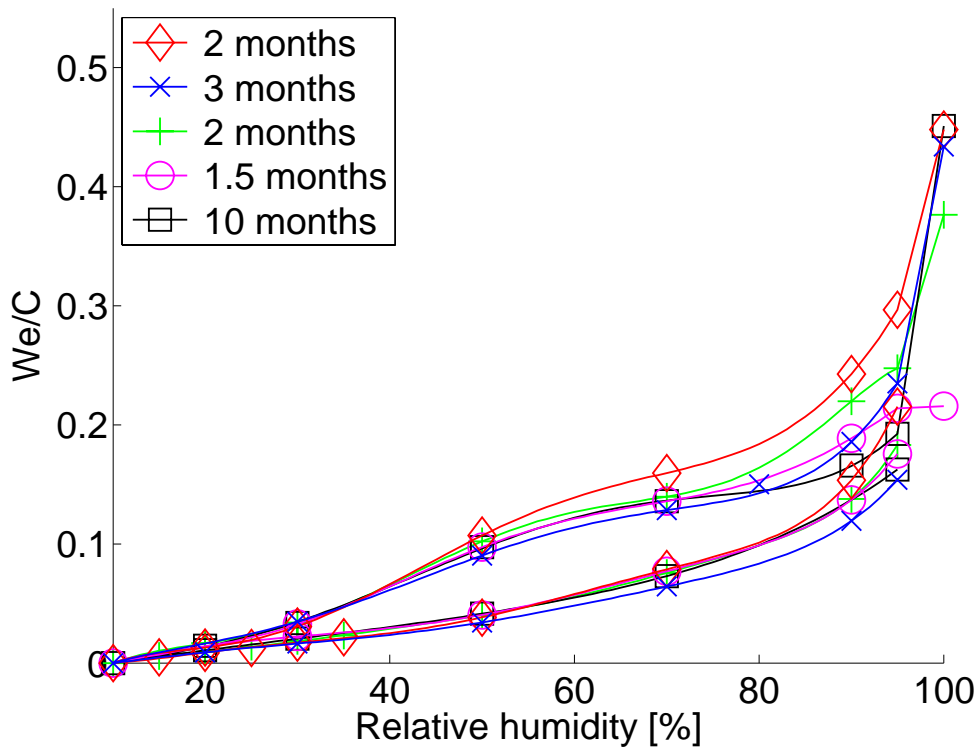


Figure 4. Sorption isotherms for concrete W/C 0.65, samples removed at different times from the floor slab

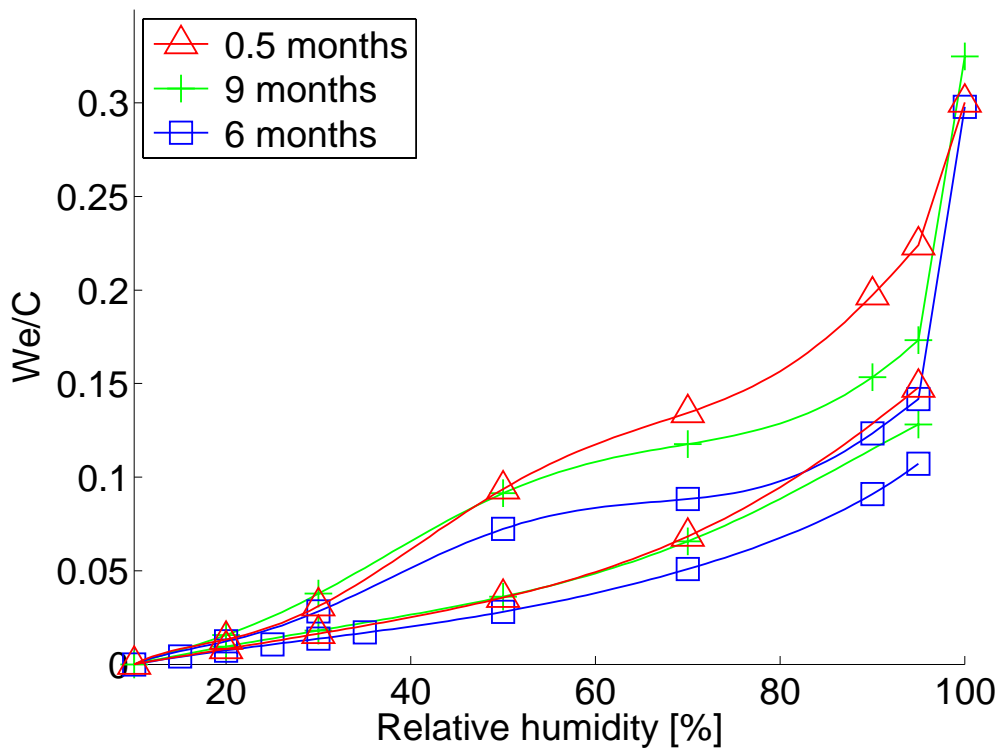


Figure 5. Sorption isotherms for concrete W/C 0.55, samples removed at different times from the floor slab

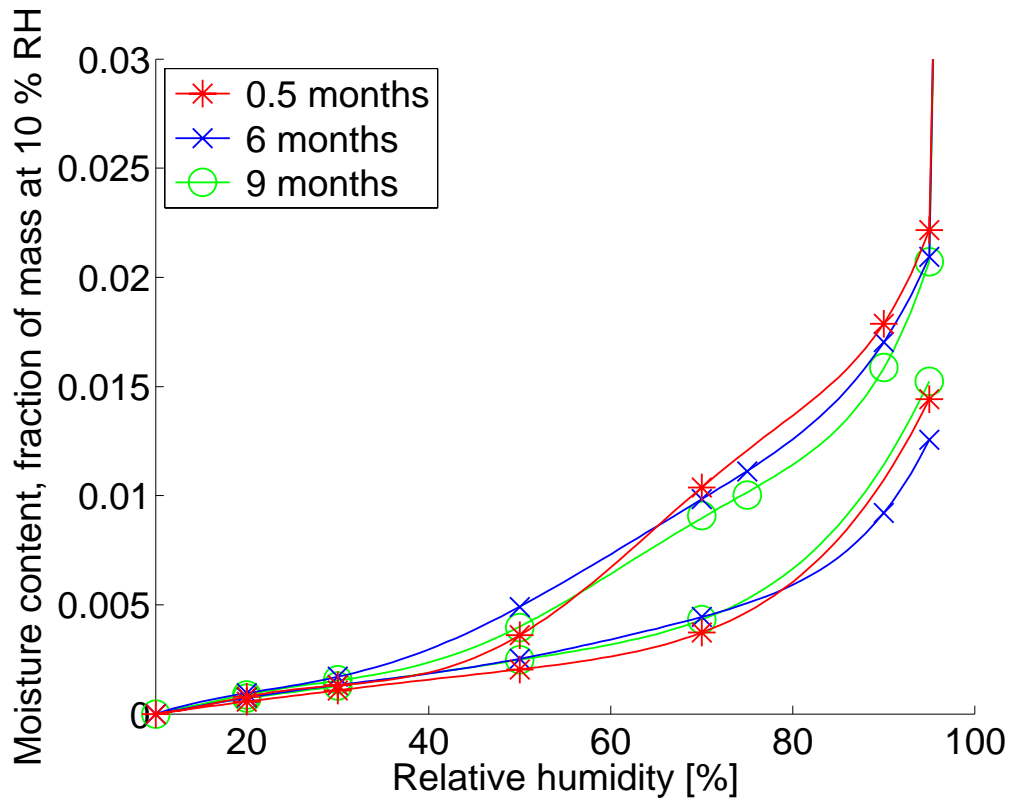


Figure 6. Sorption isotherms for Floor 4310 Fibre Flow, samples removed at different times from the floor slab

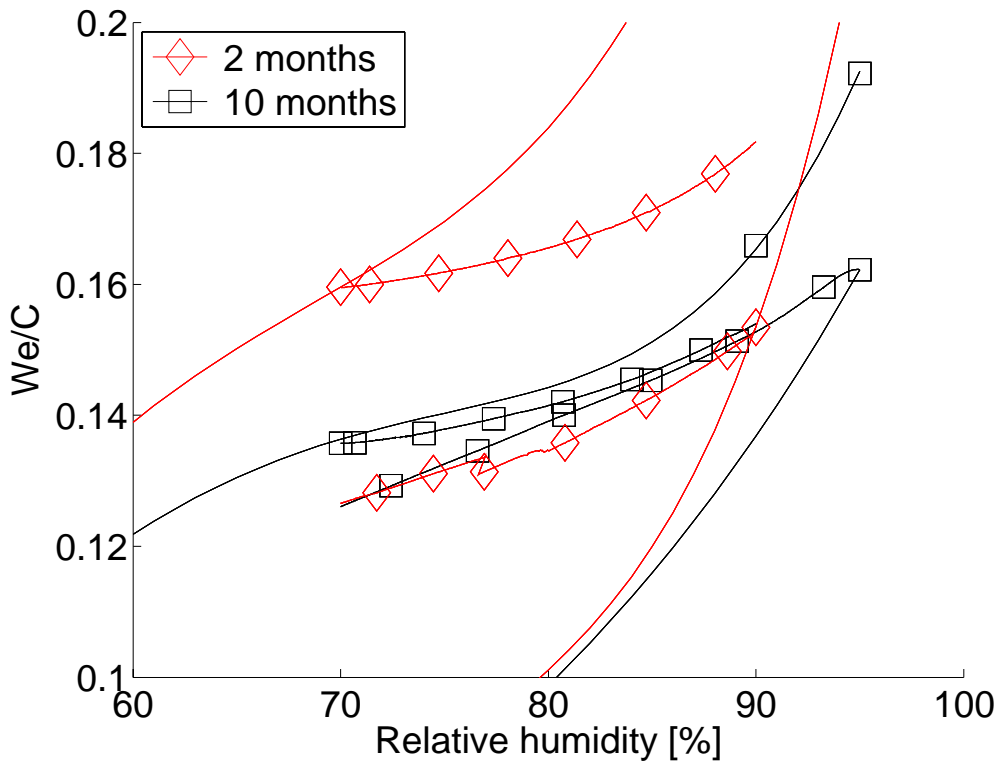


Figure 7. Sorption isotherms including absorption and desorption scanning curves for W/C 0.65

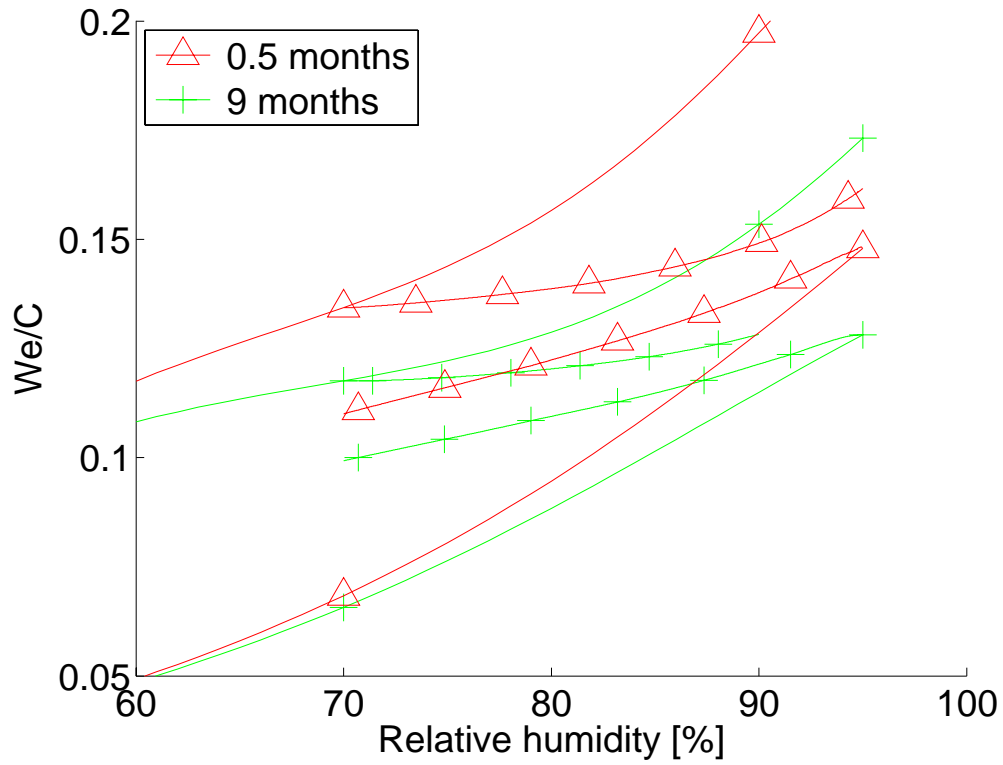


Figure 8. Sorption isotherms including absorption and desorption scanning curves for W/C 0.55

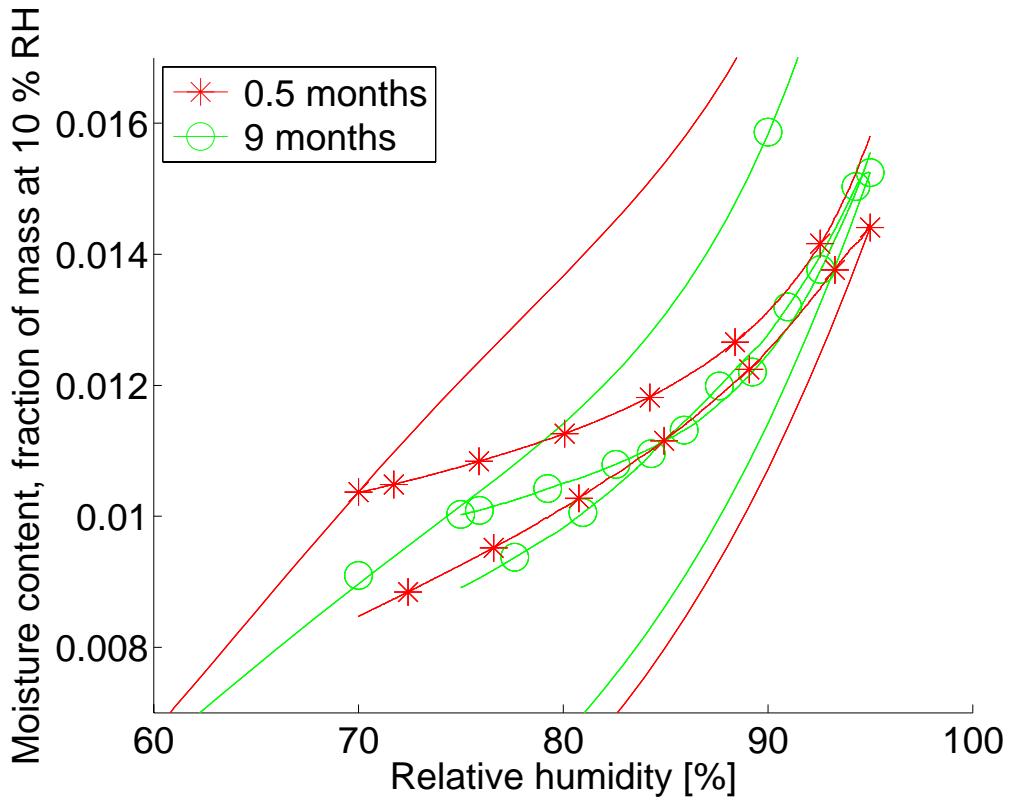


Figure 9. Sorption isotherms including absorption and desorption scanning curves for Floor 4310 Fibre Flow

Discussion

Sorption and scanning isotherms were determined for samples of concrete W/C 0.65, W/C 0.55 and SFC. Significant hysteresis was observed for desorption isotherms for concrete W/C 0.65 and W/C 0.55, between 60 % - 95 % RH, fig 4, 5. The moisture content for the desorption branch decreased with an increased drying time. As a consequence the adsorption scanning isotherm decreased considerably, fig 7, 8. This does not agree with previous findings of the desorption isotherm [15]. However, this disagreement may originate from a different sample preparation. Powers first water cured the samples and then dried them to 0 % RH before determining absorption and subsequently the desorption isotherm. In addition, later research has shown that there is a risk of damaging the pore structure when drying the specimen to levels below 10 % RH [16].

To prevent structural and physical damage of the hydrates, all sorption isotherm data was obtained without exposing samples to levels below 10 % RH. However, the most important finding is that the longer a concrete is kept in a 60 % RH environment the larger the decrease of the desorption isotherm, fig 4, 5. Only minor changes were observed in the absorption isotherm above 80 % RH. A small but noticeable decrease in desorption isotherms above 60 % RH with curing time was shown for the SFC material, fig 6. Both sorption isotherms and scanning curves for SFC agrees well with previous research on similar material [6].

The absorption scanning curves show that the moisture content increases at a low rate at an early stage. A loss of mass was recorded in the beginning (not visible in the diagram) due to time lag effects. As the relative RH level increases, the moisture content increases and the curve ascends towards the absorption isotherm. In this first phase the moisture is probably accumulated mostly as adsorption on the pore walls made available after previous drying. As the scanning curve approaches the boundary absorption curve, it curves upwards more and more. This curving upwards is most probably due to a gradual transition from adsorption on the pore walls to capillary condensation in the pores. When the RH level increases, the absorption scanning curve comes closer to the boundary absorption curve. However, the curve appears never to cross the boundary defined by the absorption isotherm. Most likely the absorption scanning curve reaches the boundary absorption isotherm at 100 % RH, as stated earlier by Powers [15].

Desorption scanning curves, starting from the absorption isotherm, is for a minute period parallel to the x-axis and then descend and softly turns towards the desorption isotherm. From the results of this study it is not possible to suggest if the desorption scanning curve hits the desorption isotherm above 0 % RH. However, the results clearly demonstrate that an ascending absorption scanning curve could cross a descending desorption scanning curve, see figure 8.

The decrease of sorption isotherms of concrete through aging is often explained as structural changes of the material due to hydration. In this study however, hydration could not completely explain the decrease of desorption isotherm branches with an increased drying time. A rough estimate showed that all samples taken from the large specimens had an equal degree of hydration, about 0.8. The hydration degree was estimated judging from both the total porosity based on water content at saturation, see figure 3 and 4, and the drying conditions of the samples. Below 80 % RH hydration of cement grains virtually ceases [17].

An equal hydration would imply an equal amount of physically bound water at the desorption branch in the range from 60 % RH to 95 % RH. However, the desorption isotherm decreased

significantly with drying time in that range. It is not possible to completely eliminate differences in hydration degree since it was never determined. There is a possibility that the desorption isotherm is affected by the moisture history of the material itself, an indication of a hysteresis effect previously not found in literature.

A comparison of the amount of sorped water at saturation showed a relatively small spread for the samples, see figure 4 and 5. However, two samples, 1.5 and 2 months old respectively, showed significantly lower moisture content at saturation. One probable cause of this difference is that these samples were removed too early from the wet cloth, thus not reaching a saturated state. This is clearly seen when comparing the water content at 100 % RH, see figure 4, where the W_e/C is about 0.22 and 0.37 for the two samples compared with 0.43 - 0.45 for the remaining samples.

Since the boundary sorption isotherms and scanning curves were determined at the same time the sample mass was checked before and after scanning to see whether the process was reversible. The results from this examination indicated that both absorption scanning starting from the desorption isotherm and desorption scanning starting from the absorption isotherm were reversible.

References

1. Nilsson, L.-O., *Hygroscopic moisture in concrete - Drying, measurements & related material properties*, in *Division of building materials*. 1984: Lund. pp. 170.
2. Wolkoff, P., et al., *Are We Measuring the Relevant Indoor Pollutants?* *Indoor Air*, 1997. **7**(2): pp. 92-106.
3. Holm, A.H. and H.M. Kuenzel, *Practical application of an uncertainty approach for hygrothermal building simulations-drying of an AAC flat roof*. *Building and Environment*, 2002. **37**(8-9): pp. 883-889.
4. West, R.P. and N. Holmes, *Predicting moisture movement during the drying of concrete floors using finite elements*. *Construction and building materials*, 2005. **19**: pp. 674-681.
5. Obeid, W., G. Mounajed, and A. Alliche, *Mathematical formulation of thermo-hygro-mechanical coupling problem in non-saturated porous media*. *Computer Methods in Applied Mechanics and Engineering*, 2001. **190**(39): pp. 5105-5122.
6. Anderberg, A. and L. Wadsö, *Moisture in self-levelling flooring compounds. Part II. Sorption isotherms*. *Nordic concrete research*, 2004. **32**(2): pp. 16-30.
7. Baroghel-Bouny, V. and T. Chaussadent, *Texture and moisture characterization of hardened cement pastes and concretes from water vapour sorption measurements*, in *The modelling of microstructure and its potential for studying transport properties and durability*. 1996, Kluwer Academic Publishers.
8. Ahlgren, L., *Fuktfixering i porösa byggnadsmaterial (in Swedish)*, in *Division of building technology*. 1972, Lund University Lund. pp. 197.
9. Atlassi, E., L.-O. Nilsson, and A. Xu. *Moisture Sorption Properties of Concrete with Admixtures and Industrial By-products - Implications for Durability*. in *Durability of Concrete: Aspects of Admixtures and Industrial By-products, 2nd International Seminar*. 1989. Stockholm: Svensk Byggtjänst.
10. Maa, Y.-F., et al., *Effect of spray drying and subsequent processing conditions on residual moisture content and physical/biochemical stability of protein inhalation powders*. *Pharmaceutical research*, 1998. **15**(5): pp. 768-775.

11. Costantino, H.R., *Water sorption behavior of lyophilized protein-sugar systems and implications for solid-state interactions*. International journal of pharmaceutics, 1998. **166**: pp. 211-221.
12. Hébrard, A., et al., *Hydration properties of durum wheat semolina: influence of particle size and temperature*. Powder technology, 2003. **130**: pp. 211-218.
13. Espinosa, R.M. and L. Franke, *Inkbottle Pore-Method: Prediction of hygroscopic water content in hardened cement paste at variable climatic conditions*. Cement and Concrete Research, 2006. **36**(10): pp. 1954-1968.
14. Åhs, M., A. Sjöberg, and A. Anderberg. *A method for study sorption phenomena*. in *Proceedings of the 10:th International Conference on Indoor Air Quality and Climate*. 2005. Beijing, China pp. 1969-1973.
15. Powers, T.C. and T.L. Brownyard. *Studies of the physical properties of hardened portland cement paste*. in *Journal of the american concrete institute*. 1948. Chicago, Illinois.: PCA Research Laboratories.
16. Zhang, I. and F.P. Glasser, *Critical examination of drying damage to cement pastes*. Advances in cement research, 2000. **12**(2): pp. 79-88.
17. Powers, T.C. *A discussion of cement hydration in relation to the curing of concrete*. in *Proceedings 27*. 1947. Washington, D.C.: Highway Research Board pp. 178-188.

VI

Moisture distribution in screeded concrete slabs

Abstract

Residual moisture in screeded concrete slabs is transported towards the screed as it redistributes from interior parts after flooring. As the humidity increases the achieved level may exceed the critical humidity level, thus promoting deterioration of adjacent materials. A qualitative model of moisture distribution in screeded concrete slabs is presented through different production phases. From this model it is possible to make clear humidity changes which are important when making predictions of the future humidity achieved beneath flooring, as corresponding moisture properties are affected by such changes. The relative humidity, RH, distribution was determined before flooring and after a certain time of redistribution in nine concrete slabs made of w/c 0.65 and w/c 0.4 concrete screeded with w/c 0.55 cement mortar and Floor 4310 Fibre Flow. The redistribution of humidity is clearly demonstrated in the results section, where the humidity increase beneath flooring is exemplified. The initial moisture distribution and subsequent changes determined in the nine screeded concrete slabs fitted the presented qualitative model. This model may be used to develop current moisture distribution prediction tools further by introducing a more complex interrelation between moisture changes and corresponding changes in moisture related properties.

Keywords:

Moisture redistribution
Qualitative model
Relative humidity
Screeded concrete slab

1 Introduction

Drying of residual moisture in concrete floor slabs has been brought into focus during the last decade. Residual moisture in concrete is water remaining after the requirements associated with i.a. pouring and curing are fulfilled. Depending on the water/cement ratio and environmental conditions, different quantities of water will be released to the surroundings until moisture equilibrium is obtained. If a moisture barrier is installed on the slab top i.a. PVC flooring, residual moisture will redistribute and increase the humidity in the surface. To reduce the humidity level attained beneath the flooring, drying of residual moisture in concrete slabs is crucial. Drying of concrete slabs is regularly overlooked at the construction site, despite the fact that it is e.g. time consuming, difficult to accelerate, and often on the critical path.

Insufficiently dried concrete slabs in the presence of high alkali levels have been accused to promote and sustain degradation of adhesives beneath PVC-floorings [1]. Degrading adhesives are known to emit volatile organic compounds, VOC, to the indoor environment [2]. Exposure of such VOC's in high concentration has a negative health impact on people living or working in such environments [3]. Emissions originating from the damaged floor constructions are of rather low concentration. The impact on health regarding long term exposure of such low concentrations is not yet established [4]. However, research has shown a

higher frequency of people experiencing diffuse health related symptoms when staying in buildings suffering from such damages. These symptoms are hard to correlate to moisture damaged floor constructions as they appear as, i.a. runny nose and irritated respiratory passages.

Moisture distribution determination in concrete floor slabs, especially screeded concrete slabs is difficult. Independent of the applied method, the outcome becomes affected by uncertainties originating from, i.a. sampling methods, equipment or unforeseen moisture losses from samples prior to testing. One recently developed method to determine the relative humidity, RH, in a concrete slab is based on long term monitoring and logging of the RH. The temperature effects on in-situ measurements of RH are easy to realize when looking on a diagram of the results obtained through long term in-situ measurements [5].

Prediction of moisture distribution in screeded concrete slabs is even more difficult. It is not only strongly dependent on precise characterization of the comprising materials but also a detailed knowledge of moisture/material interactions, drying time, drying conditions and concrete/screed moisture interactions. Common draw backs in current models [6-8] are besides simplified moisture related properties for materials used in floor constructions, often poorly described moisture interactions between flooring, screed, and concrete. Current models may therefore generate predictions impaired by large uncertainties.

This study presents a model to qualitatively analyze the moisture distribution in a screeded concrete slab. The model is described in section 2, where the moisture distribution is shown for two cases through four phases. A condensed description of vital moisture related aspects of each phase is included. In order to verify the model the moisture distribution was determined on a number of screeded slabs before flooring and after redistribution. The experimental set up is described in section 3 and the moisture distribution before and after flooring in each slab is presented in section 4. In section 5 the results are discussed and a quantitative model is proposed along with a detailed description how drying and moisture redistribution may affect the obtained humidity of a specific point in a material.

2 Qualitative model

This section presents a qualitative model describing moisture distribution in screeded concrete slabs during construction. The model covers the time from pouring of the structural slab, continues with screed casting and finishes after flooring installation.

Moisture is evenly distributed in a freshly poured concrete slab. During hydration, the humidity level decreases uniformly as a result of moisture binding chemically to the cement. Further drying occurs when the exterior humidity is lower than the interior slab humidity. The surfaces dry first as this moisture must be released prior to the interior moisture. This moisture variation through the slab is presented as a moisture distribution profile, showing the slab center humidity in relation to the surfaces.

When a screed is applied on the slab, moisture from the screed will rewet the slab surface and redistribution of the interior moisture will initiate. Owing to the wet screed the humidity in the slab top surface will increase. However, drying at the slab base and screed top continues. The screed humidity decreases as some moisture becomes chemically bound. Finally,

impermeable flooring is applied on the screed and as a result the residual moisture redistributes.

Figure 1 presents two cases of screeded concrete representing important events related to moisture distribution. The top figure illustrates a screed applied on a newly poured concrete slab and the figure below illustrates when the screed is applied on an old concrete slab subjected to years of drying. In each phase the dotted line represents initial moisture distribution and the solid line represents the moisture distribution prior to entering next phase. The double dashed/solid line separates the phases from each other and in addition also indicates maximum moisture level. It may be used for comparing the difference in absolute level between both cases and phases.

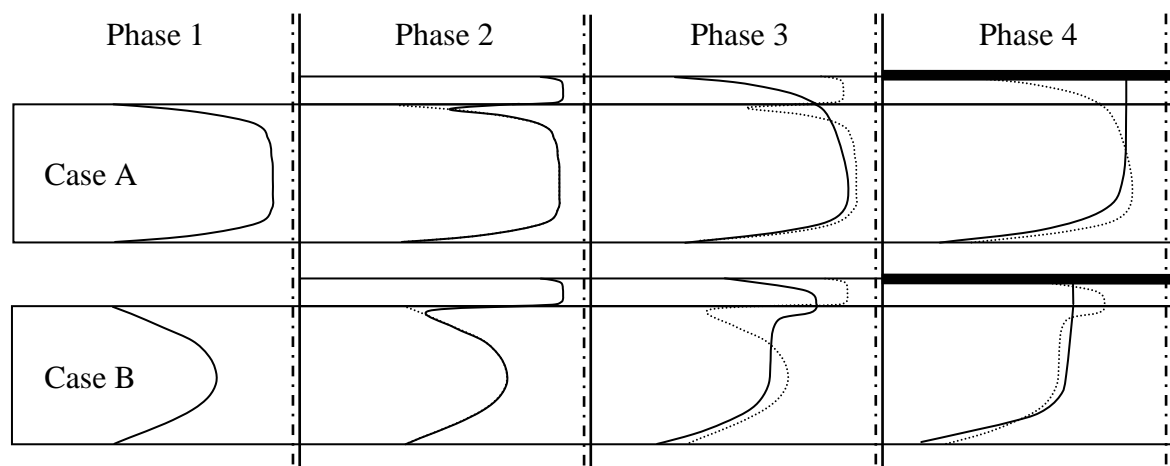


Figure 1. Phase 1 shows the distribution of residual moisture in a concrete slab. A wet screed is applied in phase 2. The applied screed dries in phase 3, and finally in phase 4 flooring is installed.

Phase 1. Drying of a concrete slab's residual moisture

- A. This profile illustrates the moisture distribution of a slab during initial drying. It is obtained as a result of a vertical moisture flow from the humid slab center through the bottom and top surfaces. The slab surfaces have lost a lot of moisture in relation to the slab interior. A steep gradient on the moisture profile indicates a larger moisture flow in relation to a flat.
- B. Like case A. However, this illustration shows a slab where drying has proceeded further. The moisture level in the central parts of the slab has dried significantly.

Phase 2. Applying a screed on top of the slab

- A. In this phase a screed is applied on the concrete slab. The screed top surface dries through a moisture release to the less humid surroundings. Moisture flow at the slab top surface becomes reversed and as a consequence the screed base dries. However, on the expense of the slab top surface becoming increasingly humid. Just above the slab center moisture transport is still directed towards the screed. However, the direction of moisture flow at the slab base remains unaffected. Additionally, drying in the screed occurs owing to the cement's chemical moisture binding.
- B. Like case A. However, the moisture level difference between slab and screed is significant, implying that the slab has a larger capacity to receive moisture from the screed compared to case A.

Phase 3. Drying of the screed's residual water

- A. A significant amount of moisture has dried from the screed. Near the slab surface a considerable humidity increase is showing. The screed's top surface humidity is lower than in the base. This is a result of moisture redistributed from the interior parts of the slab.
- B. Like case A. However, the moisture level in the slab is substantially lower than the screed. Moisture is still being transferred down from the screed into the slab.

Phase 4. Installation of an impermeable flooring and redistribution of moisture

- A. The surface is covered with moisture impermeable flooring, an efficient barrier reducing moisture transport from the screed surface. The screed no longer dries but becomes increasingly humid as a result of moisture redistributing from interior parts of the slab to the top surface. Drying will follow when the moisture flow from the screed becomes larger than the flow towards it. Future moisture profiles will never exceed this last phase, unless moisture is supplied from the exterior.
- B. Like case A. Further drying of the central parts of the screed occurs as additional moisture is relocated down into the slab and up towards the flooring. Yet some moisture is transferred from the slab center towards the screed.

3 Experimental set up

3.1 Material

Nine screeded slabs, covering an area of $800 \times 1200 \text{ mm}^2$, with PVC-flooring on top were used in this study. Eight solid slabs were cast and preconditioned in the laboratory, the ninth a hollow core slab, HCS, was cast in a factory. The solid slabs were made of concrete, C, see table 1, and separated into two batches by their thicknesses, see table 2. Batch 1, consisted of slab 1-4, 110 mm thick and batch 2, slab 5-8, 220 mm thick. Batch 3 the HCS was manufactured with C_{HCS} , 265 mm thick with 5 longitudinal core holes.

Two different screeds were applied on the slab surfaces, cement mortar, M, and a self-leveling flooring compound, SFC. The SFC labeled Floor 4310 Fibre Flow, manufactured by Maxit, was delivered as a dry powder mix in 25 kg bags. A detailed description of concrete, mortar and SFC mixes is found in table 1.

Table 1. Mixture description of the used materials. The quantities are presented in kg/m³.

Material w/c ratio	C 0.65	M 0.55	C_{HCS}* 0.4	SFC*
CEM II/A-LL 42,5 R	250	400		
CEM I 52,5 R			390	
Portland Cement				1-5
Aluminous cement				5- 20
Gypsum				2 -10
Water	162	220	147	20
Dolomite 0.002-0.1 mm				31
Sand 0.1-1 mm				47
Sand 0-8 mm	976	1672	973	
Sand 6-13 mm			851	
Sand 8-12 mm	489			
Gravel 8-16 mm	489			
Polymer				1-5
P30			1,2	
Glenium 51	1,5	2,9		

* Mixture according to manufacturer, mass-% of dry powder, density~1900 kg/m³

All surfaces and material connections around the circumference were sealed with self adhesive bitumen aluminum sheets, aluminum tape without bitumen were also used. Cavities remaining after RH distribution sampling were filled with a self expanding foam, DANA Joint - & insulation foam 591.

3.2 Methods

Formwork

Coated plywood, 13 mm, was used as formwork for the solid concrete slabs. Each form was put on a pallet, 800*1200 mm. Before pouring the forms were prepared with form oil, using an ordinary paint brush. No reinforcement bars were put inside the form. However, lifting tools were fixed on one vertical plywood sheet prior to pouring, to facilitate handling of the heavy concrete slabs in the laboratory. The web above the HCS mid core hole was cut off forming a 100*800 mm slit. Coated plywood sheets painted with form oil were used as formwork on each side of the mid core.

Pouring slab

Concrete pouring was carried out in laboratory conditions, in formwork prepared for each of the three different batches. The HCS mid core hole was filled with material C through the slit. All castings were cured for 2 days covered by a plastic sheet, thereafter the formwork was stripped. Subsequently the vertical edges on each slab were sealed with self adhesive bitumen coated aluminum sheets to obtain one dimensional moisture flow.

First drying

All slabs were drying in a climate room at 20 °C and 60 % RH. Batch 1 was dried laying flat on coated plywood and Batch 2 was vertically tilted to better obtain double sided drying.

In order to accelerate drying, slab 7 and 8 were put in a climate box, for 269 days at 32 °C, 39 days after pouring. The humidity in the climate box was obtained with Sodium Bromide,

NaBr, saturated salt solution, which generates an equilibrium humidity of 55 % RH at 32 °C, [9].

Pouring screed

Prior to screed application a primer, Optiroc 6000, was evenly spread on each slab top surface by using an ordinary paint brush. Mixing was carried out in the laboratory by using a concrete mixer. Slab 1, 2, 6, and 8 were applied with 40 mm of material SFC, slab 3, 4, 5, and 7 with 40 mm of material M, see table 2. The HCS was applied with 60 mm of material SFC. All screeds were cured for 2 days, covered by a plastic sheet. Sealing of vertical screed edges were completed subsequent to curing, by using self adhesive bitumen coated aluminum sheets.

Second drying

After curing the screed, all slabs were put in a 20 °C and 60 % RH climate for additional screed drying. Slabs in batch 2 were once again vertically tilted.

Installation of flooring

At the day of flooring, adhesive was applied on the screed top surface. The quantity of applied adhesive is found in table 2. Flooring installation was completed within 10 minutes after adhesive application. Immediately after flooring, additional aluminum tape without bitumen was used to seal the flooring rim to the previously installed aluminum sheets on the vertical slab edges.

Table 2. Description of drying and material application sequence

Batch No.	1				2				3
Slab	1	2	3	4	5	6	7	8	9
Material	C	C	C	C	C	C	C	C	C _{HCS}
1 st Drying [days]	105	105	110	110	9	11	408	408	28 ¹
Screed	SFC	SFC	M	M	M	SFC	M	SFC	SFC
2 nd Drying [days]	48	96	98	90	261	259	40	40	138
Adhesive [m ² /l]	3,6	3,6	3,5	4,3	3,1	3,0	3,3	3,0	3,0
Flooring	PVC	PVC	PVC	PVC	PVC	PVC	PVC	PVC	PVC
Redistr.[days]	206	158	149	157	269	269	91	91	273

¹ Initial drying time of the C filling of the mid core. The HCS is cast approx. 60 days earlier.

Determination of moisture distribution

The RH profile in all nine slabs was determined prior to flooring and after a certain time of moisture redistribution. All samples were obtained at least 100 mm from the vertical aluminum sealing on the slab to avoid possible edge effects. To avoid possible drying disturbances, moisture profiles were always obtained no less than 260 mm from prior sampling.

Samples were obtained vertically through the slab using a 90 mm core drill gradually penetrating the concrete in sections of 20 – 30 mm. Each section was chiseled off and crushed into gravel size pieces. Immediately after crushing, pieces of 5-15 mm size were put in glass test tubes, instantly sealed with elastic rubber plugs. Pieces considered to contain a high degree of cement pasta were selected in order to maximize the moisture quantity.

The RH was measured by using a carefully calibrated RH sensor, Vaisala HMP-44, inserted in the test tube. These sensors were connected to a computer logging system displaying the

readings as curves in a diagram on a screen. When the curve in the diagram had leveled out the actual reading was performed, some 12-48 hours after inserting the sensor in the test tube. The RH sensors were preconditioned in 20 °C and 55 % RH prior to measurements.

One day after drilling, the cavities were filled with self expanding foam DANA 591. No water was used for lubricating the core drill when sampling.

4 Results

Moisture distribution was determined in each slab prior to flooring, thin dashed lines, and after redistribution, thick solid lines, see fig 2. RH is shown on the x-axis in % RH and the y-axis represents the vertical distance in mm from the slab surface, positive figures for increasing depth. Each line marker represents the obtained RH level in each section. Flooring installation is defined as day 0 (zero) and each legend states when the profile was obtained in relation to flooring. The screed/concrete boundary is visualized in the top of each figure using a horizontal thick solid line. Dashed lines in the HCS figure represent edges of the longitudinal mid core hole.

The diagram representing slab 1 displays the RH distribution 1 day and 206 days after flooring. Each RH measurement has an uncertainty of 1 - 2 % RH, therefore changes within this range may not be significant. Drying of the screed base, at the 30 mm level has decreased the RH from 93 to 87 % RH; a virtually uniform moisture profile in the screed is shown. Throughout the concrete slab, a considerable decrease exceeding 5 % RH is shown after moisture redistribution.

The moisture distribution in slab 2 was obtained 47 and 5 days prior to flooring and after 158 days of redistribution. Before flooring significant drying in excess of 10 % RH is shown in the top 60 mm of the slab. The screed humidity increase after 158 days of redistribution is about 5 % RH. The humidity decrease of nearly 10 % RH in the concrete base indicates significant drying through the coated plywood.

In slab 3 the RH distribution is shown 56 and 14 days prior to and 158 days after flooring. Duplicate samples were obtained from different locations in the slab, 56 days before flooring. Screed humidity drops considerably about 7 -10 % RH during the first 42 days of drying. After flooring the humidity level increases significantly, from 74 to 86 % RH in the top 20 mms of screed. Additionally, after 158 days of redistribution slab humidity has decreased about 4 % RH almost uniformly.

The moisture distribution in slab 4 is shown 48 and 6 days prior to flooring, and 157 days after redistribution. The screed humidity has decreased substantially during the initial 42 days of drying, about 7 - 5 % RH. The moisture level 50 mm below flooring has decreased about 2 - 4 % RH, showing larger decrease at the base, comparing the moisture profile obtained 6 days prior to flooring with 157 days of redistribution. The screed humidity has increased about 2 - 7 % RH after redistribution, the larger increase was found at the 10 mm level close to the flooring.

After 269 days of redistribution shown in slab 5, humidity increases considerably about 10 % RH in the screed compared with the profile obtained 3 days before flooring. A minor humidity increase in the slab top section is also indicated. The performed measurements also suggest a humidity decrease in the slab base after redistribution.

In slab 6 measurements performed, day -3 and 269, clearly show an increase of humidity from 68 to 81 % RH in the screed. A humidity decrease of 5 % RH is demonstrated in the slab base. Notice the moisture level is nearly unchanged around the slab centre. Over all moisture has redistributed and drying of the slab base has occurred.

Moisture distribution determined for the drier slab 7 shows a slight decrease in the screed top of about 1 - 4 % RH after 91 days of redistribution. Over all the moisture profile obtained after redistribution is more or less equal to the moisture distribution obtained prior to flooring. However, the RH profile has flattened out in the screed layer and the slab bottom surface has dried further.

After 91 days of redistribution, the RH level in slab 8 increases 10 mm beneath the flooring. A moisture level decrease is shown both 30 mm and 50 mm below the screed top surface. The RH has increased between the 70 mm and 190 mm level.

The last three moisture profiles, HCS 1-3, shows the moisture distribution on samples obtained from the HCS, 16 days prior to flooring and 273 days after. HCS 1 represents the humidity above the core hole next to the concrete filled mid core hole. A significant humidity increase, from 68 to 78 % RH is shown in the screed surface and a minor decrease from 75 to 72 % RH in the HCS web at 90 mm level.

HCS 2 displays the results from RH determination performed on material from the wall separating mid core hole from the neighbour core hole. Top screed humidity has increased some 3 - 5 % RH. The results from the slab mid section, at 175 mm depth, shows a strange looking profile before flooring and after redistribution. This could be a result of the horizontal moisture distribution. However, a clear 5 % RH decrease in humidity is shown in the slab base.

HCS 3 diagram shows the moisture profiles on samples obtained from the concrete filled mid core hole. A minor increase 1 - 2 % RH is shown in the top screed. Throughout the concrete filling, 60 mm and below, the moisture level has decreased from about 4 - 5 % RH, slightly lower levels in the HCS base.

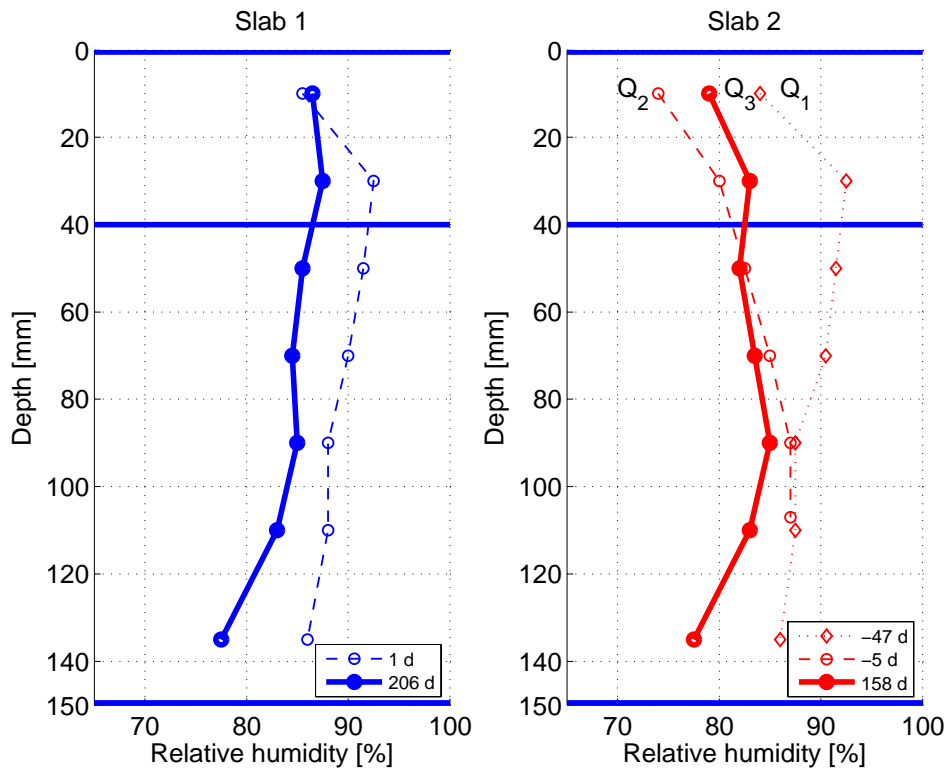


Figure 2. Moisture distribution determined for two SFC screeded concrete slabs on plywood before flooring (dashed lines) and after a certain time of redistribution (solid lines).

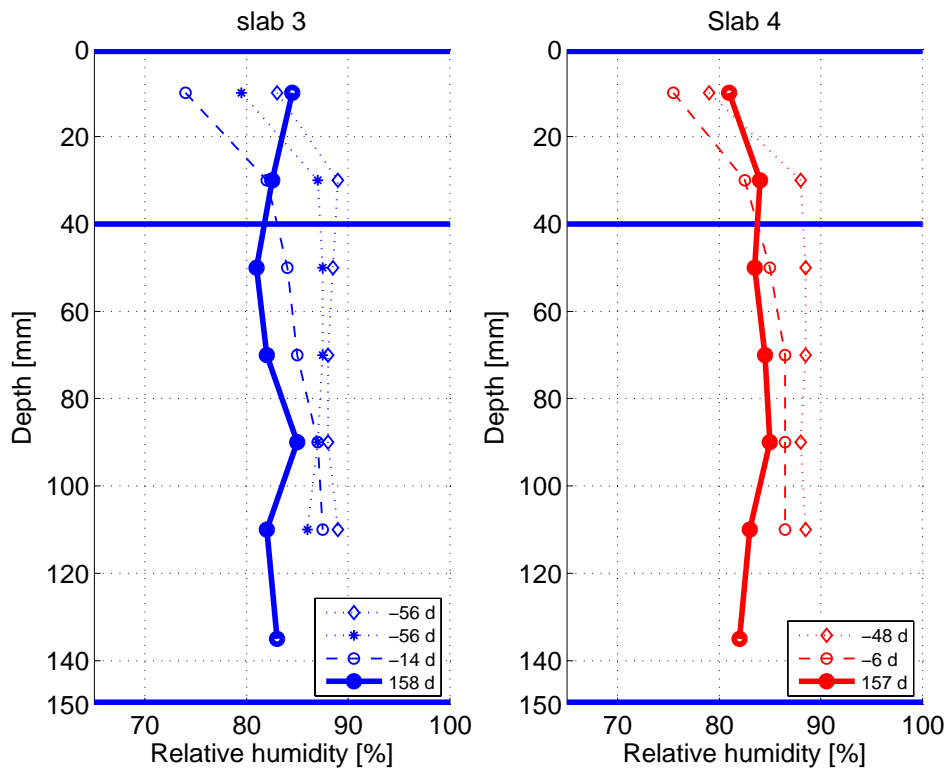


Figure 3. Moisture distribution determined for two M screeded concrete slabs on plywood before flooring (dashed lines) and after a certain time of redistribution (solid lines).

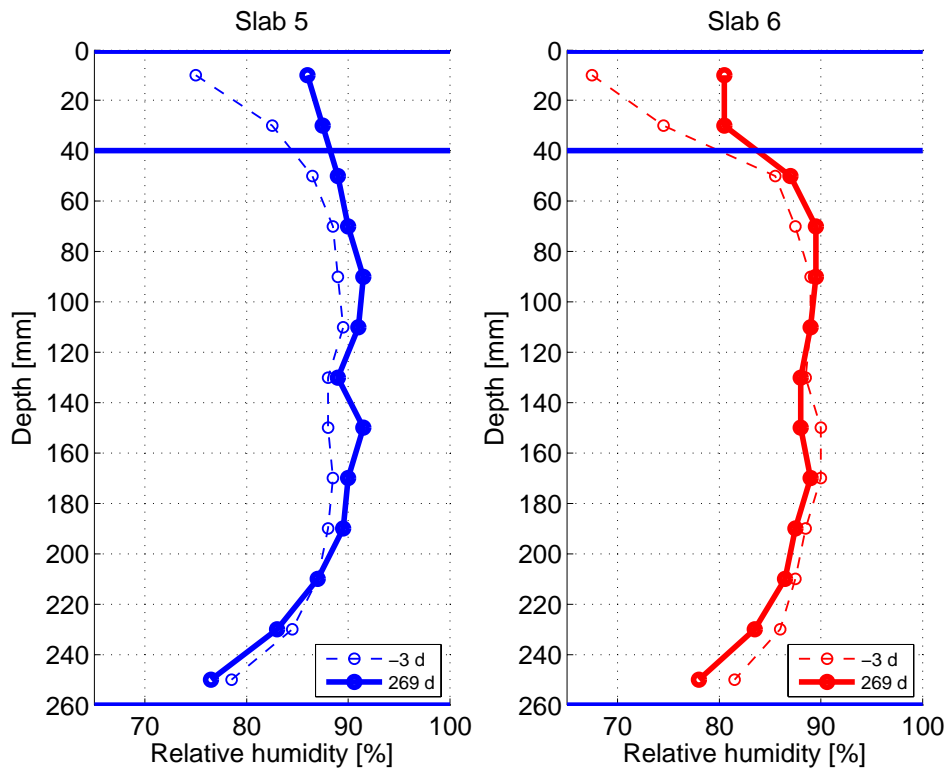


Figure 4. Moisture distribution determined for one M (left) and one SFC (right) screeded concrete slabs before flooring (dashed lines) and after a certain time of redistribution (solid lines).

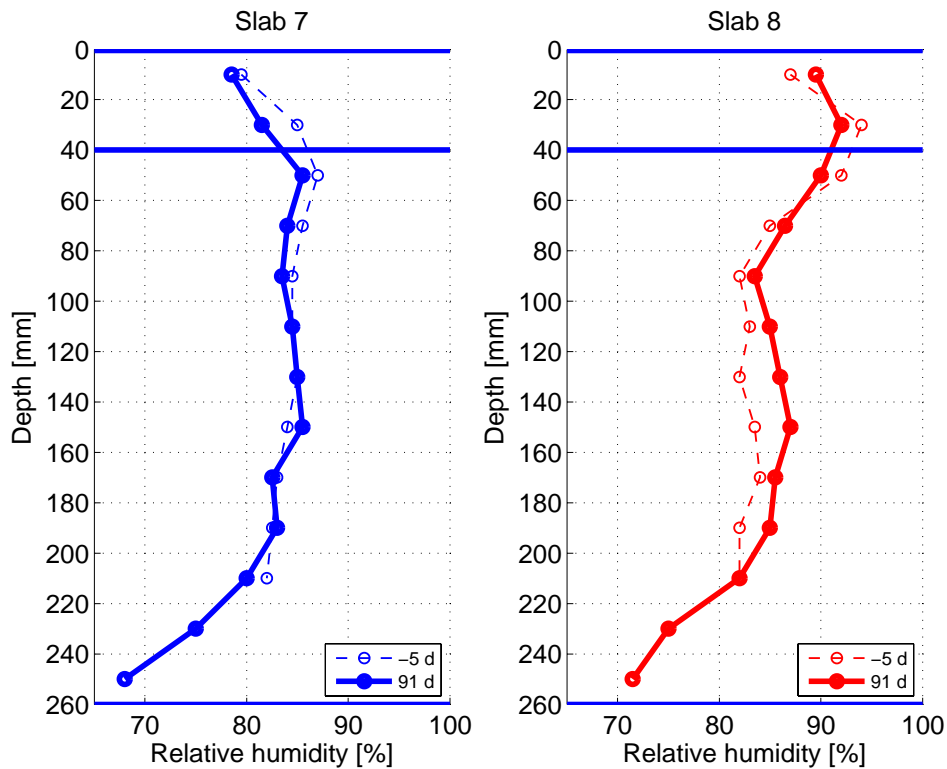


Figure 5. Moisture distribution determined for one M (left) and one SFC (right) screeded concrete slab before flooring (dashed lines) and after a certain time of redistribution (solid lines).

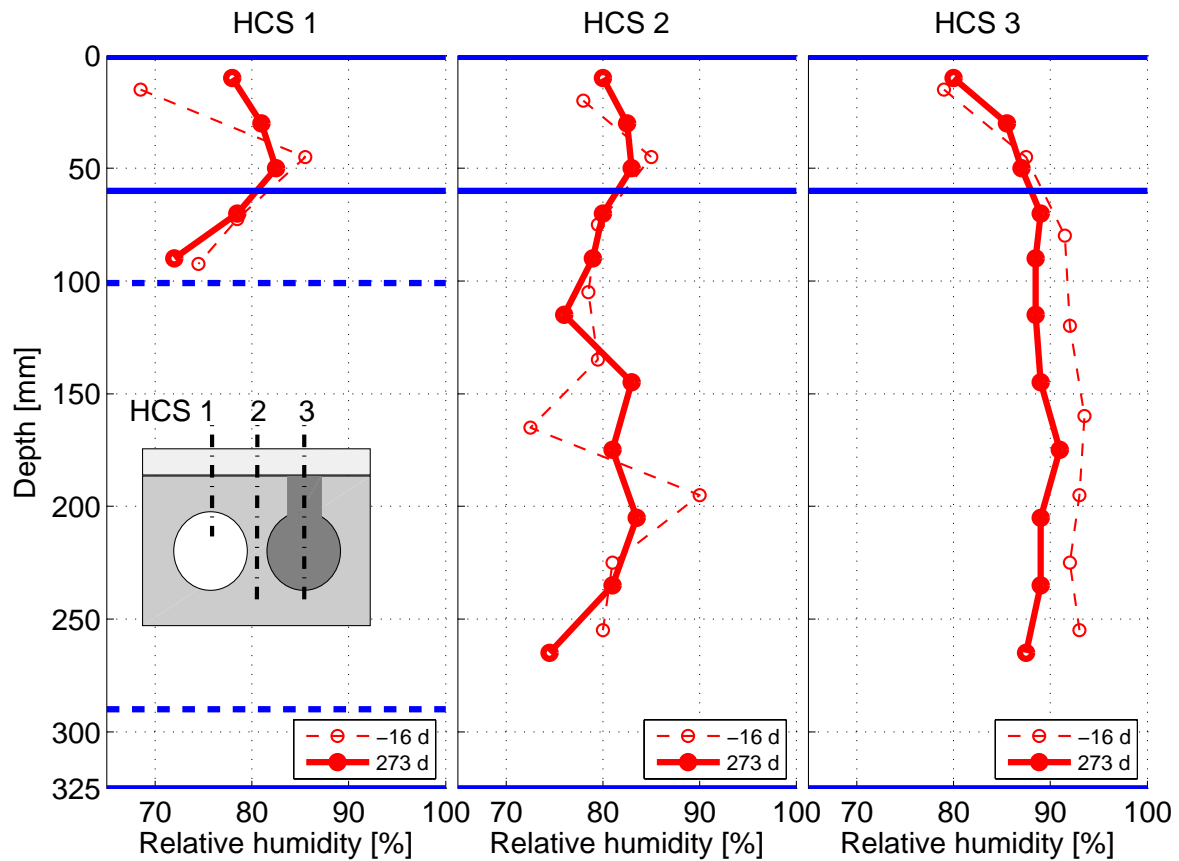


Figure 6. Moisture distribution determined in three sections of the SFC screeded hollow core slab, with one hollow core filled with material C, before flooring and after a certain time of redistribution.

5 Discussion

5.1 Comparing slab 1 and 2, Case B

The influence of screed drying time on redistribution is discussed by comparing slab 1 and 2. The screed on both slab 1 and 2 had dried for 48 days, see table 2, when moisture profile 1 d and -47 d was obtained in slab 1 and 2 respectively. Both these profiles are therefore almost identical. These two profiles show an elevated RH level in the screed/concrete corresponding to Case B phase 3 in the qualitative model. Slab 2 dried additional 42 days before a new RH profile -5 d was obtained. Judging from the obtained -5 d moisture profile in slab 2, drying has occurred mainly through the screed. The profiles 206 d, slab 1, and 157 d, slab 2, were obtained at the same day. Slab 1's shorter drying and longer moisture redistribution resulted in a more uniform screed moisture profile compared to slab 2. The moisture profile obtained in slab 1 after redistribution corresponds to phase 4 case B in the qualitative model. Further drying before flooring in slab 2 was accompanied by 158 days of moisture redistribution. This time was insufficient to achieve complete moisture redistribution in the screed. The moisture levels in slab 1 and 2 are almost equal from slab center and below, both before flooring and after redistribution, clearly demonstrating equal drying conditions were achieved through the coated plywood at the base.

5.2 Comparing slab 2 with 3 and 4, Case B

The influence of different screed materials with respect to moisture redistribution is discussed by comparing slab 2 with slab 3 and 4. The screed dried for 48 days before the moisture

profiles were determined on slab 3, -56 d, and slab 4, -48 d. Almost identical moisture profiles were obtained from slab 3 and 4. The elevated screed humidity in (slab 2) is not showing, probably a consequence of self desiccation in the mortar. Additional moisture profiles -14 d and -6 d were obtained the same day as profile -5 d for slab 2. These three moisture profiles are rather similar indicating that moisture has dried mainly through the screed as for slab 2 and moisture transfer rate is higher through hardened SFC compared to hardened mortar. They also indicate that the self desiccation diminishes with time as hydration mainly occurs early after pouring. The moisture distribution was finally determined after 149 and 157 days of redistribution in slab 3 and 4, on the same day as slab 2. Moisture in the screed of slab 4 still needs additional time to achieve a uniform distribution. The lower part of slab 3 and 4 shows equal moisture profiles with regards taken to uncertainties. Finally, further drying of the slabs would occur mostly through the slab base as this is more open to moisture transport than PVC flooring. Therefore it is likely that the future profile will concur with phase 4 in the proposed qualitative model

5.3 Comparing slab 7 with 8, Case B

The affect on residual moisture redistribution due to long drying of different screeds is discussed by comparing slab 7 and 8. Screed drying on slab 7 and 8 lasted for 35 days prior to determining the moisture profiles, - 5 d. The achieved RH profiles demonstrated the elevated moisture levels in the screed, corresponding to Case B phase 3 in the qualitative model. However, mortar self desiccation diminished the elevated screed moisture level in slab 7 compared to slab 8. In addition the benefits of the open SFC did not occur as a result of the short drying time. Both slabs were showing, within uncertainties, equally dry slab centers and bases. Flooring was applied on both slabs 40 days after screed application followed by 91 days of redistribution. A complete redistribution was not obtained 91 days after flooring. The moisture distribution after 91 days in slab 7 shows a drying of the screed and the slab top. This may be a result of uncertainties having an unfavorable impact on the achieved results. The determined humidity after redistribution may be too low compared to the true humidity in the 10 mm level and too high before the flooring. Regarding slab 8's redistribution, moisture from the screed center has redistributed down into the top, but also upwards to the screed top. Both slabs, in particular slab 8, correspond to Case B's 4th phase in the qualitative model.

5.4 Comparing slab 5 with 6, Case A

The influence of early flooring application on two different screed materials on moisture redistribution is discussed by comparing slab 5 and 6. Drying of the mortar in slab 5 and SFC in slab 6 lasted for 261 and 259 days respectively until the moisture profiles, -3 d, were obtained. The determined moisture profiles correspond well to phase 3 Case A in the qualitative model as the moisture profile for slab 5 and 6 both show pronounced drying of the screed and an equally pronounced drying of the slab base. The mortar in slab 5 has dried less compared with the SFC in slab 6. This benefit is achieved through initial self desiccation in the mortar. However, the benefit diminishes in the long run as the hardened mortar becomes less open to moisture transport compared to the SFC. The moisture profile was determined after 269 days of redistribution. The humidity increase in the mortar in slab 5 is considerable and clearly shows the effect of moisture redistributing from the slab center and up. The moisture level increase showing in the upper 200 mm of slab 5 is within the uncertainties and is therefore not significant. In slab 6, moisture from the slab center has redistributed to the top and increased the screed humidity, thus obtaining a uniform moisture profile. However, besides the continuing drying of the slab base, additional moisture will redistribute to the screed top as the maximum level is not yet achieved after 269 days of redistribution. Moisture

profiles determined for slab 5 and 6 after the achieved redistribution concur to phase 4 Case A in the qualitative model.

5.5 HCS1-3

Moisture profiles obtained from the hollow core slab in section HCS1-3 are not compared with the qualitative model owing to the significant horizontal moisture transfer occurring as a consequence of the non solid slab*.

Moisture profiles labeled -16 d in HCS1-3 were obtained after 122 days after screed application. Flooring application was completed 16 days after obtaining the first moisture profile. Redistribution maintained for 273 days until the humidity profiles after flooring were obtained. The -16 d profile of HCS1 clearly shows significant drying from the screed base and down into the HCS top as well as drying upwards. The significant downward drying may be a consequence of the reduced cross section above the empty core hole. The HCS1 redistribution profile demonstrated a significant humidity increase in the screed top originating from both vertical and horizontal moisture redistribution. Downward drying is also showing through the web top.

The moisture profile HCS2 determined for the web segment dividing the empty and the filled core hole showed some drying upwards, some moisture was also drying through the slab base. HCS2 profile shows disturbances in the slab center mainly originating from the horizontal moisture redistributing from the filling in the mid core hole through the web segment. The HCS2 screed top shows an increase as a consequence of 2-dimensional moisture redistribution. Web center profiles are less disturbed by the horizontal redistribution. Drying through the web base is significantly showing in the moisture profile of HCS2.

HCS3 moisture distribution 16 days before flooring shows drying through the screed top. The uniformly distributed moisture profile in HCS3 may be explained both by horizontal drying through the web to the neighbor core holes and vertical drying through the web base. HCS3 is showing a small increase in the top as a result of mainly vertical moisture redistribution from the filling. Further uniform drying is showing in the filling as a result of the horizontal drying through the web walls. The profile HCS3 shows lower humidity levels at the base compared to the filling center as a result from further downward drying.

* However, HCS 3 obtained in the filled core hole could judging from the obtained results without to much trouble be compared with the qualitative model Case B.

5.6 Quantitative model

One way to evaluate the moisture distribution profile in a screeded slab is to determine the moisture profile prior to flooring and suggest a complete redistribution, assuming isotherm conditions. Provided no occurrence of drying, residual moisture will redistribute until achieving a uniform RH level through the slab. Such a model needs three inputs, the distribution of RH before flooring, the thickness of each section, and the moisture capacity of each material. This model results in a simple equation, proposed below, to determine the uniform humidity distribution achieved in the screed surface, RH_{∞} [% RH],

$$RH_{\infty} = \frac{\sum_{\Delta x_i} \overline{RH}_i \cdot d_i \cdot \left(\frac{\partial w}{\partial RH} \right)_i}{\sum_{\Delta x_i} d_i \cdot \left(\frac{\partial w}{\partial RH} \right)_i} \quad (1)$$

where \overline{RH}_i [% RH] represents the average level determined in segment d_i [mm], w [kg/m³] represents the section's moisture content, $\left(\frac{\partial w}{\partial RH} \right)_i$ [kg/m³] represents average moisture capacity of each section.

Uncertainties are introduced when evaluating the RH_{∞} according to eq. 1. Provided the moisture distribution prior to flooring is close to uniform, these uncertainties are moderate. However, if flooring is applied early after screed application, the unevenly distributed moisture will need time to redistribute according to eq. 1. In such cases it becomes increasingly important to consider governing moisture transport properties, like diffusion, and time lag effects. A reduction of the uncertainties of RH_{∞} may be achieved not only through an increased accuracy of the determined moisture humidity in each section, but also by reducing each section thickness.

There is however a more profound technique to decrease the uncertainty of RH_{∞} . Moisture capacities may be obtained from the results from sorption isotherm measurements [10]. As drying/wetting cycles occur in certain sections, scanning curves between absorption and desorption isotherms also needs to be addressed in order to further decrease the uncertainties.

5.7 A description of desorption and absorption scanning

This approach to reduce uncertainties may be illustrated using the 10 mm level beneath flooring in slab 2 as an example, labeled Q. The current moisture content of a finite material element is determined by the preceding moisture history. As the humidity decreases during initial drying, Q will first follow a descending path along the boundary desorption isotherm, 1st phase of case B in the qualitative model represented by Q₁ in figure 2. 5 days prior to flooring point Q has descended on the desorption curve to Q₂, see figure 7. As the screed is applied, moisture will penetrate through the top 10 mm soon increasing the humidity in Q, 2nd phase. As the humidity increases Q's path will leave the boundary desorption curve and ascend along a new curve, scanning curve, crossing the area between desorption and absorption isotherms, represented by Q₃, see figure 7. The moisture capacity of the scanning curve is low which implies that a small increase in moisture content results in a large increase in humidity [% RH]. This scanning is a consequence of the hysteresis [11] exhibited by cement based materials. During redistribution, the humidity once again starts to decrease, in Q. The descending scanning curve will not retrace the preceding ascending scanning curve when the humidity decreases.

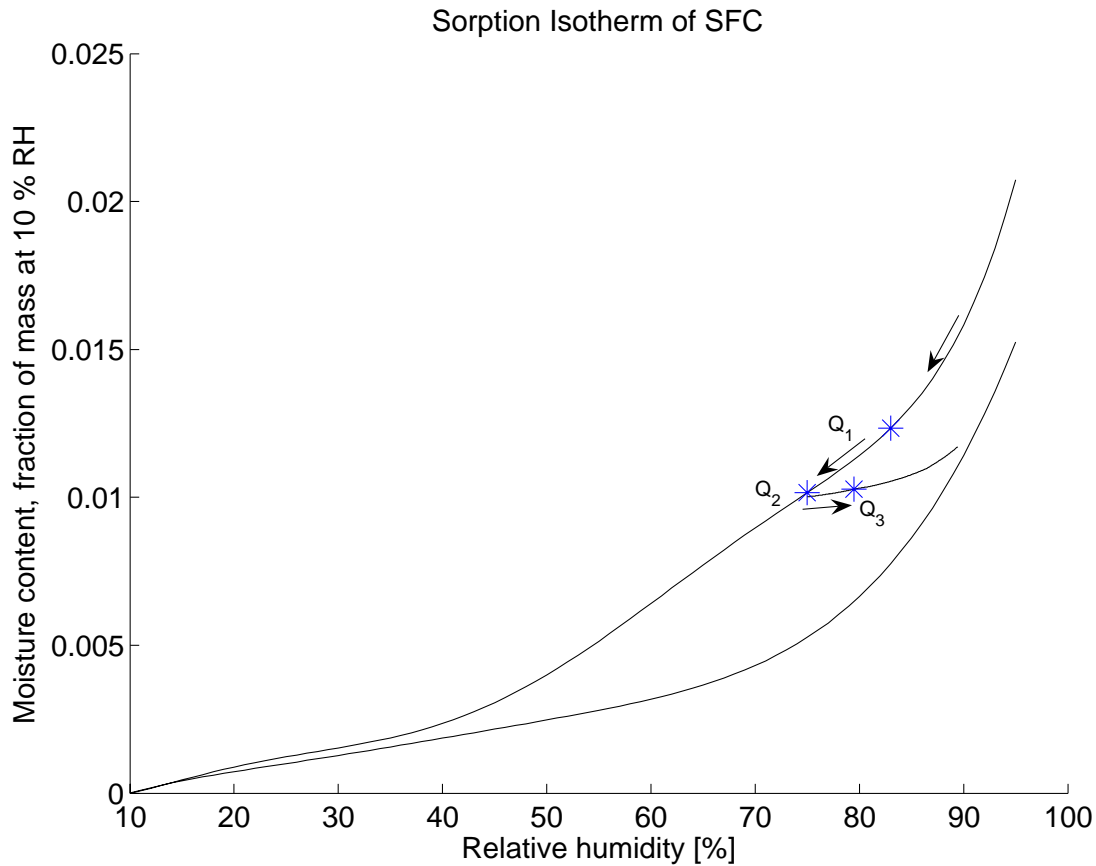


Figure 7. Illustration of Q's moisture path through drying and redistribution, y axis representing the moisture content, x axis represents the relative humidity. The stars indicate the achieved moisture state for point Q_1 at -47 days, Q_2 at -5 days and Q_3 at 158 days.

If these theories and scanning curves also were implicated in moisture redistribution calculations uncertainties would decrease further. At present a new theory has been developed for prediction of both ascending and descending scanning curves in concrete [12]. This model needs to be scrutinized before implicated in moisture distribution prediction models. So far only a few scanning curves for a few cement based materials are attainable in the literature [12-15].

6 Conclusions

Comparing the qualitative model of the moisture redistribution with the results obtained before flooring and after a certain time of redistribution indicate that moisture after flooring will redistribute according to the proposed model. This is useful with regards to moisture redistribution simulations, as simulating tools should include the hysteresis concrete exhibits. If hysteresis is not included the simulations should be performed step wise in order to grasp the scanning phenomenon, thus reducing the obtained uncertainty.

7 References

1. Wessén, B. and T. Hall. *Directed Non-Destructive VOC-sampling: A method for source location of indoor air pollutants*. in *Proceedings of the 7:th International Conference on Indoor Air Quality and Climate*. 1999. Edinburgh, Scotland: Construction Research Communications Ltd, pp. 420-425.

2. Sjöberg, A. and C. Engström, *Measurements of stored decomposition products from flooring adhesives in a concrete floor, as a basis for choosing a new floor surface construction*, in *Building Physics 2002 - 6th Nordic Symposium*. 2002.
3. Salthammer, T., *Organic Indoor Air Pollutants. Occurance, Measurement, Evaluation*, ed. T. Salthammer. 1999, Wienheim, Germany: WILEY-VCH. 329.
4. Andersson, K., et al., *TVOC and Health in Non-Industrial Indoor Environments*. *Indoor Air*, 1996. **7**(2): pp. 78-91.
5. Åhs, M. *Remote monitoring and logging of relative humidity in concrete*. in *Proceedings of the 7th symposium on building physics in the nordic countries* 2005. Reykjavik, Iceland: The icelandic building research institute pp. 181-187.
6. West, R.P. and N. Holmes, *Predicting moisture movement during the drying of concrete floors using finite elements*. *Construction and building materials*, 2005. **19**: pp. 674-681.
7. Obeid, W., G. Mounajed, and A. Alliche, *Mathematical formulation of thermo-hygro-mechanical coupling problem in non-saturated porous media*. *Computer Methods in Applied Mechanics and Engineering*, 2001. **190**(39): pp. 5105-5122.
8. Leivo, V. and J. Rantala, *Moisture behaviour of a massive concrete slab with a low temperature floor heating system during the initial drying period*. *Construction and building materials*, 2005. **19**: pp. 297-305.
9. Greenspan, L., *Humidity fixed point of binary saturated aqueous Solutions*. *Journal of research of the national bureau of standards- A. Physics and Chemistry*, 1977. **81**(1): pp. 89-96.
10. Åhs, M., A. Sjöberg, and A. Anderberg. *A method for study sorption phenomena*. in *Proceedings of the 10:th International Conference on Indoor Air Quality and Climate*. 2005. Beijing, China pp. 1969-1973.
11. Everett, D.H., *Adsorption hysteresis*, in *The Solid-Gas interface Vol. 2*, E.A. Flood, Editor. 1967, Marcel Dekker: New York. pp. 1055-1113.
12. Espinosa, R.M. and L. Franke, *Inkbottle Pore-Method: Prediction of hygroscopic water content in hardened cement paste at variable climatic conditions*. *Cement and Concrete Research*, 2006. **36**(10): pp. 1954-1968.
13. Baroghel-Bouny, V. and T. Chaussadent, *Texture and moisture characterization of hardened cement pastes and concretes from water vapour sorption measurements*, in *The modelling of microstructure and its potential for studying transport properties and durability*. 1996, Kluwer Academic Publishers.
14. Anderberg, A. and L. Wadsö, *Moisture in self-levelling flooring compounds. Part II. Sorption isotherms*. *Nordic concrete research*, 2004. **32**(2): pp. 16-30.
15. Ahlgren, L., *Fuktfixering i porösa byggnadsmaterial (in Swedish)*, in *Division of building technology*. 1972, Lund University Lund. pp. 197.